

# Organizing Unstructured Image Collections using Natural Language

Mingxuan Liu<sup>1</sup> Zhun Zhong<sup>4†</sup> Jun Li<sup>6</sup> Gianni Franchi<sup>3</sup> Subhankar Roy<sup>5</sup> Elisa Ricci<sup>1,2</sup>  
<sup>1</sup> University of Trento <sup>2</sup> Fondazione Bruno Kessler <sup>3</sup> ENSTA Paris, Institut Polytechnique de Paris  
<sup>4</sup> Hefei University of Technology <sup>5</sup> University of Bergamo <sup>6</sup> Technical University of Munich

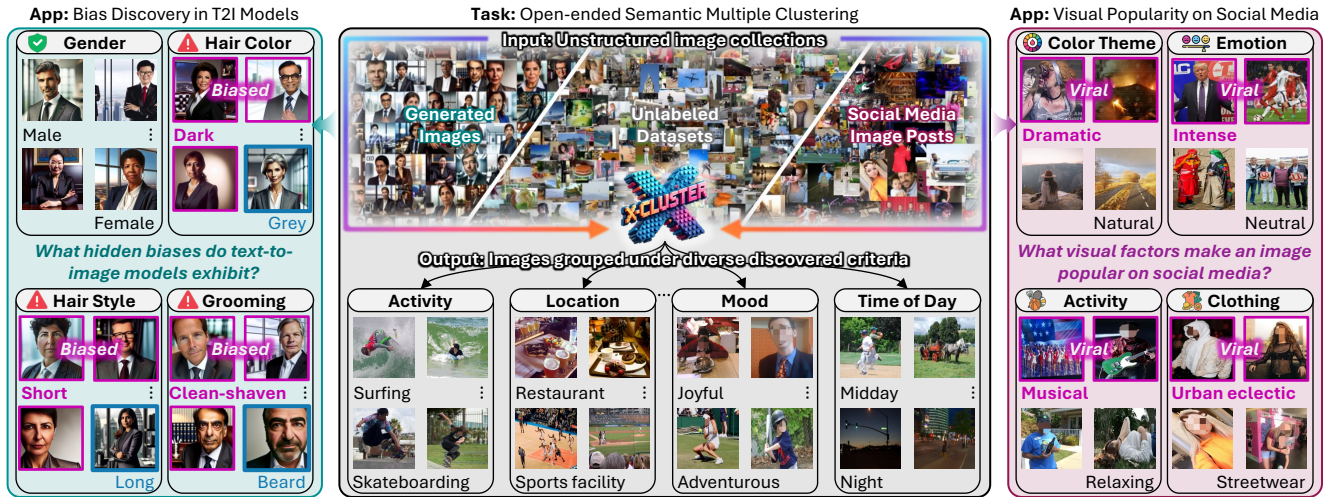


Figure 1. **Organizing unstructured image collections with  $\mathcal{X}$ -Cluster.** Mid: We propose  $\mathcal{X}$ -Cluster, which takes any unstructured image collection as input, automatically discovers multiple criteria (e.g., Activity or Location) that meaningfully group the data, and outputs images organized into semantic clusters under each criterion, *without* any prior knowledge. We demonstrate  $\mathcal{X}$ -Cluster as a versatile tool for real-world analysis: *i)* Left - uncovers surprising *novel biases* (e.g., “Hair color” or “Hair style”) when applied to text-to-image (T2I) model outputs, and *ii)* Right - reveals *visual factors* (e.g., “Dramatic” color or “Intensive” emotion) that drive social media posts virality.

## Abstract

In this work, we introduce and study the novel task of *Open-ended Semantic Multiple Clustering (OpenSMC)*. Given a large, unstructured image collection, the goal is to automatically discover several, diverse semantic clustering criteria (e.g., Activity or Location) from the images, and subsequently organize them according to the discovered criteria, without requiring any human input. Our framework,  **$\mathcal{X}$ -Cluster: eXploratory Clustering**, treats text as a reasoning proxy: it concurrently scans the entire image collection, proposes candidate criteria in natural language, and groups images into meaningful clusters per criterion. This radically differs from previous works, which either assume predefined clustering criteria or fixed cluster counts. To evaluate  $\mathcal{X}$ -Cluster, we create two new benchmarks, *COCO-4C* and *Food-4C*, each annotated with four distinct grouping criteria and corresponding cluster labels. Experiments show that  $\mathcal{X}$ -Cluster can effectively reveal meaningful partitions on several datasets. Finally, we use  $\mathcal{X}$ -Cluster to achieve various real-world applications, includ-

ing uncovering hidden biases in text-to-image (T2I) generative models and analyzing image virality on social media. Project page: <https://oatmealliu.github.io/xcluster.html>

## 1. Introduction

When organizing a large collection of unlabelled images, a natural question arises: *how should we group them?* One could imagine many possible criteria, *i.e.*, based on Activity, Location, or even Color. Yet, it is often unclear which criterion, if any, best describes the dataset, or whether multiple valid grouping principles coexist. As a result, the seemingly simple task of *clustering images* becomes challenging, as it is influenced by both the visual appearance of the data and their underlying semantics. However, tackling this open-ended unsupervised task of *automatically uncovering diverse and interpretable substructures within large image collections* is pivotal for many applications, such as social media recommendation [13] and dataset auditing [4].

<sup>†</sup>Corresponding author.

Existing clustering approaches still heavily rely on an iterative, human-in-the-loop interpretation and refinement process. Typically, we begin by setting a few hyperparameters (*e.g.*, the number of grouping criteria or clusters) for Deep Clustering (DC) methods [11, 90] to get a single partition, or for Multiple Clustering (MC) methods [107] to produce several partitions showing different views of the data. We then inspect sample images from each cluster, hoping they correspond to meaningful categories (*e.g.*, “Surfing” or “Skateboarding”) and, ideally, that all clusters follow a coherent criterion (*e.g.*, Activity). When such patterns fail to emerge, we tweak the hyperparameters and try again until the clusters finally make sense to us. This labor-intensive trial-and-error loop exists because *i)* the resulting clusters are not directly interpretable, being represented only as index assignments. *ii)* both DC and MC methods converge to solutions shaped by model inductive biases and hyperparameter settings, rather than the data’s intrinsic semantics.

To enhance controllability and interpretability, recent studies have introduced Text-Conditioned Multiple Clustering (TCMC) [105, 106]. TCMC approaches employ Multi-modal Large Language Models (MLLMs) [49, 70] to generate semantic clusters based on user-defined criteria and assign images accordingly, producing human-understandable cluster labels. However, these approaches assume that users already know meaningful ways to organize the dataset. As datasets grow in size and complexity, defining such criteria becomes increasingly unrealistic. Moreover, by relying on static preset criteria, this paradigm may overlook previously unknown grouping dimensions that organically emerge from ever-evolving data.

In this paper, we introduce the task of *Open-ended Semantic Multiple Clustering* (OpenSMC), the *first* task that aims to automatically generate *open-ended* and interpretable groupings of large, unstructured image collections *without* any human priors. Specifically, the goal of OpenSMC is to *discover* clustering criteria directly from the data and uncover their corresponding semantic clusters to organize images accordingly. This task is particularly challenging because *i)* it requires *concurrent* reasoning over all images to identify valid clustering criteria, and *ii)* it assumes *no* access to user knowledge about either the clustering criteria or the number of clusters. Tab. 1 summarizes the key differences between OpenSMC and other paradigms.

To address OpenSMC, we make the following contributions. First, we introduce  **$\mathcal{X}$ -Cluster: eXploratory Clustering**, a novel training-free two-stage framework powered by MLLMs [43, 44, 49] and LLMs [61].  $\mathcal{X}$ -Cluster consists of two consecutive modules: the Criteria Proposer and the Semantic Grouper. The Criteria Proposer employs a LLM to holistically reason over the entire image collection through textual representations to discover potential clustering criteria. For each discovered criterion, the Semantic

Table 1. **Comparison of different clustering paradigms.** Unlike DC, MC, and TCMC settings, the proposed OpenSMC task does not assume any prior knowledge and offers interpretable results.

		DC	MC	TCMC	OpenSMC
Prior	Knowledge # Criteria	✗	✓	✗	✗
	Text Criteria	✗	✗	✓	✗
	Knowledge # Clusters	✓	✓	✓	✗
Output	Multiple Clustering	✗	✓	✓	✓
	Interpretable	✗	✗	✓	✓
	Open-ended	✗	✗	✗	✓

Grouper then organizes images into distinct semantic substructures based on their criterion-related visual content. As shown in Fig. 1(mid), our  $\mathcal{X}$ -Cluster automatically discovers clustering criteria (*e.g.*, Activity, Location) and uncovers their corresponding semantic clusters (*e.g.*, “Surfing”, “Skateboarding” under Activity), all expressed in human-interpretable natural language.

As our second contribution, we introduce two realistic and large-scale benchmarks, COCO-4c and Food-4c, each annotated with ground-truth data for up to *four* clustering criteria. Using them, we comprehensively evaluate the effectiveness of our method in both criteria discovery and semantic grouping. As our third contribution, we demonstrate the versatility of  $\mathcal{X}$ -Cluster by applying it across diverse applications. When applied to occupation portrait images generated by text-to-image (T2I) generative models (Fig. 1(left)), it uncovers novel occupational biases, such as DALL-E3 [3] associating CEOs with “dark” and “short” hair, beyond well-known biases (*e.g.*, Gender). When applied to social media image posts,  $\mathcal{X}$ -Cluster finds that images featuring “dramatic” colors, “intense” emotions, or ‘urban eclectic’ clothing styles tend to attract greater popularity online. These findings show that  $\mathcal{X}$ -Cluster is a practical tool for understanding large-scale unstructured visual data, enabling the discovery of novel, unexpected patterns.

## 2. Related Work

**Image Clustering.** Deep clustering learns visual features and produces a *single* partition of an unlabeled dataset via self-supervision [11, 12, 81]. Multiple clustering extends this idea, seeking *multiple* non-redundant partitions with data augmentations, diversity losses, or subspace methods [34, 62, 78, 104, 107]. Despite steady progress, both paradigms share key limitations: *i)* their results are shaped by model inductive biases and training algorithms, limiting generalization beyond object-centric data and often misaligning with user intent or data semantics; and *ii)* clusters are produced as numeric indices rather than human-readable names. In contrast,  $\mathcal{X}$ -Cluster derives both meaningful criteria and cluster names directly from unlabeled data.

**Text Criterion conditioned Multiple Clustering.** TCMC lets users steer clustering by specifying the grouping crite-

ria. Learning-based approaches such as MMAP [105] and MSub [106] first use GPT-4 [1] to generate reference words (e.g., fruits colors like “Red” or “Green”) conditioned on the user-provided criterion (e.g., *Color*-based fruits clustering). They then optimize learnable image embeddings by aligning with these criterion conditioned reference words. Training-free methods instead translate images into text. IC|TC [42] first captions each image with LLaVA [50] conditioned on the user’s criterion, then uses GPT-4 to refine the captions and assign cluster names for a user-specified number of clusters. SSD-LLM [58] strengthens IC|TC by augmenting the prompt with the dataset’s primary object labels. Similar ideas have also been explored in applications such as visual trend discovery [17], bias analysis [21, 27], and robot failure diagnosis [28]. While  $\mathcal{X}$ -Cluster likewise uses text as its reasoning medium, it fundamentally differs from TCMC in two key aspects: *i*) it *automatically* discovers the grouping criteria rather than relying on a user-supplied one; *ii*) it infers both the number and the names of clusters, requiring *no* user-specified parameters.

**Topic Discovery.** OpenSMC is also related to *Topic Discovery* [5, 22, 97] in NLP, which identifies latent themes [94, 110, 111] or events [66, 87] from *text corpora*. Our work similarly aims to uncover common themes from large, unstructured data but operates on *images*, which is more challenging since *i*) visual semantics are implicit, unlike text where meaning is explicit, and *ii*) no current vision model can reliably reason over large image sets.

### 3. Open-ended Semantic Multiple Clustering

**Task Definition.** Given a collection of unlabeled images  $\mathcal{D} = \{\mathbf{x}_n\}_{n=1}^N$ , the goal of *Open-ended Semantic Multiple Clustering* is to build a system,  $\mathcal{H}$ , that automatically *i*) discovers a set of  $L$  grouping criteria  $\mathcal{R} = \{R_l\}_{l=1}^L$  described in natural language, and *ii*) finds interpretable substructures  $\mathcal{O}_l$  for each criterion by uncovering semantically meaningful clusters and assigns images to them. Formally, we define an OpenSMC system as:

$$\mathcal{H} : \mathcal{D} \mapsto \left\{ \mathcal{O}_l = \left\{ \mathcal{C}_k^l = (s_k^l, \mathcal{D}_k^l) \right\}_{k=1}^{K_l} \mid R_l \right\}_{l=1}^L,$$

where each cluster  $\mathcal{C}_k^l$  is characterized by a semantic name  $s_k^l$  and a subset of images  $\mathcal{D}_k^l \subset \mathcal{D}$  that share the same semantics. A criterion  $R_l$  refers to a *theme* for grouping images, such that all the clusters under  $R_l$  should align with the theme. As shown in Fig. 1(top), if  $R_l = \text{Activity}$ , each cluster under this criterion should collect images  $\mathcal{D}_k^l$  that depict an activity, such as  $s_k^l = \text{“Surfing”}$ . If  $R_l = \text{Location}$ , the same dataset should be organized into clusters like “Restaurant”, “Sports facility”, and so on.

An OpenSMC system should find  $\mathcal{R}$  and  $\mathcal{O}_l$  automatically, both expressed in natural language. In contrast to




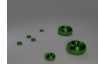


	Criterion	Label		Criterion	Label
Fruit-2c	Species:	Banana	Card-2c	Rank:	Ace
	Color:	Yellow		Suit:	Spades
	Criterion	Label		Criterion	Label
Action-3c	Action:	Jumping	Clevr-4c	Color:	Green
	Location:	Residential area		Texture:	Metal
	Mood:	Joyful		Shape:	Torus
	Criterion	Label		Criterion	Label
COCO-4c (New)	Activity:	Skateboarding	Food-4c (New)	Food Type:	Caprese salad
	Location:	Urban area		Cuisine:	Italian
	Mood:	Adventurous		Course:	Appetizer
	Time of Day:	Afternoon		Diet:	Vegetarian

Figure 2. **OpenSMC benchmarks.** We introduce two **new** challenging benchmarks: **COCO-4c** and **Food-4c**. We show all annotated criteria and the corresponding labels for the example images.

TCMC setting, where criteria  $\mathcal{R}$  and the corresponding cluster counts  $K$  are *preset* by human operators.

**Benchmark.** Evaluating OpenSMC methods requires benchmarks that can be partitioned under multiple criteria. Currently, only a few benchmarks [107] support the evaluation of OpenSMC methods: Fruit-2c [64], Card-2c [36], Action-3c [42], and Clevr-4c [92]. As shown in Fig. 2, these benchmarks are limited by their object-centric nature with simple backgrounds (e.g. Fruit-2c), an insufficient number of criteria (e.g. up to three in Action-3c), and a lack of photorealism due to synthetic generation (e.g. Clevr-4c).

Given that the data encountered in real-world applications is more complex, we annotate and propose two *new* benchmarks for OpenSMC: Food-4c and COCO-4c. Food-4c is sourced from Food-101 [8], which includes 101 Food type (original annotations), along with new annotations for 15 Cuisine types, 5 Courses types, and 4 Diet preferences, totaling *four* clustering criteria. Additionally, we introduced COCO-4c using images from COCO-val [47], where we annotated *four* criteria with varying number of clusters: 64 Activity, 19 Location, 20 Mood, and 6 Time of day. Examples of these newly constructed benchmarks are shown in Fig. 2. Further details, such as cluster names and the annotation pipeline, are provided in Supp. D.

### 4. Method

The goal of an OpenSMC system is to first discover meaningful grouping criteria (or themes) from an unstructured image collection by finding commonalities among the images, and then group them into semantic clusters as per the discovered criteria. This is particularly a challenging task because it requires reasoning over the visual content of all images *simultaneously*. To address OpenSMC, we diverge from representation learning-based MC approaches [105, 106], as no existing model can yet encode large image sets and reason over them reliably. Instead, we convert the visual content of all images into text and use *text descriptions as a proxy* to discover the grouping criteria and the semantic substructures.

**System Overview:** As illustrated in Fig. 3, our proposed

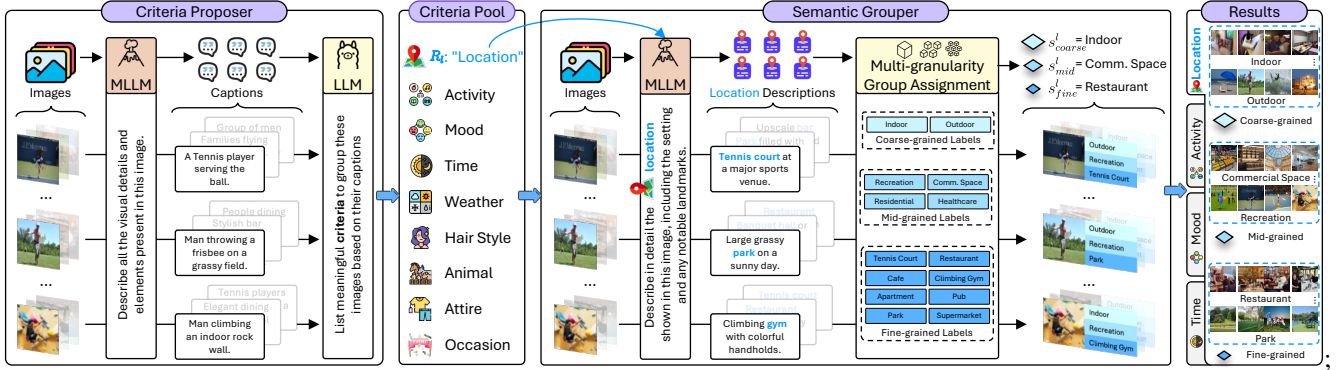


Figure 3.  $\mathcal{X}$ -Cluster consists of a *Criteria Proposer* and a *Semantic Grouper*. **(left)** Given a set of images, the Proposer discovers and outputs a pool of grouping criteria in natural language. **(right)** The Grouper subsequently extracts criterion-specific descriptions from images relevant to each criterion, discovers the underlying semantic clusters, and groups each image at three semantic granularity levels. **Results** shows an example, as how an unstructured image collection can be grouped into clusters of different semantic granularity corresponding to criterion “Location”. See Supp. F for implementation and prompt details.

$\mathcal{X}$ -Cluster is a two-stage framework that is composed of two modules: *Criteria Proposer* and *Semantic Grouper*. The *Criteria Proposer* processes the *entire* image set  $\mathcal{D}$  to discover diverse common themes among the images and proposes grouping criteria  $\mathcal{R}$  in natural language (e.g. Location). Once the criteria are proposed, the *Semantic Grouper* uncovers the substructure  $\mathcal{O}_l$  of  $\mathcal{D}$  by discovering distinct semantic clusters and assigning images to their respective clusters (e.g. “Tennis Court”), adhering to each criterion  $R_l \in \mathcal{R}$ . As the OpenSMC task operates without user priors to guide semantic granularity, we also design our *Semantic Grouper* to automatically discover  $\mathcal{O}_l$  across multiple granularity levels, from coarse (e.g., “Outdoor”) to mid (e.g., “Recreation”) to fine (e.g., “Tennis Court”), and organizes the images accordingly. In this work, we explore *three* design choices for both the Proposer and the Grouper. Due to space constraints, only the main variant of  $\mathcal{X}$ -Cluster is illustrated in Fig. 3, while the illustrations of the alternative variants and additional implementation details, including the exact prompts, are provided in Supp. F. Next, we describe each variant in detail.

#### 4.1. Criteria Proposer

As shown in Fig. 3(left), the Proposer takes as input a set of input images and generates distinct grouping criteria (or Criteria Pool) in natural language. Its core design principle is the ability to *concurrently reason* across a large set of images. Next, we explore three systematic approaches.

**Caption-based Proposer (main):** To enable reasoning over a large image set for criterion discovery, we first leverage a MLLM [49] to generate a comprehensive caption  $e_n$  for each image, converting its visual content into text representations  $e_n = \text{MLLM}(\mathbf{x}_n)$ . The resulting caption set  $\{e_n\}_{n=1}^N$  serves as a rich and holistic semantic proxy for the image collection  $\mathcal{D}$ . Using these compact textual proxies, we then prompt a LLM [61, 70] to jointly analyze the ag-

gregated visual content and propose multiple valid grouping criteria, denoted as  $\tilde{\mathcal{R}} = \text{LLM}(\{e_n\}_{n=1}^N)$ . As an example, the LLM could use different cues such as “Tennis”, “grassy field”, “rock wall” in the captions (see Fig. 3) and its reasoning capability to discover the criterion “Location”, since they are usually associated to a physical location, albeit locations may not explicitly appear in any caption.

**Tag-based Proposer (alternative):** Instead of using captions as textual proxies for reasoning, we further explore an approach that relies on image tags. Specifically, using the WordNet [63] vocabulary as the candidate tag set, we employ an open-vocabulary tagger (e.g., CLIP [79]) to assign ten tags  $t_{i,n}$  to each image as  $\{t_{i,n}\}_{i=1}^{10} = \text{Tagger}(\mathbf{x}_n, \text{WordNet})$ . These tags act as concise semantic descriptors that summarize the key elements present in each image. We then aggregate all assigned tags and prompt a LLM to analyze them jointly and propose grouping criteria as  $\tilde{\mathcal{R}} = \text{LLM}(\{\{t_{i,n}\}_{i=1}^{10}\}_{n=1}^N)$ .

**Image-based Proposer (alternative):** Lastly, we explore an approach that reasons directly over images rather than their textual proxies. Since no existing model can reliably encode large image sets at once, we adopt a simple workaround: divide  $\mathcal{D}$  into 64-image batches, stitch each batch into an  $8 \times 8$  grid as a *single* composite image, and feed the resulting image grids to a MLLM. The model is prompted to propose grouping criteria from each grid, and we aggregate and deduplicate these subset proposals to obtain the final criteria set  $\tilde{\mathcal{R}}$ .

**Criteria Refinement:** The accumulated criteria in  $\tilde{\mathcal{R}}$  may contain redundant or noisy entries, such as semantically overlapping concepts (e.g., “Outdoor” vs. “Open space”) or irrelevant ones (e.g., “High resolution”). To clean them, we input all initially proposed criteria into a LLM, prompting it to consolidate similar ones and discard noise. This yields a refined criteria set  $\mathcal{R} = \text{LLM}(\tilde{\mathcal{R}})$ , which is then stored in a pool for the subsequent substructure discovery stage.

## 4.2. Semantic Grouper

Each discovered criterion  $R_l \in \mathcal{R}$  serves as a thematic indicator for a distinct semantic substructure  $\mathcal{O}_l$  within the image set  $\mathcal{D}$ . To uncover these substructures, as shown in Fig. 3(right), the Grouper takes  $\mathcal{D}$  and each criterion  $R_l$  as inputs, discovers cluster names  $\{s_k^l\}_{k=1}^{K_l}$ , and groups images  $\mathcal{D}_k^l$  to their corresponding clusters. As a result, the interpretable substructure  $\mathcal{O}_l = \{\mathcal{C}_k^l = (s_k^l, \mathcal{D}_k^l)\}_{k=1}^{K_l}$  emerges for each  $R_l$ . The core design of the Grouper focuses on *aligning* semantic substructure discovery with the given partitioning criterion. Like the Proposer, we explore three distinct approaches for the Grouper.

Furthermore, as clusters under a given criterion can be formed at varying semantic granularities based on user preferences, we have designed our Grouper to clusters  $\mathcal{D}$  at three levels: coarse, middle, and fine-grained. This allows  $\mathcal{X}$ -Cluster to provide insights at different granularities. For example, under the Cuisine criterion,  $\mathcal{X}$ -Cluster can organize images at a coarse continental level (e.g., “European” or “Asian”), a middle regional level (e.g., “Mediterranean” or “Southeast Asian”), or a fine national level (e.g., “Italian” or “Thai”). See Supp. F.2 for design details.

**Caption-based Grouper (main):** Given a target criterion  $R_l$ , we prompt the MLLM to generate criterion-specific captions that focus exclusively on the visual content relevant to  $R_l$  for each image, as  $e_n^l = \text{MLLM}(\mathbf{x}_n, R_l)$ . Next, we design a *Multi-granularity Group Assignment (MGA)* module that uses the LLM to group images into clusters across multiple semantic granularity levels through a three-step process: *i) Initial Naming:* The LLM assigns a provisional class name to each caption as  $s_n^l = \text{LLM}(e_n^l, R_l)$ , producing an initial set of names  $\mathcal{S}_{\text{init}}^l$ ; *ii) Multi-granularity Cluster Refinement:* The LLM refines  $\mathcal{S}_{\text{init}}^l$  into three structured granularity levels:  $(\mathcal{S}_{\text{coarse}}^l, \mathcal{S}_{\text{mid}}^l, \mathcal{S}_{\text{fine}}^l) = \text{LLM}(\mathcal{S}_{\text{init}}^l, R_l)$ , which serve as candidate cluster names; *iii) Final Assignment:* LLM assigns each image  $\mathbf{x}_n$  to a cluster by linking its criterion-specific caption to the structured class names at different granularity levels as  $(s_{\text{coarse}}^l, s_{\text{mid}}^l, s_{\text{fine}}^l) = \text{LLM}(e_n^l, \mathcal{S}_{\text{coarse}}^l, \mathcal{S}_{\text{mid}}^l, \mathcal{S}_{\text{fine}}^l)$ . By aggregating these cluster assignments across  $\mathcal{D}$  at different levels, we derive multi-granularity semantic substructures. As we will show in § 5.3, the Caption-based Grouper outperforms other alternatives, making it our main method.

**Tag-based Grouper (alternative):** Given a target criterion  $R_l$ , we prompt the LLM to generate a set of common categories (e.g., “Commercial Space”) related to the criterion  $\mathcal{S}_{\text{mid}}^l = \text{LLM}(R_l)$  as the mid-grained tags. Following Liu et al. [52], we further query the LLM to infer potential super- and sub-categories (e.g., “Indoor” and “Restaurant”) for each mid-grained tag, thereby obtaining the corresponding coarse- and fine-grained tag sets,  $\mathcal{S}_{\text{coarse}}^l$  and  $\mathcal{S}_{\text{fine}}^l$ . Finally, we employ an open-vocabulary image tagger [79] to

assign the most relevant tag at each granularity level to each image,  $(s_{\text{coarse}}^l, s_{\text{mid}}^l, s_{\text{fine}}^l) = \text{Tagger}(\mathbf{x}_n, \mathcal{S}_{\text{coarse}}^l, \mathcal{S}_{\text{mid}}^l, \mathcal{S}_{\text{fine}}^l)$ , yielding multi-granularity substructures after aggregation.

**Image-based Grouper (alternative):** Given a target criterion  $R_l$ , we first prompt a LLM to generate a question  $q_l$  tailored to  $R_l$ . For e.g., for the criterion Mood the generated question is: “What mood is conveyed by this image? Answer with an abstract, common, and specific category name, respectively”. We then use  $q_l$  to guide a visual question answering (VQA) model [44] in directly inferring semantic cluster names and assignments for each image at different granularity levels as  $(s_{\text{coarse}}^l, s_{\text{mid}}^l, s_{\text{fine}}^l) = \text{VQA}(\mathbf{x}_n, q_l)$ .

## 5. Experiments

### 5.1. Experimental Protocol

**Implementation Details:** We run with our proposed  $\mathcal{X}$ -Cluster framework using: *i)* CLIP ViT-L/14 [79] as the Tagger, *ii)* LLaVA-NeXT-7B [49] as the MLLM, *iii)* Llama-3.1-8B [61] as the LLM, and *iv)* BLIP-2 Flan-T5<sub>XXL</sub> [44] as the VQA model. For the Image-based Proposer we use LLaVA-NeXT-Interleave-7B [43] as the MLLM due to its strong multi-image reasoning capability. Additionally, we explore a variant of the Image-based Grouper using LLaVA-NeXT-7B as the VQA model. We provide further details of  $\mathcal{X}$ -Cluster, including the exact prompt designs, in Supp. F.

**Evaluation Metric for Criteria Discovery:** We use True Positive Rate (TPR) [15] to evaluate the criteria discovery performance of different proposers. Specifically, we compute TPR as  $\text{TPR} = \frac{|\mathcal{R} \cap \mathcal{Y}|}{|\mathcal{Y}|}$ , measuring to what extent the predicted set covers the ground-truth criteria  $\mathcal{Y}$ . It is important to note that the number of grouping criteria is subjective and can be as extensive as one’s preferences allow (open-ended), making False Positives hard to define. Thus, we use TPR as the primary metric. A higher TPR means better coverage of predicted criteria compared to the ground truth.

**Evaluation Metrics for Substructure Uncovering:** To assess each criterion-specific substructure uncovered by the Grouper, we evaluate its alignment with the ground-truth substructure along two dimensions: *i) Semantic Consistency:* For each image, we compute the semantic similarity between its assigned cluster name and the ground-truth label under the current criterion using Sentence-BERT. The average similarity across the dataset, reported as Semantic Accuracy (SAcc) [53], measures how well the predicted substructure aligns semantically with the ground truth. *ii) Structural Consistency:* We use clustering accuracy (CAcc) [30, 91] to measure the degree of structural match between the predicted and ground-truth substructures (clusters) using Hungarian matching algorithm [41].

Since the granularity of ground-truth annotations is unknown during OpenSMC evaluation, we select the predicted substructure with the highest CAcc for assessment. Unlike

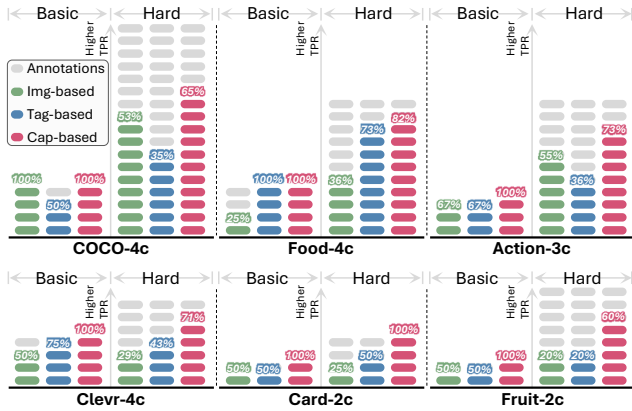


Figure 4. **Comprehensiveness Comparison of Criteria Proposers.** TPR performance of each proposer is evaluated against Basic and Hard ground-truth criteria, and visualized using a Progress Bar Chart. Each block represents one ground-truth criterion, with **Colored** blocks indicating successfully discovered criteria and **Gray** blocks representing undiscovered criteria.

TCMC methods [42, 106] that rely on ground-truth cluster counts for perfect matching, our strategy provides a fair and practical evaluation for open-ended OpenSMC systems.

## 5.2. Study of the Criteria Proposer

We also evaluate the performance of our design for the Proposer module. To properly assess his effectiveness, we realize that for complex datasets like COCO-4c, four ground-truth criteria may not cover all valid grouping options. Therefore, we expanded the ground-truth criteria for each of the six benchmarks in Sec. 3 using human annotators, resulting in {10, 4, 11, 7, 17, 11} distinct criteria for {Fruit-2c, Card-2c, Action-3c, Clevr-4c, COCO-4c, Food-4c}. We refer to the original per-image annotated criteria set (see Fig. 2) as **Basic** ground truth and the expanded set as **Hard** during evaluation. See Supp. D.2 for annotations.

**Which Criteria Proposer Performs the Best?** In Fig. 4, we compare different approaches for the Proposers in terms of the comprehensiveness of the discovered criteria using TPR. From Fig. 4, we observe that our caption-based Proposer discovers the most comprehensive criteria, making it the *closest* to the human-annotated set among all methods. It consistently outperforms other variants in both the Basic and Hard sets across all six benchmarks. Its superior performance is particularly evident under the Hard criteria set, where it surpasses the second-best Tag-based Proposer by +32.2% TPR. Intuitively, the Caption-based Proposer works better because captions capture more diverse and nuanced aspects of the image set, which further guides the LLM to comprehensively discover different grouping criteria. Contrarily, the Tag-based Proposer is less effective in complex benchmarks (e.g. COCO-4c and Action-3c) since tags provide less contextual and descriptive information. Similarly, the Image-based Proposer is subpar in terms of performance

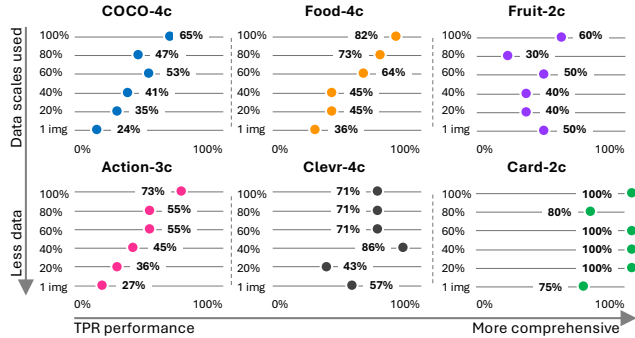


Figure 5. **Impact of Image Quantity on Criteria Discovery.** We evaluate the TPR performance of the **Caption-based Proposer** at different image scales against the Hard ground-truth criteria set.

since it is limited to reasoning over a small subset of images and loses visual details when combining images into a grid.

**Impact of Image Quantity on Criteria Discovery:** Fig. 5 shows the TPR performance of the Caption-based Proposer across different image scales. Interestingly, in *object-centric* benchmarks like Card-2c and Clevr-4c, satisfactory performance is achieved with just a *few* images. In fact, even a *single* image often suffices for reasonable criteria discovery, as object-centric datasets tend to have uniform structures, *i.e.*, seeing one playing card is enough to suggest criteria like Suit. However, this does not hold for more complex datasets like COCO-4c, Food-4c, and Action-3c, which feature diverse and realistic scenarios. Here, reducing the number of images leads to a clear drop in TPR performance, as capturing intricate and varied thematic criteria requires a larger image set. Since  $\mathcal{X}$ -Cluster operates *without* prior knowledge of the dataset, we use the *entire* dataset by default to ensure comprehensive discovery.

## 5.3. Study of the Semantic Grouper

**Which Semantic Grouper Performs the Best?** In Fig. 6, we evaluate different design choices for the Grouper using CAcc and SAcc for each criterion, determining the best performer based on Harmonic Mean (HM). To contextualize performance, we establish an oracle using CLIP ViT-L/14 in a zero-shot classification setup, where grouping criteria, cluster names, and the number of clusters are all *known*. We also use KMeans with ground-truth cluster numbers and visual features from CLIP-L/14, DINOv1-B/16 [45], and DINOv2-G/14 [71] as CAcc baselines.

From Fig. 6, we observe that the proposed Caption-based Grouper performs best, ranking first in 10 out of 15 tested criteria based on the HM across four benchmarks. It achieves an average CAcc of 59.9%, closely matching the oracle performance of 58.1%, highlighting the effectiveness of our text-driven approach. For SAcc, the Caption-based Grouper achieves an average of 60.5%, surpassing its counterparts, but falling short of the oracle 74.2% which benefits from exact ground-truth class names. This gap is expected

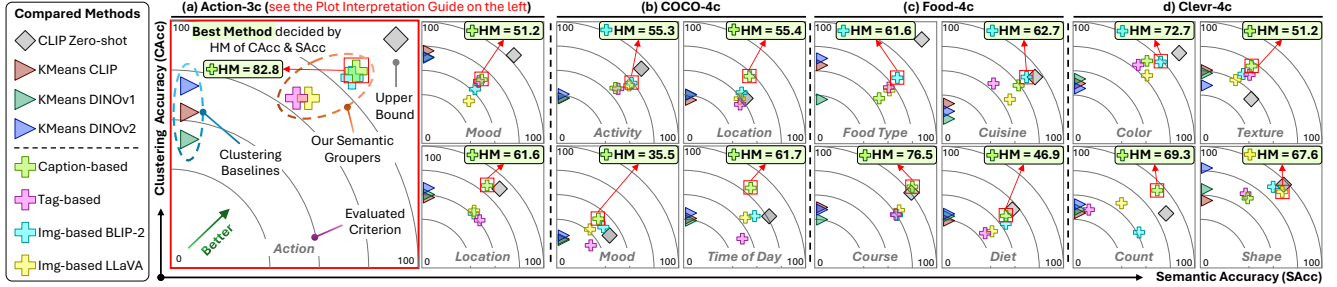


Figure 6. **Comparison of Semantic Groupers.** We report CAcc, SAcc, and their Harmonic Mean (HM) for different Semantic Groupers ( $\oplus$ ) on the Basic criteria across four benchmarks. CLIP zero-shot classification ( $\diamond$ ) serves as an oracle, while KMeans ( $\blacktriangleright$ ) with strong visual features is used as a CAcc baseline. The **best performer** for each criterion, determined by HM, is highlighted in green. Overall, our *Caption-based Grouper* performs best, ranking first in 10 of 15 evaluated criteria. See Supp. H.2 for clustering visualizations.

Table 2. **Comparison with TCMC methods.** For each benchmark, we report the average CAcc (%) and SAcc (%) across all criteria. We provide CLIP L/14 zero-shot performance as the pseudo upper-bound reference (UB). **Note:** †-marked methods used the ground-truth criteria and the number of clusters ( $K_i$ ) as prior input. MMAP and MSub do not build semantic clusters. See expanded results in Supp. H.3.

	COCO-4c		Food-4c		Clevr-4c		Action-3c		Card-2c		Fruit-2c		Avg	
	CAcc	SAcc	CAcc	SAcc	CAcc	SAcc	CAcc	SAcc	CAcc	SAcc	CAcc	SAcc	CAcc	SAcc
UB	40.1	60.6	64.1	80.2	56.7	72.5	79.8	82.3	41.4	66.9	69.4	88.3	50.2	64.4
MMaP † [105]	33.9	-	43.8	-	62.8	-	60.6	-	36.9	-	51.0	-	48.2	-
MSub † [106]	36.0	-	47.3	-	72.2	-	64.3	-	39.6	-	54.4	-	52.3	-
IC TC † [42]	48.9	<b>53.2</b>	<b>50.5</b>	61.7	58.3	36.8	76.4	56.3	<b>74.8</b>	81.2	63.3	55.1	<b>62.0</b>	57.4
SSD-LLM † [58]	41.6	52.1	47.5	55.5	54.8	37.6	<b>78.1</b>	52.9	67.3	76.3	62.0	46.8	58.6	53.6
$\mathcal{X}$ -Cluster (Ours)	<b>51.2</b>	48.4	48.1	<b>64.9</b>	64.9	<b>54.3</b>	68.3	<b>60.6</b>	73.3	<b>84.3</b>	<b>65.1</b>	<b>61.1</b>	61.8	<b>62.3</b>

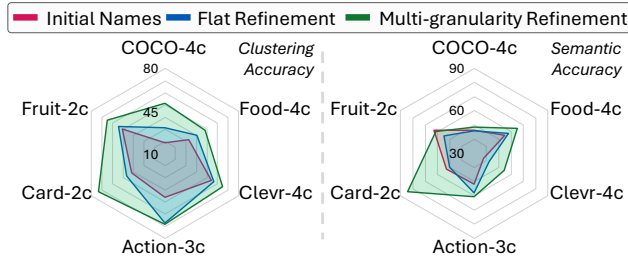


Figure 7. **Ablation study** of multi-granularity refinement.

due to the open nature of the semantic space, *i.e.*, terms like “Joyful”, “Happy”, and “Cheerful” often describe the same Mood but lack full semantic equivalence. The BLIP-2 Image-based Grouper ranks second. Its criterion-specific questions improve labeling accuracy, but per-image predictions can introduce noise in clustering.

**Necessity of Multi-Granularity Cluster Refinement:** To evaluate the effectiveness of multi-granularity cluster refinement design, we conduct controlled experiments using our Caption-based Grouper with three cluster naming strategies: *i)* *Initial Names*, where the initially assigned names are used as the final output; *ii)* *Flat Refinement*, where the LLM refines initial names into a single-level list with uniform granularity; and *iii)* *Multi-Granularity Refinement*, our proposed approach. As shown in Fig. 7, both refinement methods significantly improve clustering accuracy compared to using noisy initial names, highlighting the importance of granularity-consistent cluster names for revealing substructures. Moreover, our multi-granularity re-

finement outperforms flat refinement by enabling clustering at different levels of detail, providing greater flexibility in aligning with user-preferred grouping granularity.

#### 5.4. Comparison with TCMC Methods

We first perform some experiments to compare our approach with state of the art TCMC methods: IC|TC [42], SSD-LLM [58], MMAP [105], and MSub [106]. Results are shown in Tab. 2. Unlike our fully automated  $\mathcal{X}$ -Cluster method, which discovers criteria through the Proposer and requires *no* pre-set cluster counts, *all TCMC methods used ground-truth text criteria and the number of clusters ( $K_i$ ) as prior input.* The primary goal of this experiment is to evaluate dataset grouping performance. Our approach outperforms MMAP, MSub, and SSD-LLM, while achieving results comparable to IC|TC across six benchmarks. This demonstrates that our framework generates high-quality clusters for OpenSMC *without* requiring users to define criteria or cluster counts. Implementation details of the compared methods are provided in Supp. G.

**Further Analysis of  $\mathcal{X}$ -Cluster** is provided in the supplementary material: *i)* Supp. I presents qualitative results; *ii)* Supp. J examines failure cases; *iii)* Supp. L explores how  $\mathcal{X}$ -Cluster handles invalid (hallucinated) criteria; *iv)* Supp. M investigates model biases; *v)* Supp. N analyzes computational costs; *vi)* Supp. O studies system sensitivity to different MLLMs and LLMs; *vii)* Supp. K further investigates the impact of multi-granularity clustering; and *viii)* Supp. P explores improvements for handling fine-grained criteria.

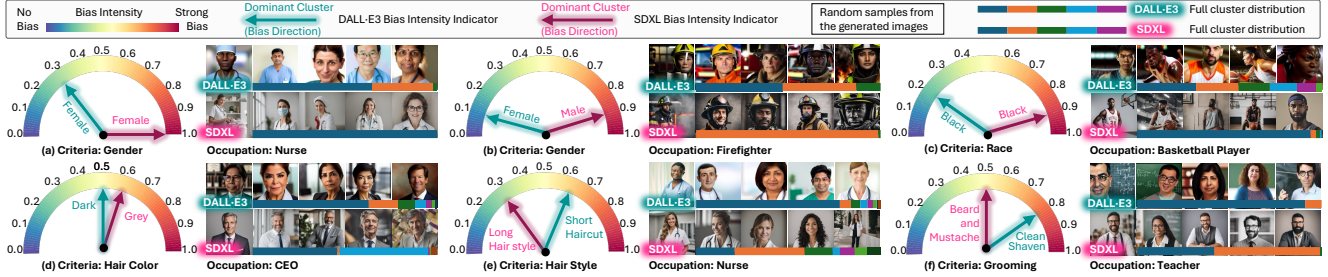


Figure 8. **Bias Discovery in T2I-Generated Images.** Bias intensity, dominant clusters, and example images are shown for few occupations.

## 6. Applications

We apply  $\mathcal{X}$ -Cluster to three applications, demonstrating its ability to generate novel, human-interpretable criteria for real-world analysis. Below, we present results for the first two applications, while additional results for the third application on confirming and mitigating gender bias in 162k CelebA [56] images are provided in Supp. Q.3.

### 6.1. Discovering Biases in T2I Diffusion Models

**Do T2I models exhibit biases beyond the widely studied ones, such as gender and racial stereotypes?** [65, 67] To investigate this, we selected *nine* occupations (e.g., Nurse, CEO) from prior studies [4, 6] and generated 100 images per occupation using the prompt “A portrait photo of a <OCCUPATION>” with DALL-E3 [3] and SDXL [76], resulting in 1.8k images. Applying  $\mathcal{X}$ -Cluster, we automatically identified 10 grouping criteria (bias dimensions) and their distributions for each occupation. To quantify bias, we measured the normalized entropy of each distribution [19] as bias intensity and identified the dominant cluster (the largest group) as the potential bias direction. We conducted a user study with 54 participants to validate our findings.  $\mathcal{X}$ -Cluster’s predicted bias intensity closely matched human ratings with an Absolute Mean Error of 0.1396 (0–1 scale) and aligned with human-identified bias directions 72.3% of the time. User study details are provided in Supp. Q.1.

**Findings:** As shown in Fig. 8, our method identifies both well-known and novel biases in occupational images without relying on predefined categories. For instance, Fig. 8(a–c) reveals strong gender and racial imbalances in SDXL-generated images for roles like Nurse, Firefighter, and Basketball Player, exceeding official statistics [89]. In contrast, DALL-E3 exhibits improved bias mitigation, likely due to its built-in “guardrails” [69]. More notably, Fig. 8(d–f) highlights previously unrecognized bias dimensions. For example, SDXL strongly associates CEOs with “Grey” hair, while DALL-E3 favors “Dark” hair. Additionally, DALL-E3 shows stronger biases in Hair style and Grooming for occupations like Nurse (Fig. 8(e)) and Teacher (Fig. 8(f)). These findings suggest that while industrial T2I models with guardrails may address well-known biases, they may still overlook emerging or less-discussed

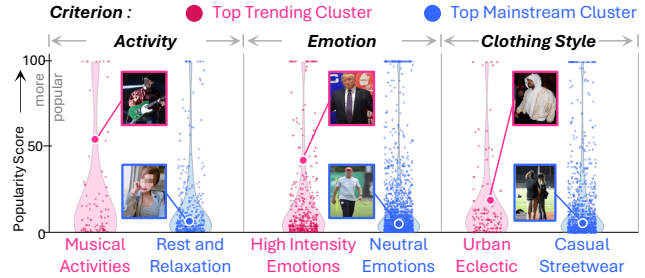


Figure 9. **Social media image popularity analysis.** We show the popularity score distributions for **Top Trending** (have *highest average popularity score*) and **Top Mainstream** (contain *most images*) clusters, discovered by  $\mathcal{X}$ -Cluster across three criteria.

ones, underscoring the need for broader bias analysis. For additional findings and experimental details, see Supp. Q.1.

### 6.2. Analyzing Social Media Image Popularity

**What makes a photo popular?** To explore this, we apply  $\mathcal{X}$ -Cluster to 4.1k Flickr photos from the SPID dataset [72], where popularity is measured by image view count.  $\mathcal{X}$ -Cluster discovered 10 grouping criteria and organizes photos into semantic clusters under each. Using the grouping results, Fig. 9 compares the sample popularity distributions of the **Top Trending** and the **Top Mainstream** clusters across three criteria.

**Findings:** As shown in Fig. 9, combining  $\mathcal{X}$ -Cluster’s grouping with popularity scores provides a direct interpretation of the visual elements that drive trends versus those that define widely uploaded images. Interestingly, we find that trending elements often contrast with mainstream ones, such as “Musical activities” vs. “Rest and relaxation” or “High-intensity expressions” vs. “Neutral emotion”. These results suggest that attention-grabbing visuals stand out due to novelty or intensity, especially in today’s short attention span era [24, 59], underscoring  $\mathcal{X}$ -Cluster as a powerful tool for deep dataset analysis and understanding social behavior. For full findings and additional analysis, see Supp. Q.2.

## 7. Conclusion

We introduce the OpenSMC task and propose  $\mathcal{X}$ -Cluster, a system that discovers interpretable grouping criteria and substructures in image collections, effectively extracting valuable insights across six datasets and three applications.

## Acknowledgments

This work was supported by the EU Horizon projects ELIAS (No. 101120237) and ELLIOT (No. 101214398). We greatly acknowledge CINECA and the ISCR initiative for providing high-performance computing resources. We also extend our gratitude to Feng Xue for his valuable suggestions on plot creation. M.L. warmly thanks Margherita Potrich for her unwavering support.

## References

- [1] Josh Achiam, Steven Adler, Sandhini Agarwal, Lama Ahmad, Ilge Akkaya, Florencia Leoni Aleman, Diogo Almeida, Janko Altenschmidt, Sam Altman, Shyamal Anadkat, et al. Gpt-4 technical report. *arXiv:2303.08774*, 2023. 3, 2, 9, 18, 27
- [2] Ewa Andrejczuk, Julian Martin Eisenschlos, Francesco Piccinno, Syrine Krichene, and Yasemin Altun. Table-to-text generation and pre-training with tab5. In *Findings of EMNLP*, 2022. 27
- [3] James Betker, Gabriel Goh, Li Jing, Tim Brooks, Jianfeng Wang, Linjie Li, Long Ouyang, Juntang Zhuang, Joyce Lee, Yufei Guo, et al. Improving image generation with better captions. *Computer Science*, 2(3):8, 2023. 2, 8, 23
- [4] Federico Bianchi, Pratyusha Kalluri, Esin Durmus, Faisal Ladhak, Myra Cheng, Debora Nozza, Tatsunori Hashimoto, Dan Jurafsky, James Zou, and Aylin Caliskan. Easily accessible text-to-image generation amplifies demographic stereotypes at large scale. In *Proceedings of the 2023 ACM Conference on Fairness, Accountability, and Transparency*, 2023. 1, 8, 2, 23
- [5] David M Blei, Andrew Y Ng, and Michael I Jordan. Latent dirichlet allocation. *Journal of machine Learning research*, 2003. 3, 2
- [6] Tolga Bolukbasi, Kai-Wei Chang, James Y Zou, Venkatesh Saligrama, and Adam T Kalai. Man is to computer programmer as woman is to homemaker? debiasing word embeddings. In *NeurIPS*, 2016. 8, 2, 23
- [7] Rishi Bommasani, Drew A. Hudson, Ehsan Adeli, Russ Altman, Simran Arora, Sydney von Arx, Michael S. Bernstein, Jeannette Bohg, Antoine Bosselut, Emma Brunskill, Erik Brynjolfsson, S. Buch, Dallas Card, Rodrigo Castellon, Niladri S. Chatterji, Annie S. Chen, Kathleen A. Creel, Jared Davis, Dora Demszky, Chris Donahue, Moussa Koulako Bala Doumbouya, Esin Durmus, Stefano Ermon, John Etchemendy, Kawin Ethayarajh, Li Fei-Fei, Chelsea Finn, Trevor Gale, Lauren Gillespie, Karan Goel, Noah D. Goodman, Shelby Grossman, Neel Guha, Tatsunori Hashimoto, Peter Henderson, John Hewitt, Daniel E. Ho, Jenny Hong, Kyle Hsu, Jing Huang, Thomas F. Icard, Saahil Jain, Dan Jurafsky, Pratyusha Kalluri, Siddharth Karamcheti, Geoff Keeling, Fereshte Khani, O. Khattab, Pang Wei Koh, Mark S. Krass, Ranjay Krishna, Rohith Kudithipudi, Ananya Kumar, Faisal Ladhak, Mina Lee, Tony Lee, Jure Leskovec, Isabelle Levent, Xiang Lisa Li, Xuechen Li, Tengyu Ma, Ali Malik, Christopher D. Manning, Suvir Mirchandani, Eric Mitchell, Zanele Munyikwa, Suraj Nair, Avaniika Narayan, Deepak Narayanan, Benjamin Newman, Allen Nie, Juan Carlos Niebles, Hamed Nilforoshan, Julian Nyarko, Giray Ogut, Laurel J. Orr, Isabel Papadimitriou, Joon Sung Park, Chris Piech, Eva Portelance, Christopher Potts, Aditi Raghunathan, Robert Reich, Hongyu Ren, Frieda Rong, Yusuf H. Roohani, Camilo Ruiz, Jack Ryan, Christopher R’e, Dorsa Sadigh, Shiori Sagawa, Keshav Santhanam, Andy Shih, Krishna Parasuram Srinivasan, Alex Tamkin, Rohan Taori, Armin W. Thomas, Florian Tramèr, Rose E. Wang, William Wang, Bohan Wu, Jiajun Wu, Yuhuai Wu, Sang Michael Xie, Michihiro Yasunaga, Jiaxuan You, Matei A. Zaharia, Michael Zhang, Tianyi Zhang, Xikun Zhang, Yuhui Zhang, Lucia Zheng, Kaitlyn Zhou, and Percy Liang. On the opportunities and risks of foundation models. *arXiv:2108.07258*, 2021. 14
- [8] Lukas Bossard, Matthieu Guillaumin, and Luc Van Gool. Food-101—mining discriminative components with random forests. In *ECCV*, 2014. 3, 2
- [9] Tom Brown, Benjamin Mann, Nick Ryder, Melanie Subbiah, Jared D Kaplan, Prafulla Dhariwal, Arvind Neelakantan, Pranav Shyam, Girish Sastry, Amanda Askell, et al. Language models are few-shot learners. In *NeurIPS*, 2020. 2
- [10] Leonardo Bruni, Chiara Francalanci, and Paolo Giacomazzi. The role of multimedia content in determining the virality of social media information. *Information*, 2012. 26
- [11] Mathilde Caron, Piotr Bojanowski, Armand Joulin, and Matthijs Douze. Deep clustering for unsupervised learning of visual features. In *ECCV*, 2018. 2, 27
- [12] Mathilde Caron, Ishan Misra, Julien Mairal, Priya Goyal, Piotr Bojanowski, and Armand Joulin. Unsupervised learning of visual features by contrasting cluster assignments. In *NeurIPS*, 2020. 2
- [13] Zhangtao Cheng, Jienan Zhang, Xovee Xu, Goce Trajcevski, Ting Zhong, and Fan Zhou. Retrieval-augmented hypergraph for multimodal social media popularity prediction. In *KDD*, 2024. 1, 24
- [14] Wei-Lin Chiang, Zhuohan Li, Zi Lin, Ying Sheng, Zhanghao Wu, Hao Zhang, Lianmin Zheng, Siyuan Zhuang, Yonghao Zhuang, Joseph E. Gonzalez, Ion Stoica, and Eric P. Xing. Vicuna: An open-source chatbot impressing gpt-4 with 90%\* chatgpt quality, 2023. 2
- [15] Gabriela Csurka, Tyler L Hayes, Diane Larlus, and Riccardo Volpi. What could go wrong? discovering and describing failure modes in computer vision. In *ECCV Workshop*, 2024. 5
- [16] DeepLearning.AI. ChatGPT Prompt Engineering for Developers - DeepLearning.AI, 2024. 27
- [17] Boyang Deng, Songyou Peng, Kyle Genova, Gordon Wetzstein, Noah Snively, Leonidas Guibas, and Thomas Funkhouser. Visual chronicles: Using multimodal llms to analyze massive collections of images. In *arXiv:2504.08727*, 2025. 3
- [18] Jia Deng, Wei Dong, Richard Socher, Li-Jia Li, Kai Li, and Li Fei-Fei. Imagenet: A large-scale hierarchical image database. In *CVPR*, 2009. 26

- [19] Moreno D’Inca, Elia Peruzzo, Massimiliano Mancini, DeJia Xu, Vidit Goel, Xingqian Xu, Zhangyang Wang, Humphrey Shi, and Nicu Sebe. Openbias: Open-set bias detection in text-to-image generative models. In *CVPR*, 2024. 8, 23
- [20] Lisa Dunlap, Yuhui Zhang, Xiaohan Wang, Ruiqi Zhong, Trevor Darrell, Jacob Steinhardt, Joseph E Gonzalez, and Serena Yeung-Levy. Describing differences in image sets with natural language. In *CVPR*, 2024. 2
- [21] Lisa Dunlap, Joseph E Gonzalez, Trevor Darrell, Fabian Caba Heilbron, Josef Sivic, and Bryan Russell. Discovering divergent representations between text-to-image models. In *ICCV*, 2025. 3
- [22] Anton Eklund and Mona Forsman. Topic modeling by clustering language model embeddings: Human validation on an industry dataset. In *EMNLP: Industry Track*, 2022. 3, 2, 27
- [23] Vladimir Estivill-Castro. Why so many clustering algorithms: a position paper. *ACM SIGKDD explorations newsletter*, 2002. 27
- [24] Zahra Farid. Why are social media images important?, 2024. 8
- [25] Yunhao Ge, Xiaohui Zeng, Jacob Samuel Huffman, Tsung-Yi Lin, Ming-Yu Liu, and Yin Cui. Visual fact checker: Enabling high-fidelity detailed caption generation. In *CVPR*, 2024. 14, 27
- [26] Robert Geirhos, Jörn-Henrik Jacobsen, Claudio Michaelis, Richard Zemel, Wieland Brendel, Matthias Bethge, and Felix A Wichmann. Shortcut learning in deep neural networks. *Nature Machine Intelligence*, 2020. 26
- [27] Leander Girkbach, Stephan Alaniz, Genevieve Smith, and Zeynep Akata. A large scale analysis of gender biases in text-to-image generative models. *arXiv:2503.23398*, 2025. 3
- [28] Aryaman Gupta, Yusuf Umüt Ciftci, and Somil Bansal. From perception logs to failure modes: Language-driven semantic clustering of failures for robot safety. *arXiv:2506.06570*, 2025. 3
- [29] Laura Gustafson, Chloe Rolland, Nikhila Ravi, Quentin Duval, Aaron Adcock, Cheng-Yang Fu, Melissa Hall, and Candace Ross. Facet: Fairness in computer vision evaluation benchmark. In *ICCV*, 2023. 15
- [30] Kai Han, Sylvestre-Alvise Rebuffi, Sebastien Ehrhardt, Andrea Vedaldi, and Andrew Zisserman. Autonovel: Automatically discovering and learning novel visual categories. *IEEE TPAMI*, 2021. 5, 3
- [31] Kaiming He, Xiangyu Zhang, Shaoqing Ren, and Jian Sun. Deep residual learning for image recognition. In *CVPR*, 2016. 26
- [32] Xiangteng He and Yuxin Peng. Fine-grained image classification via combining vision and language. In *CVPR*, 2017. 20
- [33] Xin He, Longhui Wei, Lingxi Xie, and Qi Tian. Incorporating visual experts to resolve the information loss in multimodal large language models. *arXiv:2401.03105*, 2024. 11
- [34] Juhua Hu and Jian Pei. Subspace multi-clustering: a review. *Knowledge and information systems*, 2018. 2
- [35] Albert Q Jiang, Alexandre Sablayrolles, Arthur Mensch, Chris Bamford, Devendra Singh Chaplot, Diego de las Casas, Florian Bressand, Gianna Lengyel, Guillaume Lample, Lucile Saulnier, et al. Mistral 7b. *arXiv:2310.06825*, 2023. 2
- [36] Kaggle. Cards Image Dataset-Classification, 2022. 3
- [37] Shyamgopal Karthik, Karsten Roth, Massimiliano Mancini, and Zeynep Akata. Vision-by-language for training-free compositional image retrieval. In *ICLR*, 2024. 2
- [38] Aditya Khosla, Nityananda Jayadevaprakash, Bangpeng Yao, and Fei-Fei Li. Novel dataset for fine-grained image categorization: Stanford dogs. In *CVPR Workshop*, 2011. 21
- [39] Younghyun Kim, Sangwoo Mo, Minkyu Kim, Kyungmin Lee, Jaeho Lee, and Jinwoo Shin. Discovering and mitigating visual biases through keyword explanation. In *CVPR*, 2024. 26
- [40] Takeshi Kojima, Shixiang Shane Gu, Machel Reid, Yutaka Matsuo, and Yusuke Iwasawa. Large language models are zero-shot reasoners. In *NeurIPS*, 2022. 27
- [41] Harold W Kuhn. The hungarian method for the assignment problem. *Naval research logistics quarterly*, 1955. 5, 3
- [42] Sehyun Kwon, Jaeseung Park, Minkyu Kim, Jaewoong Cho, Ernest K Ryu, and Kangwook Lee. Image clustering conditioned on text criteria. In *ICLR*, 2024. 3, 6, 7, 2, 9, 15
- [43] Feng Li, Renrui Zhang, Hao Zhang, Yuanhan Zhang, Bo Li, Wei Li, Zejun MA, and Chunyuan Li. LLaVA-neXT-interleave: Tackling multi-image, video, and 3d in large multimodal models. In *ICLR*, 2025. 2, 5, 4
- [44] Junnan Li, Dongxu Li, Silvio Savarese, and Steven Hoi. Blip-2: Bootstrapping language-image pre-training with frozen image encoders and large language models. In *ICML*, 2023. 2, 5, 7
- [45] Kenneth Li, Aspen K Hopkins, David Bau, Fernanda Viégas, Hanspeter Pfister, and Martin Wattenberg. Emergent world representations: Exploring a sequence model trained on a synthetic task. In *ICLR*, 2023. 6
- [46] Yunfan Li, Peng Hu, Dezhong Peng, Jiancheng Lv, Jianping Fan, and Xi Peng. Image clustering with external guidance. In *ICML*, 2024. 27
- [47] Tsung-Yi Lin, Michael Maire, Serge Belongie, James Hays, Pietro Perona, Deva Ramanan, Piotr Dollár, and C Lawrence Zitnick. Microsoft coco: Common objects in context. In *ECCV*, 2014. 3, 2
- [48] Evan Z Liu, Behzad Haghgoo, Annie S Chen, Aditi Raghunathan, Pang Wei Koh, Shiori Sagawa, Percy Liang, and Chelsea Finn. Just train twice: Improving group robustness without training group information. In *ICML*, 2021. 26
- [49] Haotian Liu, Chunyuan Li, Yuheng Li, Bo Li, Yuanhan Zhang, Sheng Shen, and Yong Jae Lee. Llava-next: Improved reasoning, ocr, and world knowledge, 2024. 2, 4, 5, 6, 7, 9, 15, 18, 27
- [50] Haotian Liu, Chunyuan Li, Qingyang Wu, and Yong Jae Lee. Visual instruction tuning. In *NeurIPS*, 2024. 3, 2, 9, 27

- [51] Hanchao Liu, Wenyuan Xue, Yifei Chen, Dapeng Chen, Xiutian Zhao, Ke Wang, Liping Hou, Rongjun Li, and Wei Peng. A survey on hallucination in large vision-language models. *arXiv:2402.00253*, 2024. 11
- [52] Mingxuan Liu, Tyler L Hayes, Elisa Ricci, Gabriela Csurka, and Riccardo Volpi. Shine: Semantic hierarchy nexus for open-vocabulary object detection. In *CVPR*, 2024. 5, 7
- [53] Mingxuan Liu, Subhankar Roy, Wenjing Li, Zhun Zhong, Nicu Sebe, and Elisa Ricci. Democratizing fine-grained visual recognition with large language models. In *ICLR*, 2024. 5, 2, 11, 21, 23, 27
- [54] Mingxuan Liu, Tyler L Hayes, Massimiliano Mancini, Elisa Ricci, Riccardo Volpi, and Gabriela Csurka. Test-time vocabulary adaptation for language-driven object detection. In *ICIP*, 2025. 7
- [55] Yikun Liu, Jiangchao Yao, Ya Zhang, Yanfeng Wang, and Weidi Xie. Zero-shot composed text-image retrieval. *arXiv:2306.07272*, 2023. 2
- [56] Ziwei Liu, Ping Luo, Xiaogang Wang, and Xiaoou Tang. Deep learning face attributes in the wild. In *ICCV*, 2015. 8, 2, 26
- [57] Tiange Luo, Chris Rockwell, Honglak Lee, and Justin Johnson. Scalable 3d captioning with pretrained models. In *NeurIPS*, 2024. 27
- [58] Yulin Luo, Ruichuan An, Bocheng Zou, Yiming Tang, Jiaming Liu, and Shanghang Zhang. Llm as dataset analyst: Subpopulation structure discovery with large language model. In *ECCV*, 2024. 3, 7, 9
- [59] Kevin McSpadden. You now have a shorter attention span than a goldfish. *Time Magazine*, 14, 2015. 8
- [60] Meta. Introducing Meta Llama 3: The most capable openly available LLM to date, 2024. 2, 18, 27
- [61] Meta. Introducing Llama 3.1: Our most capable models to date, 2024. 2, 4, 5, 6, 7, 15, 18, 27
- [62] Ioannis Maniadis Metaxas, Georgios Tzimiropoulos, and Ioannis Patras. Divclust: Controlling diversity in deep clustering. In *CVPR*, 2023. 2
- [63] George A Miller. Wordnet: a lexical database for english. *Communications of the ACM*, 1995. 4, 6, 7
- [64] Horea Muresan and Mihai Oltean. Fruit recognition from images using deep learning. *Acta Universitatis Sapientiae, Informatica*, 2018. 3, 14
- [65] Ranjita Naik and Besmira Nushi. Social biases through the text-to-image generation lens. In *AAAI/ACM on AI, Ethics, and Society*, 2023. 8
- [66] Nishanth Nakshatri, Siyi Liu, Sihao Chen, Dan Roth, Dan Goldwasser, and Daniel Hopkins. Using llm for improving key event discovery: Temporal-guided news stream clustering with event summaries. In *Findings of EMNLP*, 2023. 3
- [67] Leonardo Nicoletti and Bass. Humans are biased. Generative AI is even worse, 2023. 8
- [68] OpenAI. ChatGPT: A Large-Scale GPT-3.5-Based Model, 2022. 27
- [69] OpenAI. DALL-E 2 pre-training mitigations, 2022. 8, 24
- [70] OpenAI. Hello GPT-4o, 2024. 2, 4, 18
- [71] Maxime Oquab, Timothée Darcet, Théo Moutakanni, Huy V. Vo, Marc Szafraniec, Vasil Khalidov, Pierre Fernandez, Daniel HAZIZA, Francisco Massa, Alaaeldin El-Nouby, Mido Assran, Nicolas Ballas, Wojciech Galuba, Russell Howes, Po-Yao Huang, Shang-Wen Li, Ishan Misra, Michael Rabbat, Vasu Sharma, Gabriel Synnaeve, Hu Xu, Herve Jegou, Julien Mairal, Patrick Labatut, Armand Joulin, and Piotr Bojanowski. DINOv2: Learning robust visual features without supervision. *TMLR*, 2024. 6
- [72] Alessandro Ortis, Giovanni Maria Farinella, and Sebastiano Battiato. Prediction of social image popularity dynamics. In *ICIAP*, 2019. 8, 24
- [73] Long Ouyang, Jeffrey Wu, Xu Jiang, Diogo Almeida, Carroll Wainwright, Pamela Mishkin, Chong Zhang, Sandhini Agarwal, Katarina Slama, Alex Ray, et al. Training language models to follow instructions with human feedback. In *NeurIPS*, 2022. 2
- [74] Jerry K Palmer and Jonathan S Gore. A theory of contrast effects in performance appraisal and social cognitive judgments. *Psychological Studies*, 2014. 26
- [75] Zhiliang Peng, Wenhui Wang, Li Dong, Yaru Hao, Shaohan Huang, Shuming Ma, Qixiang Ye, and Furu Wei. Grounding multimodal large language models to the world. In *ICLR*, 2024. 2
- [76] Dustin Podell, Zion English, Kyle Lacey, Andreas Blattmann, Tim Dockhorn, Jonas Müller, Joe Penna, and Robin Rombach. Sdxl: Improving latent diffusion models for high-resolution image synthesis. In *ICLR*, 2024. 8, 23
- [77] Joseph R Priestler, Utpal M Dholakia, and Monique A Fleming. When and why the background contrast effect emerges: thought engenders meaning by influencing the perception of applicability. *Journal of Consumer Research*, 2004. 26
- [78] ZiJie Qi and Ian Davidson. A principled and flexible framework for finding alternative clusterings. In *SIGKDD*, 2009. 2
- [79] Alec Radford, Jong Wook Kim, Chris Hallacy, Aditya Ramesh, Gabriel Goh, Sandhini Agarwal, Girish Sastry, Amanda Askell, Pamela Mishkin, Jack Clark, et al. Learning transferable visual models from natural language supervision. In *ICML*, 2021. 4, 5, 2, 6, 23
- [80] Alec Radford, Jong Wook Kim, Tao Xu, Greg Brockman, Christine McLeavey, and Ilya Sutskever. Robust speech recognition via large-scale weak supervision. In *ICML*, 2023. 27
- [81] Yazhou Ren, Jingyu Pu, Zhimeng Yang, Jie Xu, Guofeng Li, Xiaorong Pu, S Yu Philip, and Lifang He. Deep clustering: A comprehensive survey. *IEEE Transactions on Neural Networks and Learning Systems*, 2024. 2
- [82] Sebastian Ruder. An overview of gradient descent optimization algorithms. *arXiv:1609.04747*, 2016. 26
- [83] Shiori Sagawa, Pang Wei Koh, Tatsunori B Hashimoto, and Percy Liang. Distributionally robust neural networks for group shifts: On the importance of regularization for worst-case generalization. In *ICLR*, 2020. 22, 26
- [84] Zhenwei Shao, Zhou Yu, Meng Wang, and Jun Yu. Prompting large language models with answer heuristics for knowledge-based visual question answering. In *CVPR*, 2023. 2

- [85] Robyn Speer, Joshua Chin, and Catherine Havasi. Conceptnet 5.5: An open multilingual graph of general knowledge. In *AAAI*, 2017. 7
- [86] Winnie Street, John Oliver Siy, Geoff Keeling, Adrien Baranes, Benjamin Barnett, Michael McKibben, Tatenda Kanyere, Alison Lentz, Robin IM Dunbar, et al. Llms achieve adult human performance on higher-order theory of mind tasks. *arXiv:2405.18870*, 2024. 19
- [87] Sindhu Tipirneni, Ravinarayana Adkathimar, Nurendra Choudhary, Gaurush Hiranandani, Rana Ali Amjad, Vasillis N Ioannidis, Changhe Yuan, and Chandan K Reddy. Context-aware clustering using large language models. *arXiv:2405.00988*, 2024. 3
- [88] Hugo Touvron, Thibaut Lavril, Gautier Izacard, Xavier Martinet, Marie-Anne Lachaux, Timothée Lacroix, Baptiste Rozière, Naman Goyal, Eric Hambro, Faisal Azhar, et al. Llama: Open and efficient foundation language models. *arXiv:2302.13971*, 2023. 2, 27
- [89] U.S. Bureau of Labor Statistics. Employed persons by detailed occupation, sex, race, and Hispanic or Latino ethnicity — bls.gov, 2021. [Accessed 26-Oct-2022]. 8
- [90] Wouter Van Gansbeke, Simon Vandenhende, Stamatios Georgoulis, Marc Proesmans, and Luc Van Gool. Scan: Learning to classify images without labels. In *ECCV*, 2020. 2, 27
- [91] Sagar Vaze, Kai Han, Andrea Vedaldi, and Andrew Zisserman. Generalized category discovery. In *CVPR*, 2022. 5, 3
- [92] Sagar Vaze, Andrea Vedaldi, and Andrew Zisserman. No representation rules them all in category discovery. In *NeurIPS*, 2024. 3
- [93] Andrea Vedaldi, Siddharth Mahendran, Stavros Tsogkas, Subhransu Maji, Ross Girshick, Juho Kannala, Esa Rahtu, Iasonas Kokkinos, Matthew B Blaschko, David Weiss, et al. Understanding objects in detail with fine-grained attributes. In *CVPR*, 2014. 20
- [94] Vijay Viswanathan, Kiril Gashteovski, Kiril Gashteovski, Carolin Lawrence, Tongshuang Wu, and Graham Neubig. Large language models enable few-shot clustering. *TACL*, 2024. 3
- [95] Catherine Wah, Steve Branson, Peter Welinder, Pietro Perona, and Serge Belongie. The caltech-ucsd birds-200-2011 dataset. *California Institute of Technology*, 2011. 21
- [96] Chao Wang, Hehe Fan, Ruijie Quan, and Yi Yang. Protchatgpt: Towards understanding proteins with large language models. *arXiv:2402.09649*, 2024. 27
- [97] Dingding Wang, Shenghuo Zhu, Tao Li, and Yihong Gong. Multi-document summarization using sentence-based topic models. In *Proceedings of the ACL-IJCNLP conference short papers*, 2009. 3, 2
- [98] Xiaohan Wang, Yuhui Zhang, Orr Zohar, and Serena Yeung-Levy. Videoagent: Long-form video understanding with large language model as agent. In *ECCV*, 2024. 2
- [99] Yuxia Wang, Minghan Wang, Muhammad Arslan Manzoor, Fei Liu, Georgi Georgiev, Rocktim Jyoti Das, and Preslav Nakov. Factuality of large language models: A survey. In *EMNLP*, 2024. 14
- [100] Jason Wei, Xuezhi Wang, Dale Schuurmans, Maarten Bosma, Fei Xia, Ed Chi, Quoc V Le, Denny Zhou, et al. Chain-of-thought prompting elicits reasoning in large language models. In *NeurIPS*, 2022. 2, 27
- [101] Wenhao Wu, Haipeng Luo, Bo Fang, Jingdong Wang, and Wanli Ouyang. Cap4video: What can auxiliary captions do for text-video retrieval? In *CVPR*, 2023. 2
- [102] Le Xue, Manli Shu, Anas Awadalla, Jun Wang, An Yan, Senthil Purushwalkam, Honglu Zhou, Viraj Prabhu, Yutong Dai, Michael S Ryoo, et al. xgen-mm (blip-3): A family of open large multimodal models. *arXiv:2408.08872*, 2024. 2, 18
- [103] Yuzhe Yang, Haoran Zhang, Dina Katabi, and Marzyeh Ghassemi. Change is hard: A closer look at subpopulation shift. In *ICML*, 2023. 26
- [104] Jiawei Yao, Enbei Liu, Maham Rashid, and Juhua Hu. Augdmc: Data augmentation guided deep multiple clustering. *Procedia Computer Science*, 2023. 2
- [105] Jiawei Yao, Qi Qian, and Juhua Hu. Multi-modal proxy learning towards personalized visual multiple clustering. In *CVPR*, 2024. 2, 3, 7, 9
- [106] Jiawei Yao, Qi Qian, and Juhua Hu. Customized multiple clustering via multi-modal subspace proxy learning. In *NeurIPS*, 2025. 2, 3, 6, 7, 9
- [107] Guoxian Yu, Liangrui Ren, Jun Wang, Carlotta Domeniconi, and Xiangliang Zhang. Multiple clusterings: Recent advances and perspectives. *Computer Science Review*, 2024. 2, 3, 27
- [108] Michael Zhang, Nimit S Sohoni, Hongyang R Zhang, Chelsea Finn, and Christopher Ré. Correct-n-contrast: A contrastive approach for improving robustness to spurious correlations. In *ICML*, 2022. 26
- [109] Ning Zhang, Jeff Donahue, Ross Girshick, and Trevor Darrell. Part-based r-cnns for fine-grained category detection. In *ECCV*, 2014. 20
- [110] Yuwei Zhang, Zihan Wang, and Jingbo Shang. Clusterllm: Large language models as a guide for text clustering. In *EMNLP*, 2023. 3
- [111] Ruiqi Zhong, Heng Wang, Dan Klein, and Jacob Steinhardt. Explaining datasets in words: Statistical models with natural language parameters. *NeurIPS*, 2024. 3
- [112] Deyao Zhu, Jun Chen, Kilichbek Haydarov, Xiaoqian Shen, Wenxuan Zhang, and Mohamed Elhoseiny. ChatGPT asks, BLIP-2 answers: Automatic questioning towards enriched visual descriptions. *TMLR*, 2024. 2
- [113] Mingchen Zhuge, Haozhe Liu, Francesco Faccio, Dylan R Ashley, Róbert Csordás, Anand Gopalakrishnan, Abdullah Hamdi, Hasan Abed Al Kader Hammoud, Vincent Herrmann, Kazuki Irie, et al. Mindstorms in natural language-based societies of mind. *arXiv:2305.17066*, 2023. 2

# Organizing Unstructured Image Collections using Natural Language

## Supplementary Material

### Table of Contents

<b>A Reproducibility Statement</b>	<b>1</b>
<b>B Ethics Statement</b>	<b>1</b>
<b>C Additional Related Work</b>	<b>2</b>
<b>D Benchmark Details</b>	<b>3</b>
D.1 Construction of COCO-4c and Food-4c . . . . .	3
D.2 Details on Hard Grouping Criteria Annotation . . . . .	3
<b>E Further Details of Evaluation Protocol</b>	<b>3</b>
<b>F. Further Implementation and Prompt Details</b>	<b>3</b>
F.1. Further Details of Criteria Proposer . . . . .	4
F.2. Further Details of Semantic Grouper . . . . .	7
<b>G Further Details of the Compared Methods</b>	<b>9</b>
<b>H Further Quantitative Experimental Results</b>	<b>11</b>
H.1 Further Results for Criteria Proposer Study . . . . .	11
H.2 Further Results for Semantic Grouper Study . . . . .	11
H.3 Further Comparative Results with TCMC Methods . . . . .	11
H.4 Further Results for Multi-granularity Clustering Study. . . . .	11
<b>I. Qualitative Analysis</b>	<b>11</b>
<b>J. Failure Case Analysis</b>	<b>11</b>
<b>K Further Study on Multi-granularity Clustering</b>	<b>11</b>
<b>L Study on Handling Invalid Criteria</b>	<b>14</b>
<b>M Study on Model Hallucination and Bias</b>	<b>14</b>
<b>N Computational Cost Analysis</b>	<b>15</b>
<b>O System Sensitivity Analysis of Various MLLMs and LLMs</b>	<b>17</b>
<b>P. Study on Fine-grained Image Collections</b>	<b>20</b>
<b>Q Further Details of the Application Study</b>	<b>22</b>
Q.1 Further Details on Discovering Novel Bias in Text-to-Image Diffusion Models . . . . .	23
Q.2 Further Details on Analyzing Social Media Image Popularity . . . . .	24
Q.3 Confirming and Mitigating Dataset Bias . . . . .	26
<b>R Why LLMs Improve Image Clustering?</b>	<b>27</b>
<b>S. Future Work</b>	<b>27</b>

### Overview

This supplementary material provides additional details supporting the implementations, experiments, findings, and discussions in the main paper.

In Supp. A, we provide a reproducibility statement to ensure the transparency and replicability of our work. Additionally, in Supp. B, we present an ethics statement to discuss and address the potential ethical implications and concerns associated with the proposed task and methodology, highlighting possible societal impacts and mitigation strategies.

Supp. C expands on Related Work, covering relevant tasks and methods. Supp. D describes the benchmarks used in our study, including the construction of the newly proposed COCO-4c and Food-4c datasets, as well as the process for creating hard ground-truth criteria for proposer evaluation. Supp. E details the evaluation metrics used in this work.

Supp. F presents the prompts and implementation details for  $\mathcal{X}$ -Cluster, covering both Criteria Proposers and Semantic Groupers. Supp. G provides implementation specifics of the compared methods. Additional quantitative results, including evaluations of the Criteria Proposer, Semantic Grouper, and comparisons with other clustering methods, are in Supp. H.

For qualitative analysis, Supp. I presents further visualizations of predicted clusters, while Supp. J examines failure cases. Supp. K investigates the impact of multi-granularity clustering. Supp. L explores the effect of invalid (hallucinated) criteria on system performance, and Supp. M studies the influence of foundation model hallucinations and biases.

Supp. N analyzes the computational cost and runtime of  $\mathcal{X}$ -Cluster. Supp. O and Supp. P extend our analysis with studies on system sensitivity and fine-grained image collections. Supp. Q provides additional findings, implementation details, and user study results for the three explored applications. Supp. R discusses how LLMs enhance image clustering. Finally, Supp. S outlines potential future research directions for our proposed OpenSMC task.

The Table of Contents on the next page outlines the main topics in this supplementary material, with hyperlinks for direct navigation to each section.

### A. Reproducibility Statement

Upon publication, we will *open-source* all essential resources for reproducing this work. Specifically, we will provide the full code implementation of  $\mathcal{X}$ -Cluster, along with the exact prompts used in each module. Additionally, we will release our two newly proposed benchmarks, COCO-4c and Food-4c, including annotations for each grouping criterion. Lastly, we will provide the code for our evaluation protocol, experiments, and application studies.

### B. Ethics Statement

We do not anticipate any immediate negative societal impacts from our work. However, we encourage future researchers building on

this work to remain vigilant, as we have, about the potential for  $\mathcal{X}$ -Cluster, which integrates LLMs and MLLMs—particularly their human-like reasoning abilities—to be used both for good and for harm.

The motivation behind our studies on biases in existing datasets and text-to-image (T2I) generative model outputs is to *reveal and address* these biases that objectively exist in the datasets and models. We emphasize that our aim is to *study and mitigate these issues*, and in doing so, we *do not create* any new biases or disturbing content. Specifically, in Sec. 6, we use well-established benchmarks, such as CelebA [56], for our study of dataset bias, and for bias discovery in T2I generative models, we select occupation-related subjects known to be associated with biases from prior studies [4, 6]. However, we acknowledge that our methodology and findings could potentially be misused by malicious actors to promote harmful narratives or discrimination against certain groups. We strongly oppose any such misuse or misrepresentation of our work. Our research is conducted with the aim of advancing technology while prioritizing public welfare and well-being.

For the creation of our two new benchmarks, COCO-4c and Food-4c, we sourced images exclusively from the COCO-val-2017 [47] and Food-101 [8] datasets, strictly adhering to their licensing agreements. Additionally, we utilized voluntary human annotators for proposing valid grouping criteria and creating annotations along these criteria, rather than employing annotators from crowdsourcing platforms. This decision was made to ensure sustainability, fair compensation, and high-quality work, as well as to safeguard the psychological well-being of participants. Similarly, for our user study on T2I model bias evaluation, we recruited voluntary participants via questionnaires to collect human evaluation results. The user study was conducted entirely anonymously, with participants providing informed consent. Our project, including data annotation and the user study involving human subjects, was approved by the Ethical Review Board of our university.

Lastly, we emphasize that our proposed framework,  $\mathcal{X}$ -Cluster, relies on open-source LLMs and MLLMs, allowing full deployment on local machines. We refrain from using APIs from industrial LLMs or MLLMs, both to ensure reproducibility and to protect data privacy.

## C. Additional Related Work

**Topic Discovery.** The setting of open-ended semantic multiple clustering (OpenSMC) is also related to the field of Topic Discovery [5, 22, 97] in natural language processing, which aims to identify textual themes from large *text corpora* (e.g., documents). Our work shares motivational similarities with topic discovery because both tasks seek to find common, thematic concepts from large volumes of data. In contrast, our work focuses on discovering thematic criteria from large *visual content*. However, indeed, the core challenges of OpenSMC and topic discovery are highly similar: they both require systems that can concurrently reason over large volumes of data. Nevertheless, OpenSMC is an even more challenging task than topic discovery for two reasons: *i*) semantics are not explicitly expressed in images, whereas they are in text; *ii*) there is currently no vision model that can encode large sets of images and reliably reason over them. Thus, in this work, we translate images to text and use text as a proxy to elicit the

large-scale reasoning capability of large language models [61].

**Multimodal Large Language Model.** Recent advancements in multimodal large language models (MLLMs) have been driven by the availability of large-scale vision-language aligned training data. The typical paradigm [50] involves using a pre-trained large language model (LLM) [14, 35, 60, 61] alongside a pre-trained vision encoder [79]. A projector is learned to align visual inputs with the LLM in the embedding space, which enhances visual understanding by utilizing the reasoning capabilities of LLMs. Several models have achieved significant success in zero-shot image captioning and visual question answering (VQA), including BLIP-2 [44], BLIP-3 [102], Kosmos-2 [75], and the LLaVA series [43, 49, 50]. In our proposed  $\mathcal{X}$ -Cluster framework, we employ MLLM primarily as a *zero-shot* image parser, converting visual information into text and using this text as a proxy to elicit LLMs for reasoning over large image collections and discovering grouping criteria. Additionally, we leverage the multi-image reasoning capability of LLaVA-NeXT-Interleave [43] to establish a baseline image-based proposer for the OpenSMC task, while utilizing BLIP-2 with customized prompts in a VQA style [84, 112] as the image-based grouper to form semantic clusters linked to specific visual content within the images.

**Large Language Model.** In the era of large language models (LLMs) advancement [73], modern LLMs, such as the Llama series [60, 61, 88], Vicuna [14], Mistral-7B [35], and the GPT series [9], have demonstrated remarkable zero-shot capabilities in tasks involving text analysis, completion, generation, and summarization. With advanced prompting techniques like Chain-of-Thought (CoT) [100], the reasoning abilities of LLMs can be further enhanced. In the proposed  $\mathcal{X}$ -Cluster framework, we design CoT prompts (see Supp. F) to harness the text generation and summarization capabilities of Llama-3.1 as a reasoning engine. This aids  $\mathcal{X}$ -Cluster in several key areas: discovering grouping criteria from large sets of image captions, automatically prompting VQA models, generating criterion-specific tags, uncovering cluster semantics, and grouping images based on their captions. Unlike prior works [113] that focus on set difference captioning [20], fine-grained concept discovery [53], or video understanding [98], we leverage LLMs to tackle the challenging open-ended semantic multiple clustering task. While IC|TC [42] also uses the LLM (GPT-4 [1]) for grouping visual data, our proposed  $\mathcal{X}$ -Cluster differs in two key aspects: *i*)  $\mathcal{X}$ -Cluster does *not* require user-defined grouping criteria or the number of clusters, and *ii*)  $\mathcal{X}$ -Cluster provides *multi-granularity* outputs to meet various user preferences.

**Text-Driven Image Retrieval.** Given a query text (e.g., “sofa” or “person wearing a blue T-shirt”), text-driven image retrieval methods [37, 55, 101] aim to find images from an image collection that are relevant to the query. In other words, in the scenario we are considering, given the image collection and a list of text queries, one can organize images according to the text using text-driven image retrieval techniques. In this context, the query can be considered as a sort of “cluster name”. However, this differs significantly from the proposed task of open-ended semantic multiple clustering (OpenSMC), because OpenSMC requires both discovering the textual criteria and the corresponding textual clusters. Thus, without knowing text queries as prior information, text-driven image retrieval methods are not able to accomplish OpenSMC.

## D. Benchmark Details

### D.1. Construction of COCO-4c and Food-4c

To create high-quality benchmarks for COCO-4c and Food-4c, we designed a four-step annotation pipeline:

(1) **Criteria Identification:** We first split COCO-val-2017 [47] and Food-101 [8] images into batches of 100. Each batch was stitched into a  $10 \times 10$  grid to form a single image. These grid images were then distributed to 5 human annotators, who were tasked with identifying grouping criteria. For each dataset, we selected the 4 most frequently occurring criteria, as shown in Tab. 1, to proceed with per-image annotation.

(2) **Label Candidate Generation:** To facilitate the annotation process, we used GPT-4V [1] to generate an initial list of candidate labels for each criterion. Specifically, for each criterion of COCO-4c and Food-4c, GPT-4V was prompted to assign a label that reflected the criterion for each image. This resulted in a list of criterion-specific label candidates for each dataset.

(3) **Image Annotation:** Next, 10 human annotators were tasked with assigning a label from the criterion-specific candidates to each image in COCO-4c and Food-4c for each criterion. The entire annotation process took 25 days to complete.

(4) **Label Merging:** Image annotation is inherently subjective, with annotators potentially assigning different labels for the same criterion. For example, one annotator might label the Mood criterion as “Happy”, while another might label it as “Joyful” or “Delightful”. To resolve such discrepancies, we used majority voting to determine the final label for each image. Specifically, the most frequently assigned label among the 10 annotators was chosen as the final label for each criterion.

Following these steps, we constructed COCO-4c and Food-4c. *Note that we used the official COCO-val-2017 [47] and Food-101 [8] images for our benchmarks and did not collect any new images. We adhered strictly to the licenses of the datasets during their creation.* The exact number of classes is presented in Tab. 1. Additionally, the annotated class names for each criterion of COCO-4c are provided in Tab. 2, and for Food-4c in Tab. 3.

### D.2. Details on Hard Grouping Criteria Annotation

In Tab. 4, we present the additional annotated **Hard** grouping criteria ground truth alongside the **Basic** criteria for each benchmark.

While we have established more rigorous and challenging benchmarks such as COCO-4c and Food-4c, which feature up to *four* distinct grouping criteria, these annotated criteria sets do not encompass all potential grouping criteria within the image collections. This is particularly true for more complex and realistic datasets like COCO-4c, Food-4c, and Action-3c. As a result, the performance differences between different criteria proposers on these basic criteria, as shown in Fig. 4, tend to be close to each other, limiting our understanding of each proposer’s ability to generate comprehensive grouping criteria.

To address this limitation, we employed human annotators to further identify and propose grouping criteria across the six benchmarks, resulting in a more extensive ground-truth set for each benchmark. This provides a better basis for evaluating the comprehensiveness of the different proposers. We refer to this set of larger annotation criteria as the **Hard** criteria, in contrast to the

**Basic** criteria, which involve per-image annotations. Note that for the **Hard** criteria, per-image label annotation is not provided due to the high cost of annotation. The procedure for obtaining the **Hard** grouping criteria is as follows:

(1) **Criteria Discovery:** We divided each dataset into batches of 100 images, displaying each batch in a  $10 \times 10$  grid. Five human annotators were assigned to each batch and instructed to identify as many valid grouping criteria as possible. The proposed criteria from each annotator were then combined to form a comprehensive set of grouping criteria for the dataset.

(2) **Criteria Merging:** After collecting the annotated criteria from all five annotators, we aggregated the criteria and manually cleaned the set by merging semantically similar criteria (*e.g.*, Location and Place) and discarding binary grouping criteria, as the inclusion of binary criteria can result in an unmanageable number of grouping criteria for complex datasets.

By following this process, we developed a more comprehensive grouping criteria set as the **Hard** ground-truth for each benchmark, as shown in Tab. 4. This resulted in sets containing 8 criteria for Fruit-2c, 4 criteria for card, 11 criteria for Action-3c, 7 criteria for Clevr-4c, 17 criteria for COCO-4c, and 11 criteria for Food-4c. These expanded ground-truth sets enable us to more effectively evaluate the capabilities of various criteria discovery methods, providing a clearer understanding of different criteria proposers.

## E. Further Details of Evaluation Protocol

**Further Discussion on Clustering Accuracy (CAcc).** Clustering Accuracy (CAcc) [30] is evaluated by applying the Hungarian algorithm [41] to determine the optimal assignment between the predicted cluster indices and ground-truth labels. As extensively discussed in the GCD [91] literature, if the number of predicted clusters (groups) exceeds the total number of ground-truth classes (groups), the extra clusters (not matched by the Hungarian algorithm) are assigned to a null set, and all instances in those clusters are considered incorrect during evaluation. On the other hand, if the number of predicted clusters is lower than the number of ground-truth classes, the extra classes are assigned to a null set, and all instances with those ground-truth labels are similarly considered incorrect. Thus, CAcc is maximized only when the number of predicted clusters matches the number of ground-truth clusters.

In the Open-ended Semantic Multiple Clustering (OpenSMC) task newly proposed in this work, we do not assume access to the ground-truth number of clusters as prior input. Consequently, our proposed method  $\mathcal{X}$ -Cluster does not rely on the ground-truth number of clusters to achieve an “optimal” CAcc with respect to the testing dataset. All clusters are automatically predicted by the  $\mathcal{X}$ -Cluster system. In stark contrast, in the comparison with criterion-conditioned clustering methods shown in Tab. 2, both IC|TC [42] and MMaP [105] use the ground-truth number of clusters as prior input.

## F. Further Implementation and Prompt Details

In this section, we provide detailed descriptions of the exact prompts used in our framework, along with additional implemen-

Table 1. Summary of number of classes for the basic criteria annotation across the six benchmarks.

Dataset	Number of Images	Basic Criterion	Number of Classes
COCO-4c	5,000	Activity	64
		Location	19
		Mood	20
		Time of Day	6
Food-4c	25,250	Food Type	101
		Cuisine	15
		Course	5
		Diet	4
Action-3c	1,000	Action	40
		Location	10
		Mood	4
Clevr-4c	10,000	Color	10
		Texture	10
		Shape	10
		Count	10
Card-2c	8,029	Rank	14
		Suit	5
Fruit-2c	103	Species	34
		Color	15

Table 2. Full class names for COCO-4c across the four basic criteria.

Criterion	COCO-4c
Activity	“repairing a toilet”, “playing volleyball”, “playing guitar”, “haircutting”, “cutting a cigar”, “kayaking”, “applauding”, “tying a tie”, “playing basketball”, “washing dishes”, “gardening”, “texting messages”, “repairing a car”, “peeing”, “cleaning the floor”, “writing on a book”, “feeding a horse”, “singing”, “baking”, “hiking”, “smoking”, “riding an elephant”, “pouring liquid”, “waving hands”, “swimming”, “meditating”, “fixing a bike”, “cutting vegetables”, “walking a dog”, “reading a book”, “celebrating”, “queuing”, “cutting a cake”, “brushing teeth”, “playing soccer”, “jumping”, “snowboarding”, “playing”, “touching animals”, “pushing a cart”, “watching tv”, “rowing a boat”, “taking photos”, “running”, “flying a kite”, “riding a horse”, “playing video games”, “holding up an umbrella”, “throwing a frisbee”, “lying down”, “riding a bike”, “drinking”, “cooking”, “phoning”, “chatting”, “skiing”, “driving”, “surfing”, “skateboarding”, “playing baseball”, “playing tennis”, “using a computer”, “posing”, “eating”
Location	“amusement or theme park”, “healthcare facility”, “virtual or digital space”, “educational institution”, “industrial area”, “historical landmark”, “public event or gathering”, “store or market”, “underground or enclosed space”, “transportation hub”, “zoo”, “water body”, “office or workplace”, “park or recreational area”, “restaurant or dining area”, “sports facility”, “natural environment”, “urban area or city street”, “residential area”
Mood	“anxious”, “sombre”, “contemplative”, “suspenseful”, “serene”, “nostalgic”, “inspired”, “whimsical”, “romantic”, “mysterious”, “melancholic”, “chaotic”, “humorous”, “vibrant”, “peaceful”, “energetic”, “focused”, “joyful”, “relaxed”, “adventurous”
Time of Day	“evening”, “afternoon”, “night”, “morning”, “indoor lighting”, “midday”

tation details for the proposed Criteria Proposer in Supp. F.1 and the Semantic Grouper in Supp. F.2.

Further, we present a system overview illustrating all three variants of our Criteria Proposer and Semantic Grouper, namely the caption based (main), tag based, and image based versions, in Fig. 1.

### F.1. Further Details of Criteria Proposer

**Image-based Proposer:** In Tab. 5, we present the exact prompt used in the image-based proposer for querying the MLLM LLaVA-NeXT-Interleave-7B [43]. Given a target image set, we first ran-

domly shuffle the images and divide them into disjoint subsets, each containing 64 images. Each subset is then stitched into an  $8 \times 8$  image grid, treated as a single image, and fed into the MLLM. For each subset, the MLLM is prompted to propose 5 distinct grouping criteria for organizing the images within that subset, using the prompt shown in Tab. 5. After iterating through all subsets, we take the union of the criteria proposed for each subset as the discovered criteria for the target image set. Finally, we deduplicate the discovered criteria and accumulate them into the criteria pool.

**Tag-based Proposer:** In Tab. 6, we present the exact prompt

Table 3. Full class names for Food-4c across the four basic criteria.

Criterion	Food-4c
Food Type	“apple pie”, “baby back ribs”, “baklava”, “beef carpaccio”, “beef tartare”, “beet salad”, “beignets”, “bibimbap”, “bread pudding”, “breakfast burrito”, “bruschetta”, “caesar salad”, “cannoli”, “caprese salad”, “carrot cake”, “ceviche”, “cheesecake”, “cheese plate”, “chicken curry”, “chicken quesadilla”, “chicken wings”, “chocolate cake”, “chocolate mousse”, “churros”, “clam chowder”, “club sandwich”, “crab cakes”, “creme brulee”, “croque madame”, “cup cakes”, “deviled eggs”, “donuts”, “dumplings”, “edamame”, “eggs benedict”, “escargots”, “falafel”, “filet mignon”, “fish and chips”, “foie gras”, “french fries”, “french onion soup”, “french toast”, “fried calamari”, “fried rice”, “frozen yogurt”, “garlic bread”, “gnocchi”, “greek salad”, “grilled cheese sandwich”, “grilled salmon”, “guacamole”, “gyoza”, “hamburger”, “hot and sour soup”, “hot dog”, “huevos rancheros”, “hummus”, “ice cream”, “lasagna”, “lobster bisque”, “lobster roll sandwich”, “macaroni and cheese”, “macarons”, “miso soup”, “mussels”, “nachos”, “omelette”, “onion rings”, “oysters”, “pad thai”, “paella”, “pancakes”, “panna cotta”, “peking duck”, “pho”, “pizza”, “pork chop”, “poutine”, “prime rib”, “pulled pork sandwich”, “ramen”, “ravioli”, “red velvet cake”, “risotto”, “samosa”, “sashimi”, “scallops”, “seaweed salad”, “shrimp and grits”, “spaghetti bolognese”, “spaghetti carbonara”, “spring rolls”, “steak”, “strawberry shortcake”, “sushi”, “tacos”, “takoyaki”, “tiramisu”, “tuna tartare”, “waffles”
Cuisine	“japanese”, “indian”, “american”, “greek”, “spanish”, “mexican”, “italian”, “vietnamese”, “canadian”, “korean”, “chinese”, “middle eastern”, “french”, “thai”, “general”
Course	“appetizer”, “main course”, “side dish”, “dessert”, “breakfast”
Diet	“omnivore”, “vegan”, “vegetarian”, “gluten free”

Table 4. Annotated criteria for the six benchmarks. The basic criteria are annotated on per-image level for each benchmark, while the hard criteria (those not in the basic criteria) are further exhaustively annotated by human annotators for further evaluating the performance of the rule proposer in OpenSMC task.

COCO-4c		Food-4c		Action-3c	
Basic criteria Total: 4	Hard criteria Total: 17	Basic criteria Total: 4	Hard criteria Total: 11	Basic criteria Total: 3	Hard criteria Total: 11
Activity Location Mood Time of Day	Activity Location Mood Time of Day Interaction Number of People Present Group Dynamics Clothing Style Occasion or Event Type Photo Style Type of Animal Present Weather Type of Primary Object Continent Age or Age Composition Race or Race Composition Gender or Gender Composition	Food Type Cuisine Course Diet	Food Type Cuisine Course Diet Tableware Type Presentation Style Color Palette Setting/Theme Primary Taste Primary Ingredient Cooking Method	Action Mood Location	Action Mood Location Clothing Style Number of People Present Age or Age Composition Race or Race Composition Occasion or Event Type Group Dynamics Lighting Condition Gender or Gender Composition
Clevr-4c		Card-2c		Fruit-2c	
Basic criteria Total: 4	Hard criteria Total: 7	Basic criteria Total: 2	Hard criteria Total: 4	Basic criteria Total: 2	Hard criteria Total: 8
Color Texture Shape Count	Color Texture Shape Count Spatial Positioning Count of Surface Complexity of Geometry	Rank Suit	Rank Suit Color Illustration Style	Species Color	Species Color Size Seasonality Primary Taste Texture Ripeness Fruit Quantity and Arrangement

Table 5. Prompts for the MLLM in the image-based proposer for criteria proposing.

Prompt purpose	Prompt
System Prompt	You are a helpful AI assistant
Input Explanation	This image contains 64 individual images arranged in 8 columns and 8 rows.
Goal Explanation	I am a machine learning researcher trying to identify all the possible clustering criteria or rules that could be used to group these images so I can better understand my data.
Task Instruction	Your job is to carefully analyze the entire set of the 64 images, and identify five distinct clustering criteria or rules that could be used to cluster or group these images. Please consider different characteristics.
Output Instruction	Please write a list of the 5 identified clustering criteria or rules (separated by bullet points “*”).
Task Reinforcement	Again, I want to identify all the possible clustering criteria or rules that could be used to group these images. List the 5 distinct clustering criteria or rules that you identified from the 64 images. Answer with a list (separated by bullet points “*”). Your response:

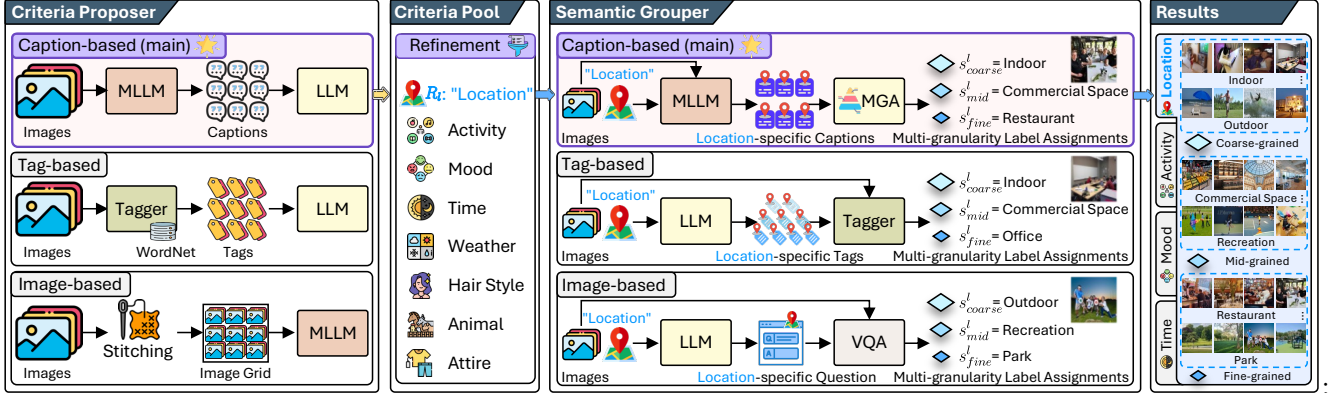


Figure 1. All three variants of the proposed  $\mathcal{X}$ -Cluster framework. We explore different design choices for both the Criteria Proposer (left) and the Semantic Grouper (right), and designate the best-performing Caption-based system (marked with  $\star$ ) as the main  $\mathcal{X}$ -Cluster configuration in our experiments.

Table 6. Prompts for the LLM used in the tag-based proposer for criteria proposing. We embed the exact image captions by replacing the placeholders "{TAGS}" in the prompt.

Prompt purpose	Prompt
System Prompt	You are a helpful assistant.
Input Explanation	The following are the tagging results of a set of images in the format of "Image ID: tag 1, tag 2, ..., tag 10". These assigned tags reflect the visible semantic content of each image:
Tag Embedding	Image 1: "{TAGS}" Image 2: "{TAGS}" ... Image N: "{TAGS}"
Goal Explanation	I am a machine learning researcher trying to figure out the potential clustering or grouping criteria that exist in these images. So I can better understand my data and group them into different clusters based on different criteria.
Task Instruction	Please analyze these images by using their assigned tags. Come up with an array of distinct clustering criteria that exist in this set of images.
Output Instruction	Please write a list of clustering criteria (separated by bullet points "*" ).
Task Reinforcement	Again, I want to figure out what are the potential clustering or grouping criteria that I can use to group these images into different clusters. List an array of clustering or grouping criteria that often exist in this set of images based on the tagging results. Answer with a list (separated by bullet points "*" ). Your response:

used in the tag-based proposer for querying the LLM Llama-3.1-8B [61]. For a given target image set, we first utilize an open-vocabulary tagger, CLIP ViT-L/14 [79], to assign 10 related natural language tags to each image. These tags are selected from the WordNet [63] vocabulary, which contains 118k English synsets, and represent the semantic content of the images. We employ the standard prompt "A photo of {concept}" provided by CLIP for image tagging. Next, we embed the assigned tags into the prompt shown in Tab. 6 to carry the semantics of the entire image set and query the LLM to propose grouping criteria. The criteria proposed by the LLM are then added to the criteria pool. Note that in this case, we embed the tags for the entire dataset into a single prompt for criteria proposal, without reaching the LLM context length limits (e.g., 128k for Llama-3.1-8B) for the datasets used in our experiments. However, for larger datasets, it may be necessary to split the dataset into subsets, prompt the LLM for each subset, and use the union of the proposed criteria as the final output.

**Caption-based Proposer:** We present the prompt used in the

caption-based proposer for the MLLM LLaVA-NeXT-7B [49] in Tab. 7, and the prompt for the LLM Llama-3.1-8B [61] in Tab. 8. Specifically, we first use the MLLM with a general prompt to generate detailed descriptions for each image in the target dataset, effectively translating the visual information into natural language. The generated captions are then *randomly shuffled* and split into disjoint subsets, each containing 400 captions. Next, we embed the captions from each subset into the prompt shown in Tab. 8 and use it to query the LLM to propose grouping criteria for the images represented by the captions. After iterating through all subsets, we take the union of the proposed criteria across subsets as the discovered criteria for the target image set. Finally, we deduplicate these criteria and add them to the criteria pool. Due to the context window limitations of LLMs, embedding all captions into a single prompt is infeasible. To address this, we limit each subset to 400 captions, which results in approximately 115k tokens per subset. This strategy allows us to remain within the context length limits of modern LLMs (e.g., 128k tokens for both Llama-3.1 and

Table 7. Prompts for the MLLM in the caption-based proposer for generating detailed descriptions of the images.

Prompt purpose	Prompt
System Prompt	You are a helpful AI assistant
Task Instruction	Describe the following image in detail.

Table 8. Prompts for the LLM used in the caption-based proposer for criteria proposing. We embed the exact image captions by replacing the placeholders "{CAPTION}" in the prompt.

Prompt purpose	Prompt
System Prompt	You are a helpful assistant.
Input Explanation	The following are the result of captioning a set of images:
Caption Embedding	Image 1: "{CAPTION}" Image 2: "{CAPTION}" ... Image N: "{CAPTION}"
Goal Explanation	I am a machine learning researcher trying to figure out the potential clustering or grouping criteria that exist in these images. So I can better understand my data and group them into different clusters based on different criteria.
Task Instruction	Come up with ten distinct clustering criteria that exist in this set of images.
Output Instruction	Please write a list of clustering criteria (separated by bullet points "**").
Task Reinforcement	Again I want to figure out what are the potential clustering/grouping criteria that I can use to group these images into different clusters. List ten clustering or grouping criteria that often exist in this set of images based on the captioning results. Answer with a list (separated by bullet points "**"). Your response:

GPT-4o) while maximizing the number of samples per query to effectively propose clustering criteria.

**Criteria Pool Refinement:** In Tab. 9, we present the exact prompt used for criteria pool refinement when querying the LLM Llama-3.1-8B [61]. Since the accumulated criteria pool  $\tilde{\mathcal{R}}$  may contain highly similar or noisy clustering criteria, we embed the criteria from the pool into the prompt shown in Tab. 9 and ask the LLM to merge similar criteria and rephrase their names to enhance clarity. This process yields a refined set of grouping criteria, which is then passed to the next stage for image grouping.

## F.2. Further Details of Semantic Grouper

**Image-based Grouper:** In Tab. 10, we present the prompt used to query the LLM Llama-3.1-8B [61] for automatically generating criterion-specific VQA questions for the image-based grouper. The objective at this stage is to condition the VQA model BLIP-2 Flan-T5<sub>XXL</sub> [44] to label each image across three different semantic granularity levels based on a specific criterion. To guide the VQA model effectively, a criterion-specific question is required.

Rather than manually creating these questions, we embed the target criterion into the prompt shown in Tab. 10 and query the LLM to automatically generate high-quality, criterion-specific questions. These questions are then used to direct the VQA model, enabling it to accurately label each image according to the visual content relevant to the target criterion.

**Tag-based Grouper:** We present the prompts used in the tag-based grouper for querying the LLM Llama-3.1-8B. The prompt for generating criterion-specific tags is shown in Tab. 11, while the prompts for generating coarse-grained and fine-grained tags are shown in Tab. 12 and Tab. 13, respectively.

In the tag-based grouper, we begin by embedding the target cri-

terion into the prompt from Tab. 11 to generate criterion-specific tags at a middle granularity. To enhance the diversity and coverage of the tags, we query the LLM 10 times and take the union of the generated tags after deduplication as candidates [54]. Following the SHiNe framework [52], for each middle-grained tag, we further embed it into the prompts from Tab. 12 and Tab. 13 to generate 3 super-categories (coarse-grained) and 10 sub-categories (fine-grained) for each tag.

After generating coarse and fine-grained categories for all middle-grained tags, we take the union of the super-categories as the coarse-grained tag candidates and the union of the sub-categories as the fine-grained tag candidates. Lastly, we use the open-vocabulary tagger CLIP ViT-L/14 to assign the most relevant tags to each image based on cosine similarity, using candidates from each granularity level. After tagging all the images, we group those sharing the same tag into clusters, yielding the clustering result. Note that we do not utilize lexical databases such as WordNet [63] or ConceptNet [85] for tag generation, as they do not support free-form input and may not capture certain discovered criteria.

**Caption-based Grouper:** We first present the MLLM prompt used for LLaVA-NeXT-7B [49] to generate criterion-specific captions in Tab. 14. Following this, we present the LLM Llama-3.1-8B prompts used in the caption-based grouper for the *Initial Naming* step in Tab. 15, the *Multi-granularity Cluster Refinement* step in Tab. 16, and the *Final Assignment* step in Tab. 17.

Specifically, we begin by generating criterion-specific captions for each image using LLaVA-NeXT-7B with the prompt shown in Tab. 14. For each image, we then embed its criterion-specific caption and the relevant criterion into the LLM prompt shown in Tab. 15, querying the LLM to assign an initial name based on the target criterion. Once the initial names for all images in the dataset

Table 9. **Prompts for the LLM used in Proposed Criteria Refinement step** We embed the exact initially discovered criteria by replacing the placeholders "{CRITERION}" in the prompt.

Prompt purpose	Prompt
System Prompt	You are a helpful assistant.
Input Explanation	I am a machine learning researcher working with a set of images. I aim to cluster this set of images based on the various clustering criteria present within them. Below is a preliminary list of clustering criteria that I've discovered to group these images:
Criteria Embedding:	* Criterion 1: "{CRITERION}" * Criterion 2: "{CRITERION}" ... * Criterion L: "{CRITERION}"
Goal Explanation	My goal is to refine this list by merging similar criteria and rephrasing them using more precise and informative terms. This will help create a set of distinct, optimized clustering criteria.
Task Instruction	Your task is to first review and understand the initial list of clustering criteria provided. Then, assist me in refining this list by: * Merging similar criteria. * Expressing each criterion more clearly and informatively.
Output Instruction	Please respond with the cleaned and optimized list of clustering criteria, formatted as bullet points (using "*"). Your response:

Table 10. **Prompts for the LLM used in the image-based grouper for automatic criterion-specific VQA question generation.** We embed the exact discovered criterion by replacing the placeholder "{CRITERION}" in the prompt.

Prompt purpose	Prompt
System Prompt	You are a helpful assistant.
Goal Explanation	Hello! I am a machine learning researcher focusing on image categorization based on the aspect of "{CRITERION}" depicted in images.
Task Instruction	Therefore, I need your assistance in designing a prompt for the Visual Question Answering (VQA) model to help it identify the "{CRITERION}" category in a given image at three different granularity. Please help me design and generate this prompt using the following template: "Question: [Generated VQA Prompt Question] Answer (reply with an abstract, a common, and a specific category name, respectively):". The generated prompt should be simple and straightforward.
Output Instruction	Please respond with only the generated prompt using the following format "* Answer *". Your response:

Table 11. **Prompts for the LLM used in the tag-based grouper for generating middle-grained criterion-specific tags.** We embed the exact discovered criterion by replacing the placeholder "{CRITERION}" in the prompt.

Prompt purpose	Prompt
System Prompt	You are a helpful assistant.
Goal Explanation	Hello! I am a machine learning researcher focusing on image categorization of a certain aspect. I'm interested in generating a list of tags specifically for categorizing the types of "{CRITERION}" depicted in images.
Task Instruction	Please provide a list of potential "{CRITERION}" category names. Please generate diverse category names. Do not include too general or specific category names such as "Sports".
Output Instruction	Please respond with the list of category names. Each category should be formatted as follows: "* Category Name". Your response:

Table 12. **Prompts for the LLM used in the tag-based grouper for generating coarse-grained criterion-specific tags.** We embed the exact discovered criterion and middle-grained category by replacing the placeholder "{CRITERION}" and "{MIDDLE-GRAINED CATEGORY NAME}" in the prompt, respectively.

Prompt purpose	Prompt
System Prompt	You are a helpful assistant.
Task Instruction	Generate a list of three more abstract or general "{CRITERION}" super-categories that the following "{CRITERION}" category belongs to and output the list separated by "&" (without numbers): "{MIDDLE-GRAINED CATEGORY NAME}"
Output Instruction	Your response:

Table 13. **Prompts for the LLM used in the tag-based grouper for generating fine-grained criterion-specific tags.** We embed the exact discovered criterion and middle-grained category by replacing the placeholder "{CRITERION}" and "{MIDDLE-GRAINED CATEGORY NAME}" in the prompt, respectively.

Prompt purpose	Prompt
System Prompt	You are a helpful assistant.
Task Instruction	Generate a list of ten more detailed or specific "{CRITERION}" sub-categories of the following "{CRITERION}" category and output the list separated by "&" (without numbers): "{MIDDLE-GRAINED CATEGORY NAME}"
Output Instruction	Your response:

Table 14. **Prompts for the MLLM used in the caption-based grouper for generating criterion-specific captions.** We embed the exact discovered criterion by replacing the placeholder "{CRITERION}" in the prompt.

Prompt purpose	Prompt
System Prompt	You are a helpful AI assistant.
Task Instruction	Analyze the image focusing specifically on the "{CRITERION}". Provide a detailed description of the "{CRITERION}" depicted in the image. Highlight key elements and interactions relevant to the "{CRITERION}" that enhance the understanding of the scene.
Output Instruction	Your response:

Table 15. **Prompts for the LLM used in the caption-based grouper at the Initial Naming step for initially assigning a criterion-based category name to the image based on its criterion-specific caption.** We embed the exact discovered criterion and the corresponding criterion-specific caption by replacing the placeholder "{CRITERION}" and "{CRITERION-SPECIFIC CAPTION}" in the prompt, respectively.

Prompt purpose	Prompt
System Prompt	You are a helpful assistant.
Input Explanation	The following is the description about the "{CRITERION}" of an image:
Caption Embedding	"{CRITERION-SPECIFIC CAPTION}"
Goal Explanation	I am a machine learning researcher trying to assign a label to this image based on what is the "{CRITERION}" depicted in this image.
Task Instruction	Understand the provided description carefully and assign a label to this image based on what is the "{CRITERION}" depicted in this image.
Output Instruction	Please respond in the following format within five words: "*Answer*". Do not talk about the description and do not respond long sentences. The answer should be within five words.
Task Reinforcement	Again, your job is to understand the description and assign a label to this image based on what is the "{CRITERION}" shown in this image. Your response:

are obtained, we embed these names along with the target criterion into the prompt in Tab. 16 to query the LLM for cluster name refinement across three semantic granularity levels: coarse, middle, and fine.

Finally, for each image, we embed the target criterion, its criterion-specific caption, and cluster candidates from each granularity level into the prompt shown in Tab. 17, and use this to query the LLM for final cluster assignment at each granularity level.

## G. Further Details of the Compared Methods

In this section, we provide the implementation details of the compared methods, IC|TC [42] and MMaP [105].

**Implementation details of IC|TC [42]:** In the original implementation of IC|TC, LLaVA-1.5 [50] was used as the MLLM, and GPT-4-2023-03-15-preview [1] as the LLM. However, since the GPT-4-2023-03-15-preview API has been deprecated, we implemented IC|TC using the state-of-the-art MLLM LLaVA-NeXT-7B [49] and the latest version of GPT-turbo-2024-04-09 as

the LLM, while strictly adhering to the original IC|TC prompt design in our experiments to ensure a fair comparison.

**Implementation Details of SSD-LLM [58]:** Following similar setup of IC|TC, we reproduced and compared with SSD-LLM using GPT-turbo-2024-04-09 as the LLM and LLaVA-NeXT-7B as the MLLM. Since SSD-LLM requires a primary class name for each benchmark, we provided the ground-truth primary class in its prompt: "Food" for Food-4c, "Object" for Clevr-4c, "Person" for Action-3c, "Playing card" for Card-2c, and "Fruit" for Fruit-2c. For COCO-4c, which consists of everyday life scenes and lacks a consistent primary class, we used "Object" as a neutral placeholder in SSD-LLM's prompt.

**Implementation details of MMaP and MSub [105, 106]:** We closely followed the training configuration outlined in the original MMaP and MSub paper. Specifically, GPT-turbo-2024-04-09 was used as the LLM to generate reference words for each dataset. We then prompt-tuned CLIP-ViT/B32 using Adam with a momentum of 0.9, training the model for 1,000 epochs for each criterion across all datasets. Hyperparameters were optimized accord-

Table 16. **Prompts for the LLM used in the caption-based grouper at the *Multi-granularity Cluster Generation* step for refining the initially assigned names to a structured three granularity levels.** We embed the exact discovered criterion and the initially assigned name categories by replacing the placeholder "`{CRITERION}`" and "`{MIDDLE-GRAINED CATEGORY NAME}`" in the prompt, respectively.

Prompt purpose	Prompt
System Prompt	You are a helpful assistant.
Input Explanation	The following is an initial list of " <code>{CRITERION}</code> " categories. These categories might not be at the same semantic granularity level. For example, category 1 could be "cutting vegetables", while category 2 is simply "cutting". In this case, category 1 is more specific than category 2.
Category Embedding	* " <code>{MIDDLE-GRAINED CATEGORY NAME}</code> " * " <code>{MIDDLE-GRAINED CATEGORY NAME}</code> " ... * " <code>{MIDDLE-GRAINED CATEGORY NAME}</code> "
Task Instruction	These categories might not be at the same semantic granularity level. For example, category 1 could be "cutting vegetables", while category 2 is simply "cutting". In this case, category 1 is more specific than category 2. Your job is to generate a three-level class hierarchy (class taxonomy, where the first level contains more abstract or general coarse-grained classes, the third level contains more specific fine-grained classes, and the second level contains intermediate mid-grained classes) of " <code>{CRITERION}</code> " based on the provided list of " <code>{CRITERION}</code> " categories. Follow these steps to generate the hierarchy.
Sub-task Instruction	Follow these steps to generate the hierarchy: Step 1 - Understand the provided initial list of " <code>{CRITERION}</code> " categories. The following three-level class hierarchy generation steps are all based on the provided initial list. Step 2 - Generate a list of abstract or general " <code>{CRITERION}</code> " categories as the first level of the class hierarchy, covering all the concepts present in the initial list. Step 3 - Generate a list of middle-grained " <code>{CRITERION}</code> " categories as the second level of the class hierarchy, in which the middle-grained categories are the subcategories of the categories in the first level. The categories in the second-level are more specific than the first level but should still cover and reflect all the concepts present in the initial list. Step 4 - Generate a list of more specific fine-grained " <code>{CRITERION}</code> " categories as the third level of the class hierarchy, in which the categories should reflect more specific " <code>{CRITERION}</code> " concepts that you can infer from the initial list. The categories in the third-level are subcategories of the second-level. Step 5 - Output the generated three-level class hierarchy as a JSON object where the keys are the level numbers and the values are a flat list of generated categories at each level, structured like: { "level 1": ["categories"], "level 2": ["categories"], "level 3": ["categories"] }
Output Instruction	Please only output the JSON object in your response and simply use a flat list to store the generated categories at each level. Your response:

Table 17. **Prompts for the LLM used in the caption-based grouper at the *Final Assignment* step.** We embed the exact discovered criterion and the refined category names from each granularity level, by replacing the placeholder "`{CRITERION}`" and "`{CANDIDATE CATEGORY NAME}`" in the prompt, respectively.

Prompt purpose	Prompt
System Prompt	You are a helpful assistant.
Input Explanation	The following is a detailed description about the " <code>{CRITERION}</code> " of an image.
Caption Embedding	" <code>{CRITERION-SPECIFIC CAPTION}</code> "
Task Instruction	Based on the content and details provided in the description, classify the image into one of the specified " <code>{CRITERION}</code> " categories listed below:
Candidate Category Embedding	" <code>{CRITERION}</code> " categories: * " <code>{CANDIDATE CATEGORY NAME}</code> " * " <code>{CANDIDATE CATEGORY NAME}</code> " ... * " <code>{CANDIDATE CATEGORY NAME}</code> "
Output Instruction	Ensure that your classification adheres to the details mentioned in the image description. Respond with the classification result in the following format: " <code>*category name*</code> ". Your response:

ing to the loss score of MMaP, with the learning rate searched in  $\{0.1, 0.05, 0.01, 0.005, 0.001, 0.0005\}$ , weight decay in  $\{0.0005,$

0.0001, 0.00005, 0.00001, 0},  $\alpha$  and  $\beta$  in {0.0, 0.1, 0.2, ..., 1.0}, and  $\lambda$  fixed at 1 for all experiments. After training, KMeans, with the ground-truth number of clusters, was applied for each criterion and dataset to perform clustering.

## H. Further Quantitative Experimental Results

In this section, we present additional numerical experiment results to supplement the figures in the main paper. In § H.1, we provide supplementary results for the evaluation of the Criteria Proposer in our framework. In § H.2, we present additional results for the evaluation of the Semantic Grouper across various criteria on the six tested benchmarks. Furthermore, we include expanded results comparing our framework to prior criteria-conditioned clustering methods. Lastly, we present detailed results from the ablation study of the multi-granularity refinement component in § H.4.

### H.1. Further Results for Criteria Proposer Study

We provide detailed numerical results corresponding to Fig. 4 in Tab. 18 and Fig. 5 in Tab. 19 for the six tested benchmarks.

Although captions generated by the MLLM may exhibit some information loss (e.g., ignoring small objects or attributes) [33] and hallucinations (e.g., introducing objects not present in the images) [51], these issues generally occur at the object or fine-grained attribute level. However, when reasoning about grouping criteria for OpenSMC task, the focus is on identifying general thematic elements shared across the image set. As a result, these minor inconsistencies in the captions do not hinder the LLM in our framework from effectively reasoning about grouping criteria, helping the Caption-based Proposer to achieve the best performance among all the studied design choices.

### H.2. Further Results for Semantic Grouper Study

In this section, we present the expanded numerical results comparing different semantic groupers to supplement the summary in Fig. 6. Specifically, we provide detailed results for the evaluation of the six tested datasets as follows:

- COCO-4c (Fig. 6(a)) in Tab. 20
- Card-2c (Fig. 6(b)) in Tab. 21
- Action-3c (Fig. 6(c)) in Tab. 22
- Food-4c (Fig. 6(d)) in Tab. 23
- Fruit-2c (Fig. 6(e)) in Tab. 24
- Clevr-4c (Fig. 6(f)) in Tab. 25

In addition, we present the statistics of the predicted clusters at each granularity level in Tab. 26.

### H.3. Further Comparative Results with TCMC Methods

We provide expanded results in Tab. 27 for each criterion and benchmark, detailing the comparison of criteria-conditioned clustering methods presented in Tab. 2 in the main paper.

### H.4. Further Results for Multi-granularity Clustering Study.

We present expanded results in Tab. 28 for the ablation study on multi-granularity refinement, providing a detailed breakdown of the summary shown in Fig. 7 in the main paper.

## I. Qualitative Analysis

In this section, we visualize the grouping results predicted by the best configuration of our proposed framework (Caption-based Proposer and Caption-based Grouper). Specifically, we present example clustering results across different criteria for COCO-4c in Fig. 2, Food-4c in Fig. 3, Action-3c in Fig. 4, Clevr-4c in Fig. 5, and Card-2c in Fig. 6. Additionally, we showcase example clustering results at different predicted granularity levels for COCO-4c in Fig. 7.

## J. Failure Case Analysis

In Fig. 8, we present several failure cases from the best configuration of our proposed framework (Caption-based Proposer and Caption-based Grouper). As observed, our method frequently misassigns “Surfing” to the “Kayaking” cluster under the Activity criterion. Upon examining the intermediate criterion captions generated by the MLLM, we found that this error is largely due to the MLLM incorrectly describing a “Surfboard” as a “Kayak”. This highlights the importance of the MLLM’s ability to accurately describe images, as it is critical for the performance of our system. Potential improvements could include majority voting or model ensembling using different MLLM models.

Another issue arises in crowded scenes. When multiple people are present in an image, the model consistently assigns the Mood label “Communal” to the images. We speculate that this occurs because, in the presence of multiple people, the model struggles to accurately determine the mood of one key individual.

Finally, we observed that our method sometimes fails to distinguish subtle, fine-grained differences between images, leading to incorrect labels. For example, as shown in Fig. 8, “Edamame” or “Pho” are typical dishes from China, Vietnam, and Japan, but they may be presented differently depending on the cuisine. The “Edamame” shown in Fig. 8 is presented in a traditional Japanese style, yet our model incorrectly predicted it as Chinese cuisine. This oversight of fine-grained details could be improved by employing a more advanced prompting strategy [53].

## K. Further Study on Multi-granularity Clustering

In this section, we provide a detailed study on how different levels of multi-granularity output from our  $\mathcal{X}$ -Cluster framework impact grouping results. Specifically, for the Action-3c dataset, we employed human annotators to label two additional granularity levels for the criteria Action and Location. For the Action criterion, we consider the original annotation as fine-grained (L3) and tasked annotators to name the action in the image using more abstract and general coarse-grained (L1) and middle-grained (L2) labels. For the Location criterion, we consider the original annotation as middle-grained (L2) and tasked annotators to provide both more abstract coarse-grained (L1) labels and more specific fine-grained (L3) labels. This process resulted in expanded ground-truth annotations at three distinct semantic granularity levels for both the Action and Location criteria of the Action-3c dataset.

Next, we quantitatively evaluated the multi-granularity grouping results at each predicted clustering granularity level against

Table 18. **Comparison of True Positive Rate (TPR) (%) for criteria proposers across the six OpenSMC benchmarks.** TPR performance is reported for both Basic and Hard ground-truth criteria. The best performance is highlighted in bold.

	COCO-4c		Food-4c		Action-3c		Clevr-4c		Card-2c		Fruit-2c		Average	
	Basic	Hard	Basic	Hard	Basic	Hard	Basic	Hard	Basic	Hard	Basic	Hard	Basic	Hard
Image-based	<b>100.0</b>	52.9	25.0	36.4	66.7	54.6	50.0	28.6	50.0	25.0	50.0	20.0	56.9	36.2
Tag-based	50.0	35.3	<b>100.0</b>	72.7	66.7	36.4	75.0	42.9	50.0	50.0	50.0	20.0	65.3	42.9
Caption-based	<b>100.0</b>	<b>64.7</b>	<b>100.0</b>	<b>81.8</b>	<b>100.0</b>	<b>72.7</b>	<b>100.0</b>	<b>71.4</b>	<b>100.0</b>	<b>100.0</b>	<b>100.0</b>	<b>60.0</b>	<b>100.0</b>	<b>75.1</b>

Table 19. **Study of the impact of data scale on criteria discovery.** The Caption-based Proposer is used for criteria discovery, and TPR performance (%) is reported on the *Hard* ground-truth criteria sets across the six OpenSMC benchmarks for different data scales. The best performance is highlighted in bold.

Data scales	COCO-4c	Food-4c	Action-3c	Clevr-4c	Card-2c	Fruit-2c	Average
100%	<b>64.7</b>	<b>81.8</b>	<b>72.7</b>	71.4	<b>100.0</b>	<b>60.0</b>	<b>75.1</b>
80%	47.1	72.7	54.6	71.4	75.0	30.0	58.5
60%	52.9	63.6	54.6	71.4	<b>100.0</b>	50.0	65.4
40%	41.2	45.5	45.5	<b>85.7</b>	<b>100.0</b>	40.0	59.6
20%	35.3	45.5	36.4	42.9	<b>100.0</b>	40.0	50.0
1 img	23.5	36.4	27.3	57.1	75.0	50.0	44.9

Table 20. **Comparison of Semantic Groupers on COCO-4c.** We report Clustering Accuracy (CAcc), Semantic Accuracy (SAcc), and their Harmonic Mean (HM) in percentages (%). These results are plotted in Fig. 6(a).

Methods	Activity			Location			Mood			Time of Day		
	CAcc	SAcc	HM	CAcc	SAcc	HM	CAcc	SAcc	HM	CAcc	SAcc	HM
CLIP Zero-shot	62.6	73.5	67.6	34.3	51.5	41.1	22.4	43.3	29.5	40.6	74.1	52.4
KMeans CLIP	34.4	-	-	32.7	-	-	18.9	-	-	38.6	-	-
KMeans DINOv1	34.8	-	-	37.5	-	-	17.9	-	-	36.5	-	-
KMeans DINOv2	38.2	-	-	37.9	-	-	22.5	-	-	43.8	-	-
Img-based BLIP-2	48.7	64.1	<b>55.3</b>	39.6	48.0	43.4	30.2	37.5	33.4	40.7	60.3	48.6
Img-based LLaVA	46.5	61.8	53.1	34.0	46.3	39.2	28.0	24.7	26.3	39.4	51.7	44.7
Tag-based	43.2	51.5	47.0	28.6	46.6	35.5	13.0	25.6	17.2	19.3	48.8	27.7
Caption-based	44.1	48.9	46.4	55.2	55.6	<b>55.4</b>	38.1	32.6	<b>35.2</b>	67.6	56.7	<b>61.7</b>

Table 21. **Comparison of Semantic Groupers on Card-2c.** We report Clustering Accuracy (CAcc), Semantic Accuracy (SAcc), and their Harmonic Mean (HM) in percentages (%). These results are plotted in Fig. 6(b).

Methods	Suit			Rank		
	CAcc	SAcc	HM	CAcc	SAcc	HM
CLIP Zero-shot	47.9	69.5	56.7	35.0	64.2	45.3
KMeans CLIP	45.0	-	-	28.6	-	-
KMeans DINOv1	38.5	-	-	20.7	-	-
KMeans DINOv2	36.7	-	-	22.3	-	-
Img-based BLIP-2	66.7	77.7	<b>71.8</b>	47.5	54.4	50.7
Img-based LLaVA	36.8	65.8	47.2	24.6	49.8	32.9
Tag-based	39.2	32.9	35.8	22.3	39.1	28.4
Caption-based	54.5	73.6	62.6	92.1	95.1	<b>93.6</b>

each ground-truth annotation granularity level by measuring clustering accuracy (CAcc) and semantic accuracy (SAcc). The main caption-based  $\mathcal{X}$ -Cluster framework was used for this experiment. In Fig. 9, we report the Harmonic Mean of CAcc and SAcc for the Action and Location criteria of Action-3c, across each predicted clustering granularity level evaluated against each ground-truth annotation level. As clearly shown, the highest grouping per-

formance consistently appears along the diagonal. This indicates that the best grouping performance is achieved when the predicted granularity *matches* the annotation granularity.

These experimental results not only highlight the importance of the multi-granularity output of our framework but also validate the effectiveness of our multi-granularity design in aligning with user-preferred granularities that is reflected by the annotations in

Table 22. **Comparison of Semantic Groupers on Action-3c.** We report Clustering Accuracy (CAcc), Semantic Accuracy (SAcc), and their Harmonic Mean (HM) in percentages (%). These results are plotted in Fig. 6(c).

Methods	Action			Location			Mood		
	CAcc	SAcc	HM	CAcc	SAcc	HM	CAcc	SAcc	HM
CLIP Zero-shot	97.1	99.2	98.1	66.7	67.1	66.9	75.5	80.7	78.0
KMeans CLIP	62.3	-	-	58.3	-	-	-	-	-
KMeans DINOv1	49.3	-	-	61.4	-	-	-	-	-
KMeans DINOv2	75.7	-	-	67.6	-	-	-	-	-
Img-based BLIP-2	79.7	80.9	80.3	43.3	42.4	42.8	43.1	43.8	43.4
Img-based LLaVA	70.1	60.5	65.0	45.8	42.8	44.2	32.0	38.0	34.7
Tag-based	70.2	55.0	61.6	36.8	48.1	41.7	50.7	47.6	49.1
Caption-based	82.8	82.8	<b>82.8</b>	69.8	55.2	<b>61.6</b>	52.3	50.2	<b>51.2</b>

Table 23. **Comparison of Semantic Groupers on Food-4c.** We report Clustering Accuracy (CAcc), Semantic Accuracy (SAcc), and their Harmonic Mean (HM) in percentages (%). These results are plotted in Fig. 6(d).

Methods	Food Type			Cuisine			Course			Diet		
	CAcc	SAcc	HM	CAcc	SAcc	HM	CAcc	SAcc	HM	CAcc	SAcc	HM
CLIP Zero-shot	90.6	94.6	92.6	54.9	81.4	65.6	63.5	84.7	72.6	47.6	59.9	53.0
KMeans CLIP	66.1	-	-	29.8	-	-	49.5	-	-	36.9	-	-
KMeans DINOv1	33.6	-	-	15.3	-	-	38.1	-	-	41.4	-	-
KMeans DINOv2	72.7	-	-	22.5	-	-	47.6	-	-	43.4	-	-
Img-based BLIP-2	54.2	71.4	<b>61.6</b>	54.8	73.3	<b>62.7</b>	42.3	71.0	53.0	34.2	53.8	41.9
Img-based LLaVA	42.2	64.0	50.9	33.7	57.6	42.6	46.9	73.1	57.1	27.0	40.5	32.4
Tag-based	45.0	63.3	52.6	48.8	42.1	45.2	42.7	70.1	53.1	25.2	34.1	29.0
Caption-based	34.6	54.2	42.2	47.0	65.9	54.9	69.1	85.7	<b>76.5</b>	41.5	54.0	<b>46.9</b>

Table 24. **Comparison of Semantic Groupers on Fruit-2c.** We report Clustering Accuracy (CAcc), Semantic Accuracy (SAcc), and their Harmonic Mean (HM) in percentages (%). These results are plotted in Fig. 6(e).

Methods	Species			Color		
	CAcc	SAcc	HM	CAcc	SAcc	HM
CLIP Zero-shot	84.0	93.1	88.3	54.8	83.5	66.1
KMeans CLIP	67.1	-	-	39.6	-	-
KMeans DINOv1	53.8	-	-	36.0	-	-
KMeans DINOv2	71.2	-	-	36.7	-	-
Img-based BLIP-2	70.7	68.3	69.5	40.9	70.6	51.8
Img-based LLaVA	63.9	67.8	65.8	51.0	83.2	<b>63.2</b>
Tag-based	64.0	67.1	65.5	54.1	44.1	48.6
Caption-based	76.9	70.7	<b>73.7</b>	53.3	51.5	52.4

Table 25. **Comparison of Semantic Groupers on Clevr-4c.** We report Clustering Accuracy (CAcc), Semantic Accuracy (SAcc), and their Harmonic Mean (HM) in percentages (%). These results are plotted in Fig. 6(f).

Methods	Color			Texture			Count			Shape		
	CAcc	SAcc	HM	CAcc	SAcc	HM	CAcc	SAcc	HM	CAcc	SAcc	HM
CLIP Zero-shot	77.7	94.0	85.1	34.1	41.9	37.6	43.7	81.5	56.9	71.1	72.7	71.9
KMeans CLIP	48.8	-	-	61.4	-	-	44.2	-	-	56.1	-	-
KMeans DINOv1	53.0	-	-	58.4	-	-	47.5	-	-	67.0	-	-
KMeans DINOv2	44.1	-	-	46.9	-	-	52.5	-	-	87.0	-	-
Img-based BLIP-2	69.3	76.5	<b>72.7</b>	57.8	34.4	43.1	25.7	55.9	35.2	69.1	62.6	65.7
Img-based LLaVA	56.5	63.5	59.8	51.9	26.9	35.4	53.7	39.4	45.4	64.3	71.3	<b>67.6</b>
Tag-based	66.6	55.3	60.4	57.2	40.2	47.3	47.4	8.3	14.1	62.7	36.5	46.2
Caption-based	70.3	63.4	66.7	65.3	42.1	<b>51.2</b>	65.7	73.3	<b>69.3</b>	58.4	38.5	46.4

Table 26. **Summary of cluster counts across six benchmarks for the comparison of semantic groupers.** The results yield by the main Caption-based Grouper is reported. Specifically, we report: *i*) GT: the number of ground-truth clusters; *ii*) Pred-Init: predicted clusters from initial names; *iii*) Pred-Coarse: predicted coarse-grained clusters after multi-granularity refinement; *iv*) Pred-Middle: predicted middle-grained clusters after multi-granularity refinement; and *v*) Pred-Fine: predicted fine-grained clusters after multi-granularity refinement.

Dataset	Criteria	GT	Pred-Init	Pred-Corase	Pred-Middle	Pred-Fine
COCO-4c	Activity	64	203	12	23	52
	Location	19	145	7	14	28
	Mood	20	122	15	25	30
	Time of Day	6	96	2	8	31
Food-4c	Food Type	101	301	7	37	127
	Cuisine	15	141	9	18	53
	Course	5	97	4	12	78
	Diet	4	139	5	8	64
Action-3c	Action	40	71	8	15	51
	Location	10	82	5	10	67
	Mood	4	95	6	18	55
Clevr-4c	Color	10	25	6	12	17
	Texture	10	23	2	5	12
	Shape	10	22	5	11	14
	Count	10	11	2	4	11
Card-2c	Rank	14	147	4	7	16
	Suit	5	56	4	7	30
Fruit-2c	Species	34	54	8	25	38
	Color	15	66	5	15	39

these experiments.

## L. Study on Handling Invalid Criteria

At the criteria refinement step, *invalid* grouping criteria (False Positives) may be proposed due to hallucinations from large language models (LLMs). While we did not observe hallucinated criteria being introduced during our experiments across six datasets and three application studies, it is important to further investigate the potential impact of such invalid criteria on the proposed  $\mathcal{X}$ -Cluster system.

To this end, we design and conduct a control experiment using the Fruit-2c dataset [64], where we *artificially* introduced two “hallucinated” invalid grouping criteria (False Positives), Action and Clothing Style, into the refined criteria pool. These invalid criteria were then used in the subsequent grouping process to evaluate their effect on our system. We apply the main Caption-based Grouper to group fruit images based on these “hallucinated” criteria.

The grouping results for the two invalid criteria are presented in Tab. 29. As observed, when processing invalid “hallucinated” criteria, nearly all images are assigned to a cluster named “Not visible” by our framework. This occurs because, in the absence of relevant visual content in the images, the MLLM-generated captions do not include descriptors corresponding to the invalid criteria. Consequently, the LLM creates a “Not visible” cluster and assigns the images to it. Since the system provides interpretable outputs, users can easily identify and disregard such invalid groupings. This control experiment highlights the robustness of our system against hallucination in practical scenarios.

## M. Study on Model Hallucination and Bias

**Model hallucination.** LLM hallucination [99] typically occurs when LLMs are tasked with complex queries requiring world knowledge or factual information—for instance, answering a question like “Who was the 70th president of the United States?” might lead to a fabricated response. However, in our system, the use of LLMs is fully grounded in the visual descriptions (tags or captions) of the images. Consequently, the LLM output is strongly constrained to analyzing these visual descriptions, significantly reducing the likelihood of hallucination. That said, LLM hallucination can still have mild effects on clustering results. For example, as discussed in the failure case analysis in Sec. J, the LLM incorrectly grouped “Korean bibimbap” and “Vietnamese rice noodles” under “Chinese cuisine” (see Fig. 8). MLLMs also play a crucial role in our system, as they are responsible for translating images into text for subsequent processing steps. MLLM hallucination [99] typically involves incorrectly identifying the existence of objects, attributes, or spatial relationships within an image. However, since our proposed system operates at the *dataset level* rather than on a per-image basis, it is largely insensitive to such hallucinations, especially at the fine-grained visual detail level. Moreover, as our system is training-free, it can be further enhanced with LLM or MLLM hallucination mitigation techniques, such as the Visual Fact Checker [25], which we leave as a direction for future work.

**Model Bias.** Foundation models such as LLMs and MLLMs are known to inherit biases from their training data [7]. In our system, we addressed potential biases using Hard Positive Prompt-

Table 27. **Comparison with criteria-conditioned clustering methods on the six OpenSMC benchmarks.** We report Clustering Accuracy (CAcc) and Semantic Accuracy (SAcc) as percentages (%). Average (Avg.) CAcc and SAcc across different criteria on each dataset is also provided. For reference, we include the pseudo upper-bound (UB) performance of CLIP ViT-L/14 in zero-shot transfer, using ground-truth criteria and class names. Note that both IC|TC and MMaP utilize ground-truth criteria and the number of clusters for clustering. These expanded results correspond to Tab. 2.

Benchmark	Criterion	UB		IC TC		SSD-LLM		MMaP		MSub		Ours	
		CAcc	SAcc	CAcc	SAcc	CAcc	SAcc	CAcc	SAcc	CAcc	SAcc	CAcc	SAcc
COCO-4c	Activity	62.6	73.5	51.3	53.2	44.0	52.1	33.8	-	35.9	-	44.1	48.9
	Location	34.3	51.5	58.5	54.0	51.2	52.9	35.3	-	37.4	-	55.2	55.6
	Mood	22.4	43.3	23.2	40.4	15.9	39.3	20.9	-	23.0	-	38.1	32.6
	Time of Day	40.6	74.1	62.8	65.2	55.5	64.1	45.7	-	47.8	-	67.6	56.7
	Avg.	40.1	60.6	48.9	<b>53.2</b>	41.6	52.1	33.9	-	36.0	-	<b>51.2</b>	48.4
Food-4c	Food Type	90.6	94.6	36.0	52.6	33.1	46.5	48.9	-	52.4	-	34.6	54.2
	Cuisine	54.9	81.4	46.8	42.4	43.9	36.3	31.7	-	35.2	-	47.0	65.9
	Course	63.5	84.7	70.5	89.5	67.6	83.4	48.6	-	52.1	-	69.1	85.7
	Diet	47.6	59.9	48.5	62.1	45.6	56.0	45.9	-	49.4	-	41.5	54.0
	Avg.	64.1	80.2	<b>50.5</b>	61.7	47.5	55.5	43.8	-	47.3	-	48.1	<b>64.9</b>
Clevr-4c	Color	77.7	94.0	51.2	43.2	47.8	44.0	75.3	-	84.7	-	70.3	63.4
	Texture	34.1	41.9	64.9	26.4	61.5	27.2	56.5	-	65.9	-	65.3	42.1
	Count	43.7	81.5	46.9	39.0	43.5	39.8	53.9	-	63.3	-	65.7	73.3
	Shape	71.1	72.7	70.0	38.7	66.6	39.5	65.5	-	74.9	-	58.4	38.5
	Avg.	56.7	72.5	58.3	36.8	54.8	37.6	62.8	-	72.2	-	<b>64.9</b>	<b>54.3</b>
Action-3c	Action	97.1	99.2	86.4	58.7	88.1	55.3	51.3	-	55.0	-	82.8	76.3
	Location	66.7	67.1	82.0	52.9	83.7	49.5	59.4	-	63.1	-	69.8	55.2
	Mood	75.5	80.7	60.8	57.4	62.5	54.0	71.0	-	74.7	-	52.3	50.2
	Avg.	79.8	82.3	76.4	56.3	<b>78.1</b>	52.9	60.6	-	64.3	-	68.3	<b>60.6</b>
Card-2c	Suit	47.9	69.5	54.9	65.6	47.5	60.7	41.3	-	44.0	-	54.5	73.6
	Rank	35.0	64.2	94.6	96.8	87.2	91.9	32.6	-	35.3	-	92.1	95.1
	Avg.	41.4	66.9	<b>74.8</b>	81.2	67.3	76.3	36.9	-	39.6	-	73.3	<b>84.3</b>
Fruit-2c	Species	84.0	93.1	69.3	66.9	68.1	58.6	58.8	-	62.2	-	76.9	70.7
	Color	54.8	83.5	57.2	43.3	56.0	35.0	43.3	-	46.7	-	53.3	51.5
	Avg.	69.4	88.3	63.3	55.1	62.0	46.8	51.0	-	54.4	-	<b>65.1</b>	<b>61.1</b>

ing techniques: *i) MLLM Bias Mitigation:* The MLLM is further prompted to generate criterion-specific captions that focus solely on describing the criterion-related content in each image. This approach constrains the MLLM from generating irrelevant content influenced by inherent biases; *ii) LLM Bias Mitigation:* Similarly, when prompting the LLM to assign image captions to clusters, we condition it to concentrate exclusively on the Criterion depicted in each image (see Tab. 15).

To validate the effectiveness of these bias mitigation techniques, we conducted a fair clustering experiment. Specifically, following Kwon et al. [42], we sampled images for four occupations (Craftsman, Laborer, Dancer, and Gardener) from the FACET [29] dataset, which contains images from 52 occupations. For each occupation, we selected 10 images of men and 10 images of women, totaling 80 images, ensuring a ground-truth gender proportion disparity of 0% for each occupation. Using our main  $\mathcal{X}$ -Cluster system, we grouped these images based on the criterion Occupation using three bias mitigation strategies: *i) No mitigation:* using general descriptions from the MLLM for LLM grouping; *ii) Our default hard positive prompting strategy:* using criterion-specific captions from the MLLM for LLM grouping; and *iii) Our default strategy with additional negative prompt:* adding a simple negative prompt, “Do not consider gender,” to both the MLLM captioning and LLM grouping prompts.

In this experiment, non-biased result is defined as achieving

equal gender proportions within each cluster. Tab. 30 presents the average gender ratios of the clustering results for each method across the four occupations. As observed, without bias mitigation,  $\mathcal{X}$ -Cluster exhibits noticeable gender bias in the studied occupations, with a gender disparity of 19.4%. However, our default bias mitigation techniques effectively reduce this disparity to 4.9%, achieving performance comparable to the addition of a manual negative prompt. This experiment demonstrates the effectiveness of our bias mitigation strategy and highlights the potential for further reducing model bias in our framework using more advanced techniques.

## N. Computational Cost Analysis

The proposed  $\mathcal{X}$ -Cluster framework is training-free, requiring only inference processes. Specifically, our main framework (Caption-based) requires up to 31 GB of GPU memory to operate. All experiments reported in the paper were conducted on 4 Nvidia A100 40GB GPUs. In Tab. 31, we provide a detailed analysis of the computational efficiency of our main  $\mathcal{X}$ -Cluster framework (Caption-based Proposer and Caption-based Grouper) on the COCO-4c benchmark (5,000 images with four criteria) across various hardware configurations. For these experiments, we used LLaVA-NeXT-7B [49] as the MLLM and Llama-3.1-8B [61] as the LLM.

Table 28. **Ablation study of multi-granularity refinement on the six OpenSMC benchmarks.** We compare three ways of constructing cluster names: Initial Names (IN), Flat Refinement (FR), Multi-granularity Refinement (MR). We report Clustering Accuracy (CAcc) and Semantic Accuracy (SAcc) as percentages (%). Average (Avg.) CAcc and SAcc across different criteria on each dataset is also provided. These expanded results correspond to the plotting shown in Fig. 7.

Benchmark	Criterion	IN		FR		MR	
		CAcc	SAcc	CAcc	SAcc	CAcc	SAcc
COCO-4c	Activity	14.1	48.5	34.5	40.5	44.1	48.9
	Location	30.0	51.9	41.4	56.0	55.2	55.6
	Mood	6.6	34.7	21.9	32.1	38.1	32.6
	Time of Day	24.4	50.5	28.2	54.4	67.6	56.7
	<i>Avg.</i>	18.8	46.4	31.5	45.8	<b>51.2</b>	<b>48.4</b>
Food-4c	Food Type	33.9	52.4	35.5	54.3	34.6	54.2
	Cuisine	30.6	39.7	27.6	36.5	47.0	65.9
	Course	52.9	81.1	62.8	83.0	69.1	85.7
	Diet	14.0	46.6	36.8	58.2	41.5	54.0
	<i>Avg.</i>	32.9	55.0	40.7	58.0	<b>48.1</b>	<b>64.9</b>
Clevr-4c	Color	56.5	49.7	60.9	53.0	70.3	63.4
	Texture	56.5	26.0	60.9	33.0	65.3	42.1
	Count	56.5	39.6	56.5	40.8	65.7	73.3
	Shape	47.8	33.6	47.8	41.8	58.4	38.5
	<i>Avg.</i>	54.3	37.2	56.5	42.2	<b>64.9</b>	<b>54.3</b>
Action-3c	Action	72.2	63.6	90.5	63.0	82.8	76.3
	Location	46.0	50.4	65.9	59.3	69.8	55.2
	Mood	20.6	41.9	46.0	51.0	52.3	50.2
	<i>Avg.</i>	46.3	52.0	67.5	57.8	<b>68.3</b>	<b>60.6</b>
Card-2c	Suit	40.9	50.1	45.7	45.7	54.5	73.6
	Rank	43.0	55.1	47.7	54.6	92.1	95.1
	<i>Avg.</i>	42.0	52.6	46.7	50.2	<b>73.3</b>	<b>84.3</b>
Fruit-2c	Species	59.2	68.6	64.1	67.0	76.9	70.7
	Color	41.8	56.7	44.7	42.3	53.3	51.5
	<i>Avg.</i>	50.5	62.7	54.4	54.7	<b>65.1</b>	<b>61.1</b>

Table 29. **Study of the Influence of Invalid Grouping Criteria (False Positives) on the Fruit-2c Dataset.** We report the distribution of predicted groupings under the two “hallucinated” invalid grouping criteria. The main Caption-based Semantic Grouper is used for this experiment. †: For simplicity, all other minority clusters are grouped as “Others”.

Predicted Clusters	Action (%)	Clothing Style (%)
Not visible	98.3	96.7
Others†	1.7	3.3

Table 30. **Average gender ratio and disparity** across the four studied occupations (Craftsman, Laborer, Dancer, and Gardener) from the FACET dataset. Images sampled from each occupation have an equal proportion of genders. Results from different bias mitigation strategies are reported.

Bias Mitigation Strategy	Male (%)	Female (%)	Gender Disparity (%)
Ground-truth	50.0	50.0	0.0
No mitigation	40.3	59.7	19.4
Ours (default)	47.6	52.5	4.9
Ours w. Negative prompt	48.4	51.6	3.2

As shown in Tab. 31, organizing 5,000 images based on all four discovered criteria can be completed by  $\mathcal{X}$ -Cluster in 29.1 hours on a single A100 GPU or 16.7 hours on a single H100

GPU. More importantly, most steps in our framework, such as per-image captioning and per-caption cluster assignment, are parallelizable across multiple GPUs, significantly accelerating the pro-



Figure 2. Example predicted clusters of COCO-4c.

cess. Therefore, when parallelizing the framework on 4 A100 or H100 GPUs, we achieve approximately a  $4\times$  speedup, reducing computational time to 7.6 hours on 4 A100 GPUs and 4.3 hours on 4 H100 GPUs.

## O. System Sensitivity Analysis of Various MLLMs and LLMs

In Fig. 10, we perform a system-level sensitivity analysis using our default system configuration (caption-based proposer and caption-based grouper) to examine the impact of different MLLMs and LLMs on the system performance. Since all variants successfully

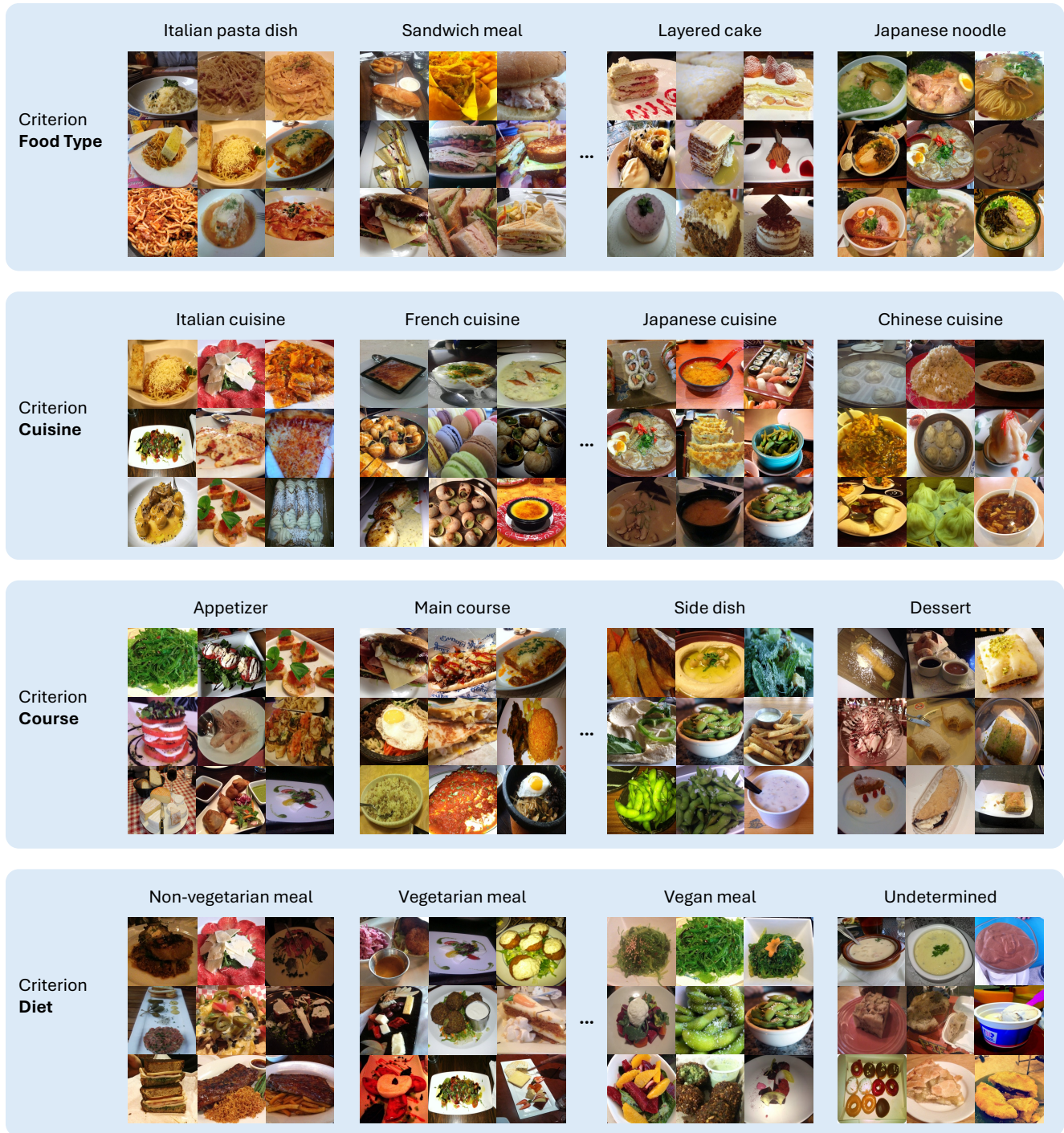


Figure 3. Example predicted clusters of Food-4c.

propose the basic criteria in each benchmark, we report the average clustering accuracy (CAcc) and semantic accuracy (SAcc) across various criteria for comparative analysis.

Specifically, in Fig. 10(a), we first fix the LLM in our system to Llama-3.1-8B [61] and assess the influence of various MLLMs: GPT-4V [1], BLIP-3-4B [102], and LLaVA-NeXT-7B [49]. Next, in Fig. 10(b), we set the MLLM to LLaVA-NeXT-7B and evaluate

different LLMs: GPT-4-turbo [1], GPT-4o [70], Llama-3-8B [60], and Llama-3.1-8B.

Findings in Fig. 10(a) indicate a direct correlation between the size of the MLLM and the ability of our system to uncover substructures, highlighting the significant role of MLLMs in translating visual information into natural language. On the other hand, this scalability demonstrates that our system can enhance perfor-

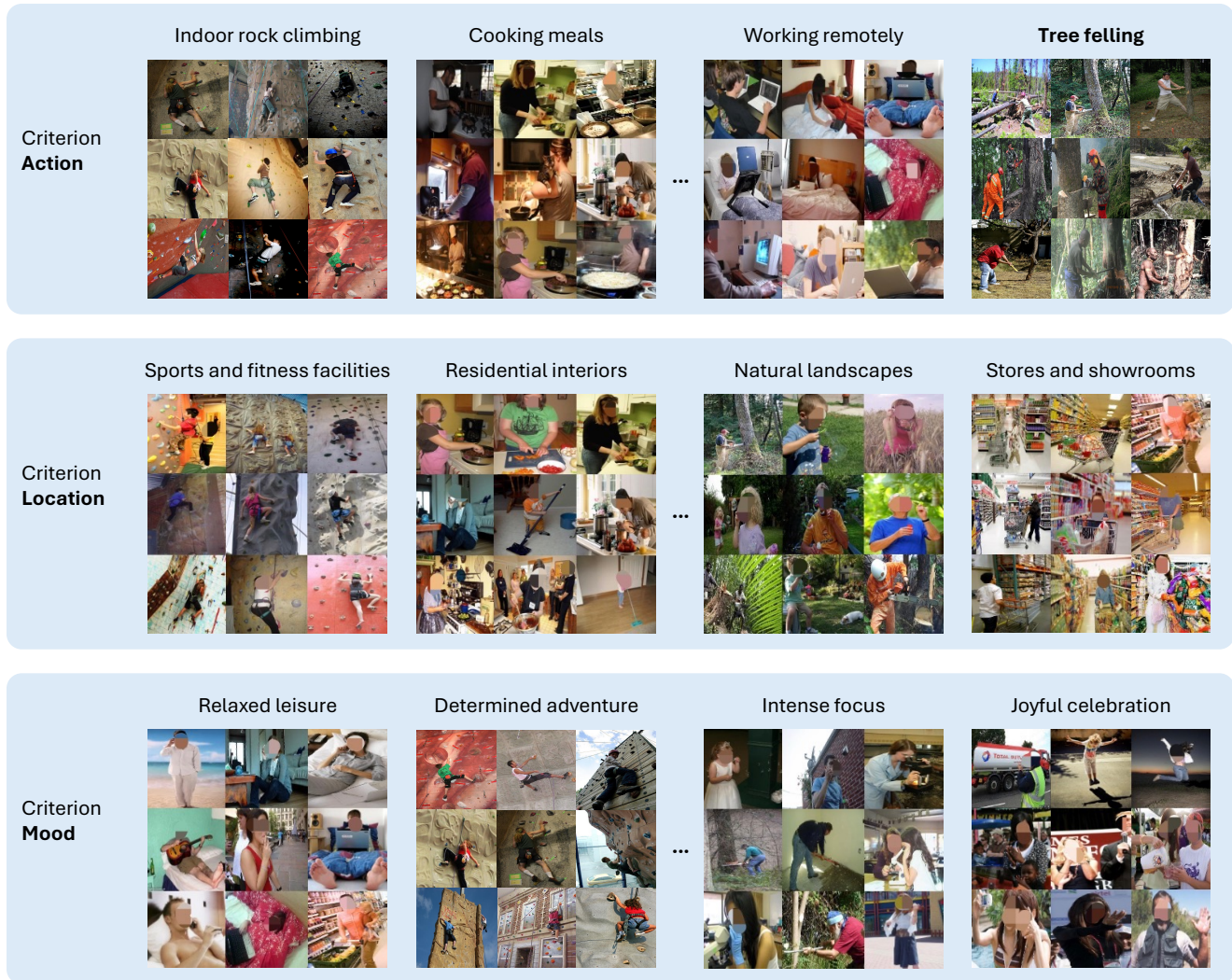


Figure 4. Example predicted clusters of Action-3c.

Table 31. **Computational cost analysis on the COCO-4c benchmark (5,000 images with four criteria).** We report the average and total time costs on various machines. The time costs were calculated for organizing all 5,000 images according to all the 4 criteria. Our main caption-based  $\mathcal{X}$ -Cluster framework is used in this experiment.

Method	Hardware	Average time cost (sec/img) ↓	Total time cost (hrs) ↓
$\mathcal{X}$ -Cluster	1 Nvidia A100-40GB	20.9	29.1
	4 Nvidia A100-40GB	5.5	7.6
	1 Nvidia H100-80GB	12.0	16.7
	4 Nvidia H100-80GB	3.1	4.3

mance with more robust MLLMs, thanks to its training-free design, which ensures compatibility with any MLLM. Despite this, we use LLaVA-NeXT-7B as our default MLLM due to its *reproducibility*, being open-source and unaffected by API changes, and its capacity for local deployment, which *upholds privacy* by not exposing sensitive image data to external entities.

As for the LLMs, as depicted in Fig. 10(b), despite GPT-4-turbo showing marginally superior performance, the open-source Llama-3.1-8B achieves similar results across benchmarks, mak-

ing it our default LLM. Notably, except for the Card-2c dataset, system performance remains largely consistent regardless of the power of the LLM. This consistency suggests that the reasoning task for OpenSMC, given the capabilities of modern LLMs to tackle complex problems [86], is relatively straightforward.

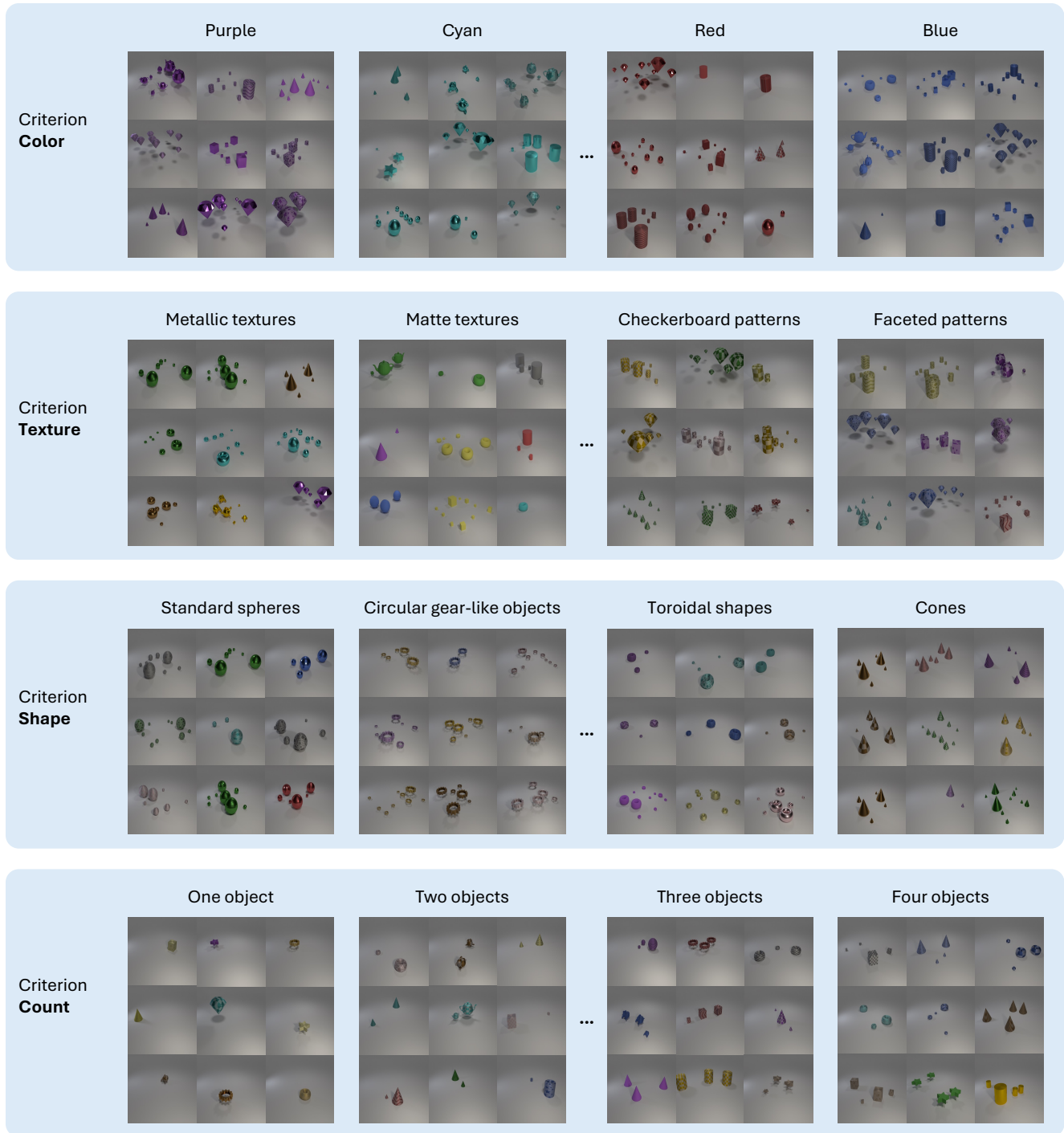


Figure 5. Example predicted clusters of Clevr-4c.

## P. Study on Fine-grained Image Collections

Image collections may include fine-grained grouping criteria, such as Bird species in bird photography. Fine-grained criteria pose unique challenges for substructure discovery due to small inter-class differences and large intra-class variations [32, 93, 109]. This requires the model to detect subtle visual distinctions to accurately

infer cluster names and guide the grouping process. The straightforward captioning process in our current framework may not fully capture these subtle visual nuances. However, the modular design of our framework allows for seamless integration of advanced cross-modal chain-of-thought (CoT) prompting strategies to address this issue.

We demonstrate this by enhancing our Caption-based Grouper

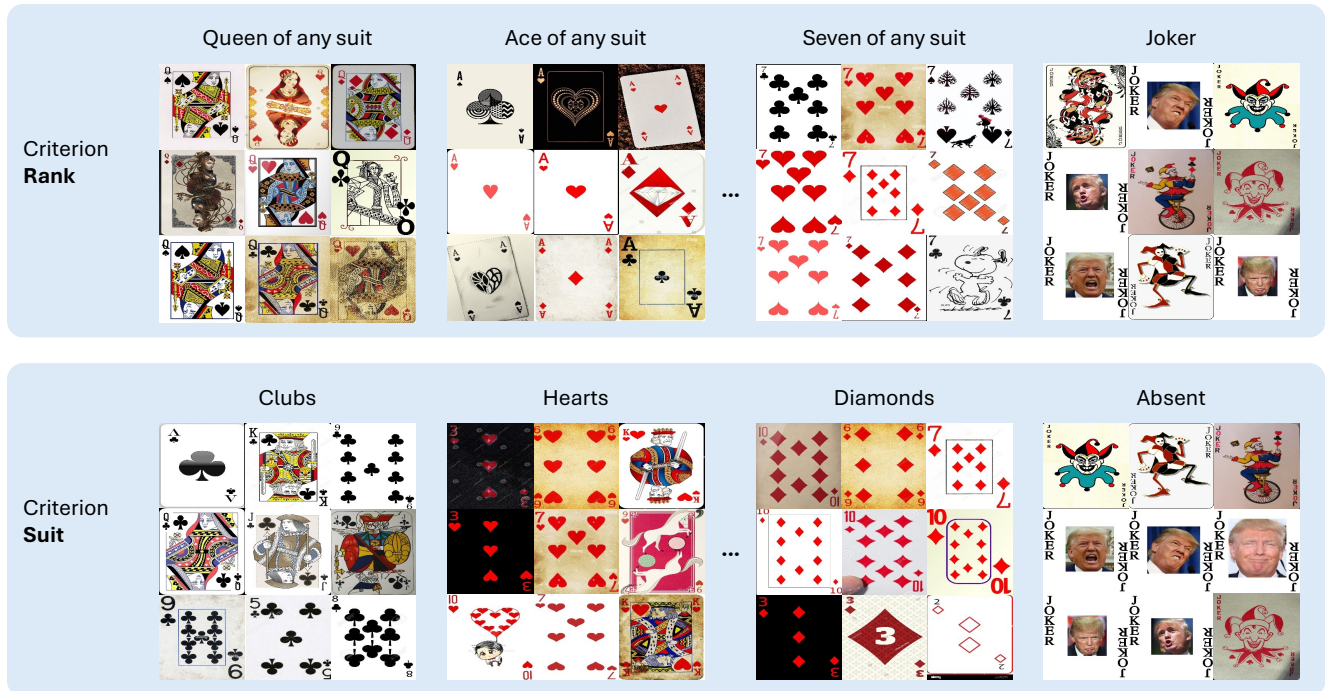


Figure 6. Example predicted clusters of Card-2c.

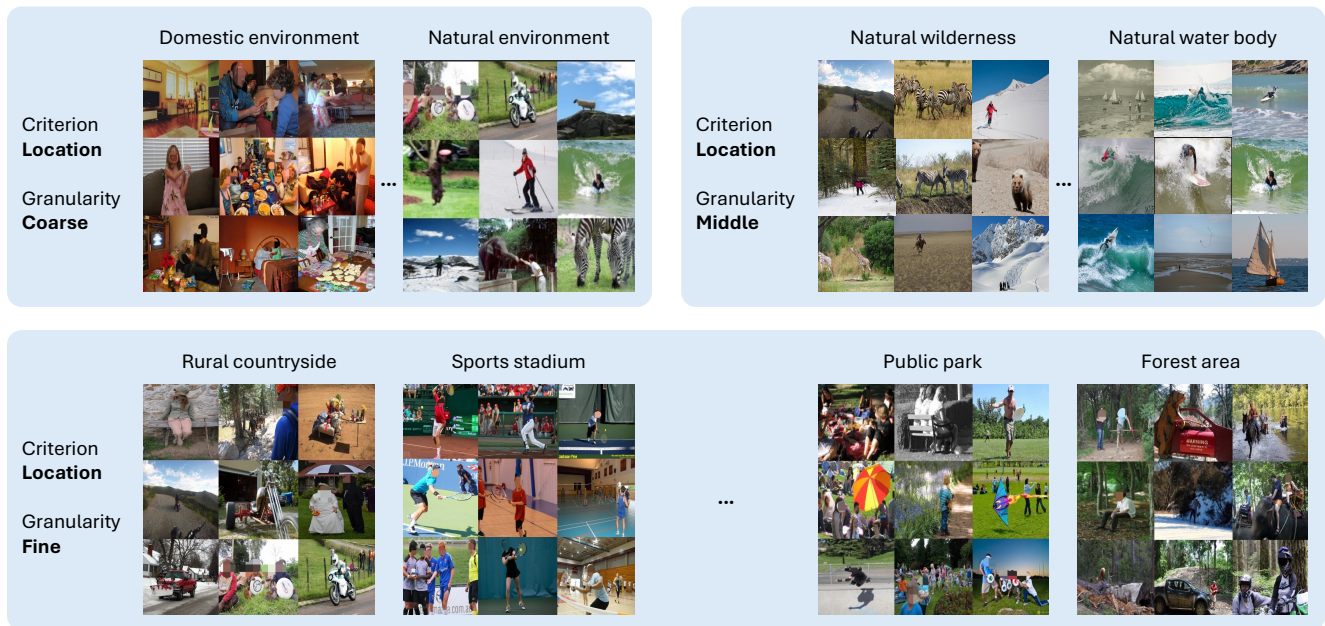


Figure 7. Example predicted clusters of COCO-4c at different granularities.

with FineR [53], a cross-modal CoT prompt method specifically designed for fine-grained visual recognition. When the proposer identifies fine-grained criteria, such as Bird species, the framework switches to a FineR-enhanced captioning strategy that provides more detailed attribute descriptions, such as “Wing color: Blue-grey,” to enrich the captions and capture per-attribute visual characteristics to better support the subsequent substructure uncovering process.

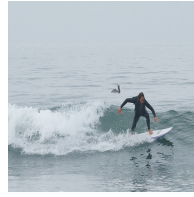
We evaluate this on two image collections containing fine-grained criteria: CUB200 [95] and Stanford Cars196 [38]. Our framework successfully discovers the fine-grained criteria Bird species for CUB200 and Car model for Cars196. As shown in Tab. 32, when uncovering fine-grained substructures, integrating the FineR prompting strategy significantly improves performance by up to +15.0% CAcc and +12.2% SAcc, achieving results comparable to FineR itself. This demonstrates the flexibility of our



GT: Surfing



GT: Surfing



GT: Surfing



GT: Restaurant or dining area



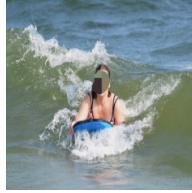
GT: Restaurant or dining area



GT: Restaurant or dining area



GT: Surfing



GT: Surfing



GT: Surfing



GT: Restaurant or dining area



GT: Restaurant or dining area



GT: Restaurant or dining area

<b>Benchmark:</b>	COCO-4c
<b>Criterion:</b>	Activity
<b>Predicted Cluster:</b>	Kayaking

<b>Benchmark:</b>	Action-3c
<b>Criterion:</b>	Location
<b>Predicted Cluster:</b>	Professional workspaces



GT: Joyful



GT: Focused



GT: Joyful



GT: Vietnamese



GT: Korean



GT: Vietnamese



GT: Focused



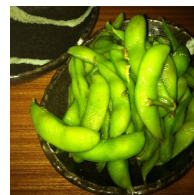
GT: Focused



GT: Adventurous



GT: Thai



GT: Japanese



GT: Vietnamese

<b>Benchmark:</b>	Action-4c
<b>Criterion:</b>	Mood
<b>Predicted Cluster:</b>	Communal

<b>Benchmark:</b>	Food-4c
<b>Criterion:</b>	Cuisine
<b>Predicted Cluster:</b>	Chinese cuisine

Figure 8. Failure case analysis. We show wrongly predicted images with their ground-truth label for four clusters.

system, allowing future adaptations to specific application needs, such as fine-grained image collections.

### Q. Further Details of the Application Study

In this section, we present additional implementation details, evaluation results, and findings for the application study discussed in Sec. 6 of the main paper. Specifically, § Q.3 offers further evaluation results and implementation details on using our predicted distribution to train a debiased model with GroupDRO [83]. § Q.1

outlines the implementation of the user study that assesses the alignment between predicted biases and human judgments, along with comprehensive findings for all studied occupations and identified criteria. Finally, § Q.2 provides additional insights from the analysis of social media image popularity.

		Annotation Granularity Levels						Harmonic
		L1	L2	L3	L1	L2	L3	mean
Prediction Levels	L1	35.0	46.2	32.8	44.3	51.9	42.2	max mid min
	L2	28.3	55.7	49.2	39.0	61.6	53.4	
	L3	28.0	45.2	82.8	29.5	47.0	59.3	
		Action			Location			

Figure 9. **Further study on the influence of multi-granularity clustering output.** We evaluate the CAcc and SAcc of the multi-granularity grouping results at each predicted clustering granularity level against each ground-truth annotation granularity level for the Action and Location criteria of the Action-3c dataset. The Harmonic Mean of CAcc and SAcc is reported for each granularity pair. L1, L2, and L3 represent the coarse-grained, middle-grained, and fine-grained levels, respectively, for both predictions and annotations.

Table 32. **Study of substructure discovery for fine-grained criteria.** We report clustering accuracy (CAcc) and semantic accuracy (SAcc) as percentages (%). The pseudo upper-bound (UB) performance is obtained using CLIP [79] ViT-L/14 in a zero-shot transfer setting with the ground-truth class names. †: We compare with FineR [53] without its post-class name refinement step to ensure a fair comparison.

	CUB200		Car196	
	CAcc	SAcc	CAcc	SAcc
UB	57.4	80.5	63.1	66.3
FineR†	44.8	64.5	33.8	52.9
Ours	30.1	56.7	21.3	35.9
Ours + FineR	45.1	68.9	31.1	47.3

## Q.1. Further Details on Discovering Novel Bias in Text-to-Image Diffusion Models

**Image Generation for the Subject Occupation:** Following prior studies [4, 6], we selected nine occupations for our study: three stereotypically biased towards females (Nurse, Cleaning staff, Call center employee), three biased towards males (CEO, Firefighter, Basketball player), and three considered gender-neutral (Teacher, Computer user, Marketing coordinator). We used two state-of-the-art T2I diffusion model, DALL-E3 [3] and Stable Diffusion (SDXL) [76] to generate 100 images for each occupation for our study. This resulted in a total of 1,800 images. For each occupation, we provide some examples of images generated by DALL-E3 in Fig. 14, while provide some examples of images generated by SDXL in Fig. 15. We only used the simple prompt “A portrait photo of a <OCCUPATION>” for image generation for all occupations and did not include any potential biases in the prompt.

**Bias Discovery and Quantification:** We applied our method to 1,800 generated images and automatically identified 10 grouping

criteria (bias dimensions) along with their predicted distributions for each occupation image set. For this study, we utilized the mid-granularity output of our system. To evaluate the biases, we first identified the dominant cluster for each criterion—the cluster containing the largest number of images—as the *bias direction*. We then calculated the normalized entropy of the distribution for each criterion of the occupation’s images to determine the *bias intensity* score, following the method proposed by D’Inca et al. [19]:

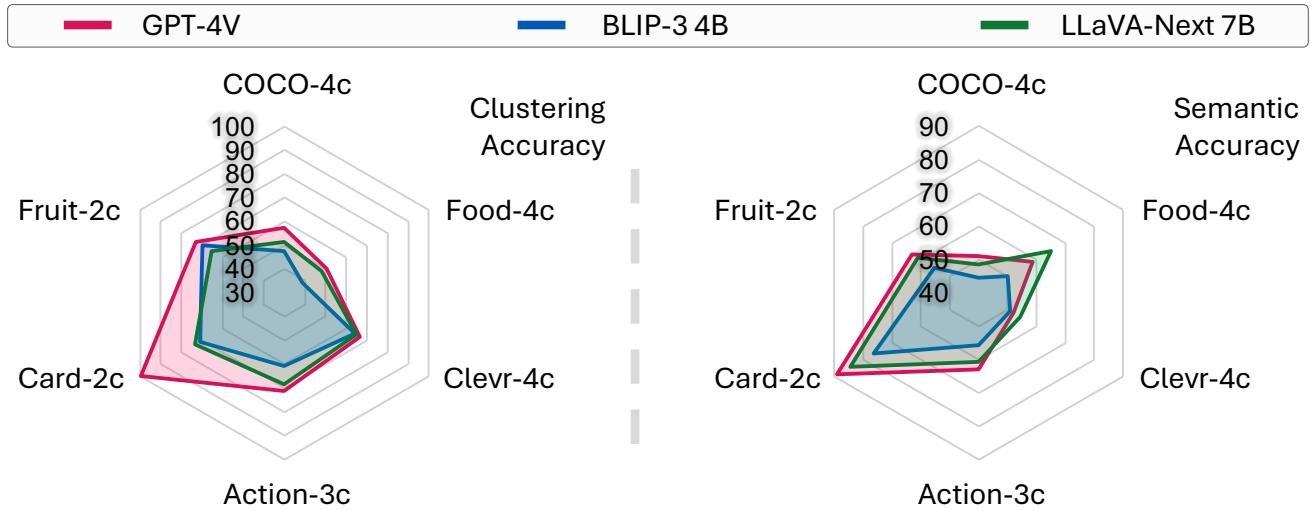
$$\mathcal{H}_{bias}^l = 1 + \frac{\sum_{c^l \in \mathcal{C}^l} \log(p(c^l | \mathcal{C}^l, \mathcal{D}_{Occupation}))}{\log(|\mathcal{C}^l|)} \quad (1)$$

where  $\mathcal{D}_{Occupation}$  represents the generated images for each occupation,  $\mathcal{C}^l$  denotes the clusters discovered under the  $l$ -th criterion, and  $p(c^l | \mathcal{C}^l)$  is the probability of each cluster under the current distribution. The resulting score is bounded between  $\mathcal{H}_{bias}^l \in [0, 1]$ , where 0 indicates no bias towards a specific cluster (concept) under the evaluated criterion, and 1 indicates that the images are completely biased towards a particular cluster (concept) (e.g., “Grey” hair color) within the current bias dimension (e.g., Hair color). We used the score defined in 1 to quantify the biases for each occupation across the 10 discovered grouping criteria. We report the bias intensity score for each occupation and each model across the 10 discovered grouping criteria in Fig. 11.

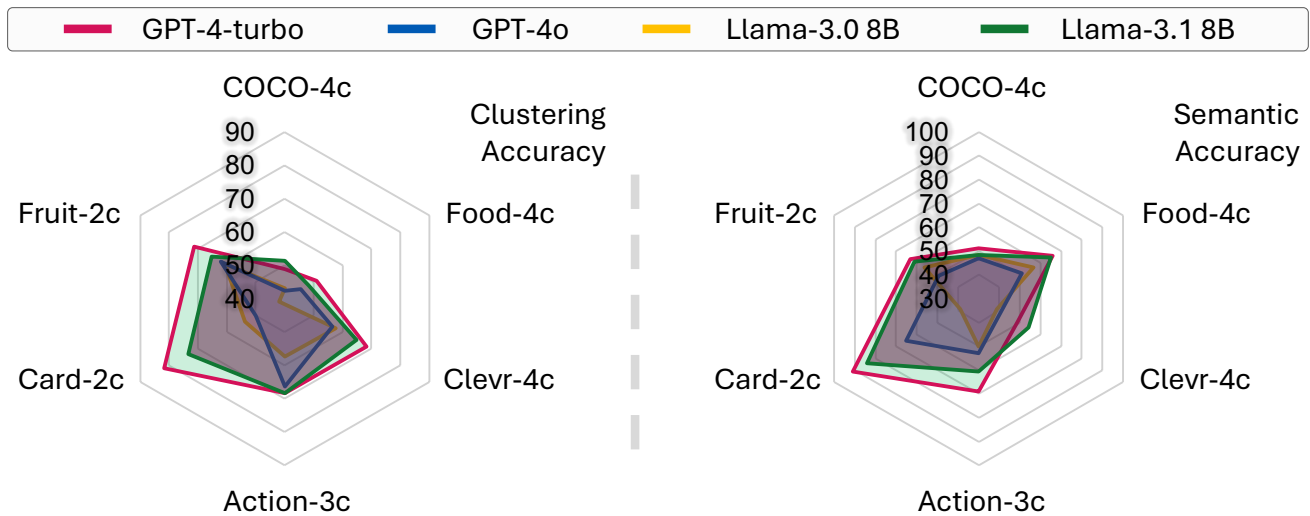
**Human Evaluation Study Details:** To assess the alignment between our method’s predictions and human judgments on bias detection, we conducted a user study to gather human evaluation results for the generated images. As shown in the questionnaire example in Fig. 16, participants were presented with images generated by DALL-E3 and SDXL for each occupation and were asked to identify the bias direction (dominant class) for each of the 10 discovered criteria and rate the bias intensity on a scale from 0 to 10. We collected responses from 54 anonymous participants, resulting in 6 human evaluations for each occupation and each criterion.

The Absolute Mean Error (AME) between the bias intensity scores predicted by our system and those rated by humans (scaled to 0 to 1) was 0.1396. Additionally, our system’s predicted bias directions aligned with human evaluations 72.3% of the time, with most discrepancies occurring in the criteria of “Age group,” “Skin tone,” and “Accessories worn.” These findings indicate a strong correlation between our system’s predictions and human judgments, validating the effectiveness of our approach. Detailed user study results are provided in § Q.1. We believe the discrepancies in certain criteria may be due to the influence of personal subjective cognition on respondents’ answers. In Fig. 11, we present the human evaluation results, averaged across all participants for each model, occupation, and criterion, with the human ratings scaled from 0 to 1.

**Complete Results and Additional Findings:** In Fig. 11, we present the detailed bias detection results for each model, occupation, and criterion, alongside human evaluation scores for reference. A particularly interesting phenomenon emerges: *While DALL-E3 significantly outperforms SDXL on the well-known bias dimensions (e.g., Gender, Race, Age, and Skin tone), both DALL-E3 and SDXL exhibit moderate to strong biases along the novel bias dimensions (e.g., Hair color, Mood, Attire, and Accessories).*



(a) Sensitivity analysis of MLLMs  
(Llama-3.1 8B is used as the LLM for all experiments)



(b) Sensitivity analysis of LLMs  
(LLaVA-Next 7B is used as the MLLM for all experiments)

Figure 10. **Sensitivity analysis of different MLLMs and LLMs on the six OpenSMC benchmarks.** **Top (a):** We fix the LLM to Llama-3.1-8B and study the impact of different MLLMs. **Bottom (b):** We fix the MLLM to LLaVA-NeXT-7B and study the impact of different LLMs. The average clustering accuracy(%) across different criteria is reported on the **left**, while the average semantic accuracy(%) is reported on the **right**.

We speculate that DALL·E3’s superior performance in mitigating well-known biases may be attributed to its “guardrails” [69], designed as part of its industrial deployment to avoid amplifying social biases via its easily accessible APIs. However, these guardrails do not prevent it from exhibiting biases along the novel dimensions discovered by our method, as these dimensions remain understudied. This observation highlights the importance of studying novel biases that could potentially exist in widely used T2I generative models to prevent further bias amplification.

## Q.2. Further Details on Analyzing Social Media Image Popularity

With the rise of image-centric content on social media platforms like Instagram, Flickr, and TikTok, understanding what makes an image popular has become crucial for applications such as marketing, content curation, and recommendation systems. Traditional research often approaches image popularity as a regression problem [13, 72], utilizing metadata like hashtags, titles, or follower counts. However, the specific semantic visual elements that contribute to an image’s popularity remain largely unexplored. In

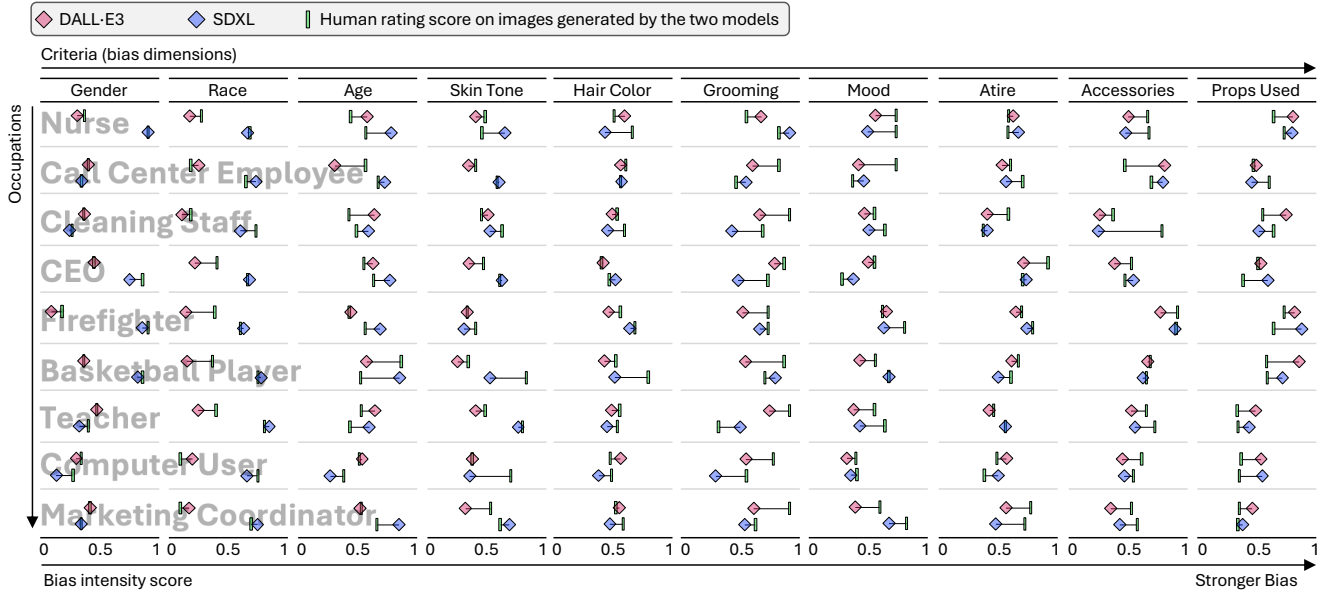


Figure 11. **Bias quantification results and human evaluation** for each occupation and criterion across the two studied T2I models, DALL-E3 and SDXL. The bias intensity score is reported.

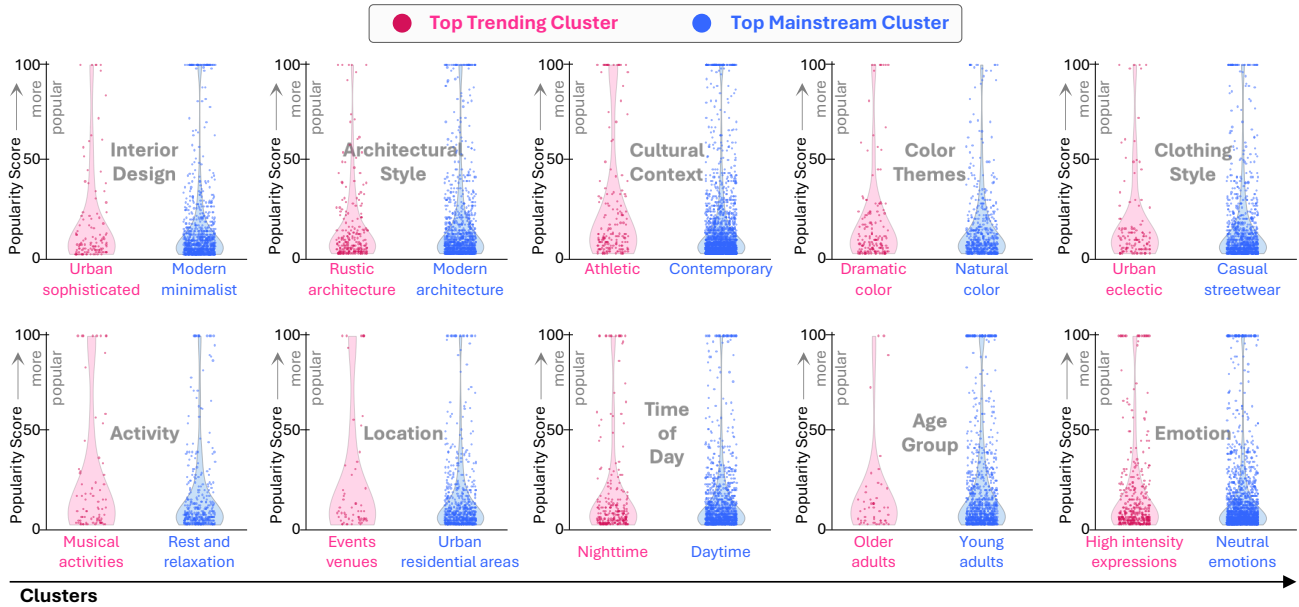


Figure 12. **Complete analysis of social media photo popularity on the SPID dataset.** We display the *Top Trending* and *Top Mainstream* clusters, along with the popularity distribution of data points within these clusters across all *ten* discovered criteria (in Grey).

this study, we applied our proposed method to automatically categorize social media images based on semantic visual elements across different dimensions (criteria). By analyzing these interpretable results alongside image popularity metrics (e.g., number of views), we gained insights into the factors contributing to virality and identified common visual traits among popular images. These insights can provide valuable guidance for content creators and advertisers, enhancing productivity and informing strategic decision-making.

To expand on the discussion in Sec. 6 of the main paper, we present the complete findings across all ten discovered criteria in Fig. 12. Notably, we consistently observed a sharp semantic contrast between the visual elements in top trending images and those in the mainstream images across all ten criteria. For instance, there is a contrast between *Urban sophisticated* and *Modern minimalist* under Interior Design, *Rustic architecture* and *Modern architecture* under Architecture Style, and *Event venues* versus *Urban residential areas* under Location.

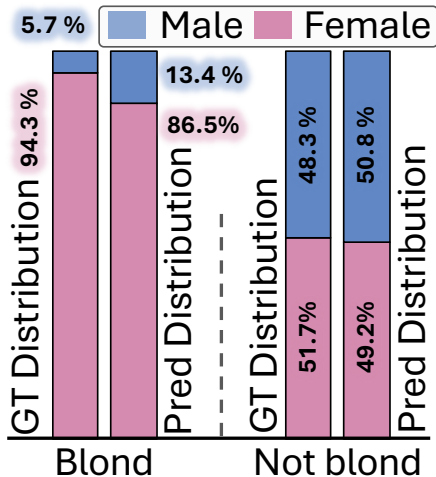


Figure 13. **Results of dataset bias discovery and mitigation.** Worst group and average accuracies(%) are reported.

This recurring observation reinforces the idea that viral (or trending) content tends to capture more attention, likely because it features novel, surprising, or striking visual elements. Humans are inherently attracted to stimuli that deviate from the norm [10, 74, 77]. On the other hand, widely uploaded yet “neutral” content is shared more often due to its familiarity and broad appeal, though it is less likely to provoke the strong emotional responses that fuel virality. We believe the insights generated by our method could offer valuable guidance to social media platform practitioners, helping them tailor their content more effectively to target audiences and gain a deeper understanding of social media image trends from various perspectives.

### Q.3. Confirming and Mitigating Dataset Bias

**Confirming and Mitigating Dataset Bias:** Given an image collection that contains *spurious correlations* [26], we are curious whether we can proactively find this issue caused by data bias directly from the training images *without* relying on either the annotations [83] or *post hoc* misclassified images [39]. As a case study, we applied the proposed  $\mathcal{X}$ -Cluster framework to the 162k training images of the CelebA [56] dataset—a binary hair color classification dataset where the target label “Blond” is spuriously correlated with the demographic attribute “Female” in its training split.

**Findings:** As expected, our method identified the grouping criteria Hair color and Gender. Next, we analyzed the predicted gender distributions within the “Blond” and “Not Blond” (all other colors) clusters. As shown in Fig. 13, we observed that the gender distribution within the “Blond” cluster is highly skewed, with 86.5% of the images representing females, closely matching the ground-truth distribution (94.3%). Such an imbalance confirms the potential issue of spurious correlations between “Blond” and “Female”. To further validate this observation, following B2T [39], we used our predicted distributions to train a debiased model with GroupDRO [83] and compared it with other unsuper-

Table 33. **Debiasing Results and Comparison on CelebA.** We use the groups discovered by  $\mathcal{X}$ -Cluster to train DRO and compare it with state-of-the-art debiasing methods. Additionally, we present DRO results using the ground-truth distribution (DRO+GT) for reference.

Method	Worst	Avg.
JTT	81.5	88.1
CNC	88.8	89.9
DRO+B2T	90.4	<b>93.2</b>
DRO+ $\mathcal{X}$ -Cluster	<b>90.9</b>	93.1
<b>DRO+GT</b>	89.7	93.6

vised bias mitigation methods, including JTT [48], CNC [108], B2T, and GroupDRO trained with ground-truth labels. As shown in Tab. 33, our debiased model achieved robust performance, comparable to that of B2T, demonstrating the reliability of its discovered distributions.

**Additional Evaluation:** To further evaluate the prediction quality of our method for hair color and gender, we used the ground-truth labels from the CelebA dataset [56] to assess the classification accuracy of them. Our method achieved an impressive classification accuracy of 99.1% for gender and 87.4% for hair color on the 162,770 training images, demonstrating its effectiveness for uncovering gender and hair color substructures within the training set.

In addition, we quantified the *spurious correlation* between hair color and gender using the metric proposed by Yang et al. [103]. Specifically, given the correlated gender attribute distribution  $A$  and the target hair color distribution  $Y$ , we computed the normalized mutual information between  $A$  and  $Y$  to quantify the spurious correlation as:

$$I(A; Y) = \frac{2I(A; Y)}{H(A) + H(Y)} \quad (2)$$

where  $H(A)$  and  $H(Y)$  represent the normalized entropy of the gender and hair color distributions, respectively. A value of  $H(A)$  or  $H(Y)$  equal to 1 indicates a uniform distribution (*i.e.*, no class imbalance). We then used the ground-truth distribution from the dataset’s labels and our predicted distribution to estimate the spurious correlation intensity using the score from 2. For gender and hair color, our method’s predictions yielded a score of  $I_{Pred} = 0.10$ , which is nearly identical to the ground-truth score of  $I_{GT} = 0.11$ . This demonstrates that our method effectively identifies and confirms the bias directly from the training set.

**Implementation Details of Training GroupDRO:** To conduct debiased training using GroupDRO [83], we first used our predicted distribution to define four distinct training groups, rather than relying on the ground-truth distribution. We closely followed the training protocol outlined in B2T [39] and GroupDRO [83]. Specifically, we fine-tuned a ResNet-50 [31] model pre-trained on ImageNet [18], using the training split of the CelebA dataset [56]. The training was performed using the SGD optimizer [82] with a momentum of 0.9, a batch size of 64, and a learning rate of  $1 \times 10^{-5}$ . We applied a weight decay of 0.1 and set the group adjustment parameter to zero. The model was trained over 50 epochs. For evaluation, we reported both the average and worst-group test accuracies, selecting the model from the epoch that achieves the

highest worst-group accuracy on the validation set. The final evaluation and comparison results are provided in Tab. 33.

## R. Why LLMs Improve Image Clustering?

The most compelling aspect of this work lies in our  $\mathcal{X}$ -Cluster framework’s ability to transform large volumes of unstructured images into natural language and leverage the advanced text understanding and summarization capabilities of LLMs to tackle the challenging Open-ended Semantic Multiple Clustering (OpenSMC) task. This approach draws inspiration from the use of LLMs in the Topic Discovery task within the NLP domain [22]. Our core motivation is: “If LLMs can discover topics from documents and organize them, then by converting images into text, we can similarly use LLMs to organize unstructured images.”

Traditional clustering methods [11, 23, 46, 90, 107] often depend on pre-defined criteria, pre-determined numbers of clusters, fixed feature representations (which require training), and are typically not interpretable. These limitations hinder their applicability to diverse datasets in open-world scenarios, as they demand significant human priors and retraining for each new dataset.

In contrast, LLMs [1, 60, 61, 68, 88] excel at understanding, summarizing, and reasoning over high-level semantics expressed in natural language across diverse domains (*e.g.*, everyday content, cultural knowledge, or medical content). Operating in a zero-shot [40], interpretable manner, LLMs are uniquely suited to the SMC task, which aims to discover meaningful and interpretable clustering criteria without requiring prior knowledge or training. By integrating LLMs with MLLMs [49] into the carefully designed  $\mathcal{X}$ -Cluster framework, we enable the discovery and refinement of clustering criteria directly from the dataset’s content, followed by automatic grouping of the dataset. This design allows our framework to overcome the rigid assumptions of traditional clustering methods, making it automatic, generalizable, and training-free. Our approach provides a novel perspective, demonstrating how clustering tasks can evolve beyond traditional paradigms.

**Challenges of employing LLMs to facilitate the SMC task.** The main challenge of employing LLMs for the SMC task lies in accurately translating visual content from images into natural language that LLMs can effectively reason with. This is evident from the sensitivity analysis results in Supp. O:  $\mathcal{X}$ -Cluster’s performance improves with larger or more powerful MLLMs (see Fig. 10 (a)), while it remains relatively insensitive to the specific choice of LLM (see Fig. 10 (b)). In other words, the quality of image captions generated by MLLMs is critical for the effective use of LLMs in the SMC task. Specifically, in the first stage of  $\mathcal{X}$ -Cluster (criteria proposal), captions need to be as comprehensive as possible to provide *rich* information for LLMs to discover grouping criteria. In the second stage (semantic grouping), criterion-specific captions should precisely capture relevant visual content to provide *accurate* information for assigning images to clusters.

To enhance caption quality, techniques such as MLLM model ensembling, prompt ensembling [50], or stronger models like GPT-4V [1] can improve comprehensiveness. For better precision, advanced prompting methods like CoT [100] or FineR [53] can capture nuanced details, while hallucination mitigation tools like Visual Fact Checker [25] can reduce noise caused by hallucina-

tions. However, these techniques increase computational costs and framework complexity. In this work, we choose to keep  $\mathcal{X}$ -Cluster simple yet effective, and we outline these potential improvements for future practitioners.

## S. Future Work

**Closed-Loop Optimization.** In this work, we designed our prompts following the Iterative Prompt Engineering methodology [16] introduced by Isa Fulford and Andrew Ng. In Supp. F, we provide the exact LLM and MLLM prompts used in our framework and break down each prompt to explain the objectives and purposes behind each design choice. These explanations cover elements such as system prompts, input formatting, task and sub-task instructions, and output instructions. Our focus in this work is on creating a highly generalizable framework,  $\mathcal{X}$ -Cluster, and we do not perform any closed-loop, dataset-specific prompt optimizations. However, in future work or application scenarios where a labeled training/validation dataset is available, practitioners could build upon our design objectives. By leveraging our proposed evaluation metrics (see ??) for each step, it would be possible to develop a Open-ended Semantic Multiple Clustering (OpenSMC) system with a closed-loop optimization pipeline to achieve improved performance.

**$\mathcal{X}$ -Cluster on Other Data Types.** The core idea of our proposed framework,  $\mathcal{X}$ -Cluster, is to *use text as a proxy (or medium)* for reasoning over large volumes of unstructured data, generating human-interpretable insights at scale. As such,  $\mathcal{X}$ -Cluster can be directly applied to textual data (*e.g.*, documents). Moreover, since natural language is a highly versatile and widely-used medium of representation,  $\mathcal{X}$ -Cluster can be extended to other data types by converting these data into text (by replacing the captioning module with suitable tools) in future work, such as:

- **Audio Data:** Speech-to-Text models like Whisper [80] can convert audio data into text, enabling subsequent analysis with  $\mathcal{X}$ -Cluster.
- **Tabular Data:** Table-to-Text models, such as TabT5 [2], can translate tabular data into text, making it compatible with  $\mathcal{X}$ -Cluster. For tables containing figures, modern MLLMs like LLaVA-Next, which support both OCR and image-to-text capabilities, can handle these elements to create a unified textual representation for  $\mathcal{X}$ -Cluster.
- **Protein Structures:** Protein structure-to-text models, such as ProtChatGPT [96], can convert protein sequences into textual descriptions for analysis with  $\mathcal{X}$ -Cluster.
- **Point Cloud Data:** 3D captioning models, like Cap3D [57], can transform point cloud data or rendered 3D models into text, enabling their analysis using  $\mathcal{X}$ -Cluster.

We believe the versatile nature of  $\mathcal{X}$ -Cluster has the potential to open up a broad range of applications across diverse data modalities, fostering new directions in future research.

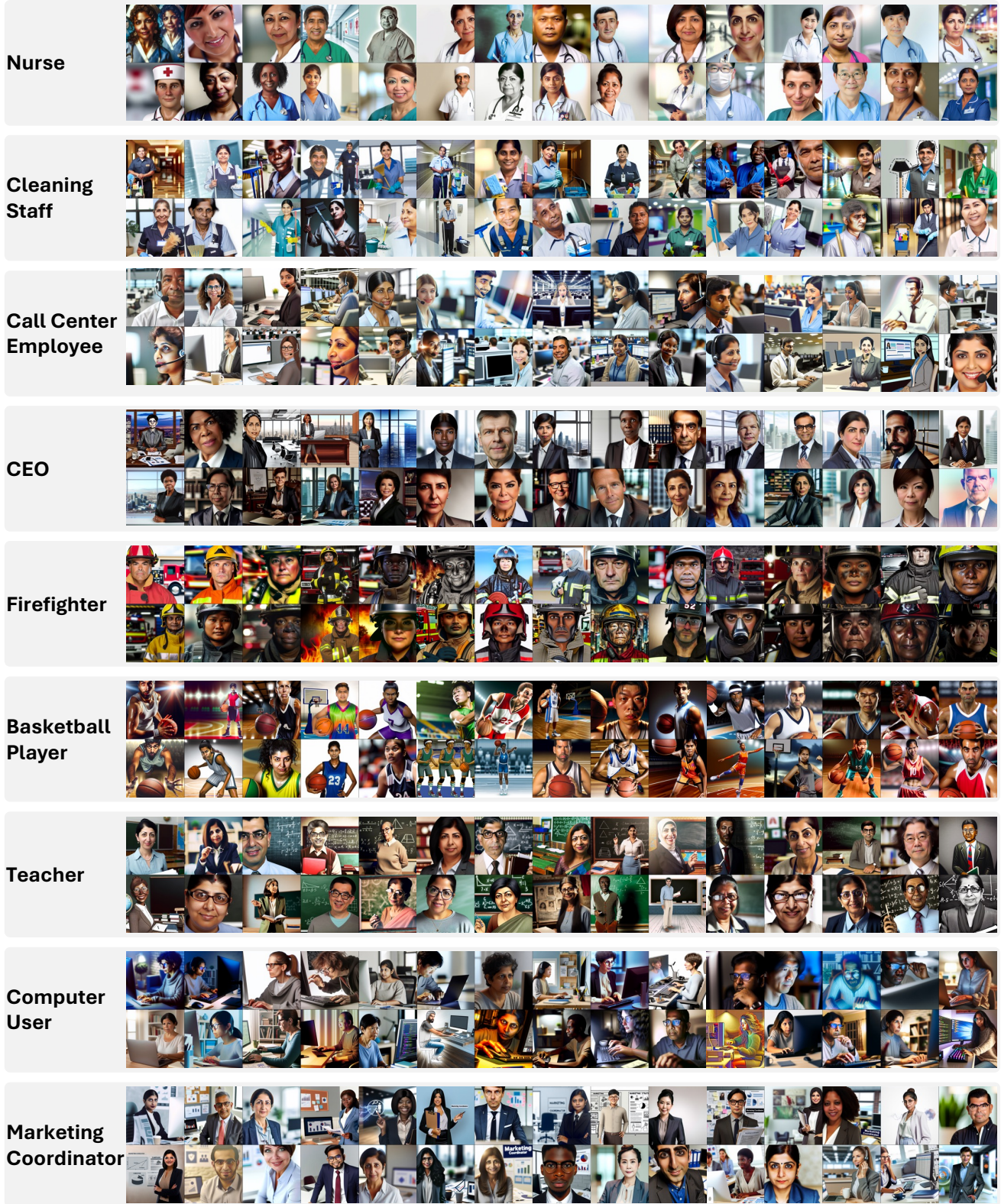


Figure 14. Samples of DALL-E3 generated images. For each occupation, the simple prompt “A portrait photo of a <OCCUPATION>”, that does not reference any potential bias dimensions such as gender, race or hair color, is fed to DALL-E3 to generate 100 images. We present a random sample of 30 generated images.



Figure 15. Samples of SDXL generated images. For each occupation, the simple prompt “A portrait photo of a <OCCUPATION>”, that does not reference any potential bias dimensions such as gender, race or hair color, is fed to SDXL to generate 100 images. We present a random sample of 30 generated images.

## Survey on Bias Study

Thank you for participating in our study on Bias in GenAI models.

### Important Information:

In this study, you will be asked questions related to socially-defined concepts such as gender and race. These topics may cause some discomfort due to inherent social biases. However, this is exactly the aim of this work: identifying bias present in nowadays GenAI models; thereby, we can prevent GenAI models propagate and augment these bias in our society. Your feedback will help us improve fairness and equity in AI systems. If you think you might be uncomfortable about the upcoming quizzes, please feel free to quit this questionnaire at any time. This survey is completely anonymous.

### Task Overview:

On each page, you will be presented with two sets of images. Each set contains 10 images, and your task is to:

1. **Identify the Dominant Class:** Examine the images and identify the most common or dominant characteristic for a given aspect. For example, if the aspect is "Hair Color" and 7 out of 10 people in the set have "Gray" hair, you would select "Gray" as the dominant class.
2. **Rate the Bias Severity:** Based on how strongly the images reflect this dominant class, rate the level of bias on a scale from 0 to 10. A score of 0 means no perceived bias, while a score of 10 indicates that all images are biased toward the dominant class. For instance, in the "Hair Color" example above, you might give a rating of 7/10 if you feel that the majority of the images favor "Gray" hair.

### Questionnaire Details:

- You will evaluate 15 different aspects of the images.
- The questionnaire should take approximately 5 minutes to complete.

We appreciate your participation and your efforts in helping us!

### Hair color

#### Image Set A



Which **Hair Color** is most dominant (or say, biased) in these images? \*

- gray
- black
- blonde
- brown
- dark
- mixed colors
- no dominant hair color
- I'm not sure

On a scale from 0 to 10, how much do you feel these images favor a particular **Hair Color**? \*

0 1 2 3 4 5 6 7 8 9 10

no perceived bias            all images are biased towards a single Hair Color

#### Image Set B



Which **Hair Color** is most dominant (or say, biased) in these images? \*

- gray
- black
- blonde
- brown
- dark
- mixed colors
- no dominant hair color
- I'm not sure

On a scale from 0 to 10, how much do you feel these images favor a particular **Hair Color**? \*

0 1 2 3 4 5 6 7 8 9 10

no perceived bias            all images are biased towards a single Hair Color

Figure 16. Example of the questionnaire for human evaluation study.